Diss. ETH NO. 24355

MODELING THE SEISMIC RESILIENCE OF ELECTRIC POWER SUPPLY SYSTEMS

A thesis submitted to attain the degree of

DOCTOR OF SCIENCES of ETH ZURICH

(Dr. sc. ETH Zurich)

presented by

LI SUN

M. Eng., Tongji University

born on 17.05.1983

citizen of P. R. China

accepted on the recommendation of

Prof. Dr. B. Stojadinovic, examiner

Prof. Dr. G. Sansavini, co-examiner

Prof. Dr. M. Bruneau, co-examiner

2017

Acknowledgement

I am heartily grateful to everybody who helped to make this thesis a reality. It turns out to be a grueling yet hugely rewarding journey.

I am particularly thankful to my supervisor Professor Bozidar Stojadinovic, whose unfaltering guidance renders it possible for me to chart and materialize the research path presented in this thesis. His unwavering support and endless patience were incredibly enlightening to my way forward.

I would also like to acknowledge the gratitude to my co-supervisor Professor Giovanni Sansavini for his consistent support throughout the entire journey. His staunch dedication and insightful suggestion always extricated me from the predicament.

I am thankful to Professor Michel Bruneau for serving as the examiner on my thesis. His gracious cooperation and generous advice were greatly encouraging to me.

I would also like to thank Professors Bruno Sudret and Eleni Chatzi for the help they have offered during my qualifying exams.

The unconditional and invaluable supports of Drs. Mirko Lukovic and Joseph Nagel always made it less scary every time when I was trying to get into the uncharted waters. I'm vehemently grateful to all of them.

I want to extend my heartfelt thanks to Ms. Neuhaus for her kind aids throughout my PhD study in ETH.

My colleagues Anastasios, Burkhart, Jonas, Max, Catherine, Michalis, Marco, Panos and Giuseppe have made our Chair a delightful atmosphere, whereupon all of us can rejoice at and focus on our research. I'm genuinely grateful to your magnificent help.

Lastly but importantly, I want to thank my family from the bottom of my heart, for their constant and firm support over the past decades. My parent and two uncles were always the enduring supply of encouragement and uplift. To my dear grandmother who passed away three years ago, I will be eternally mindful of your love. I can barely imagine a better way to pay you back with this hard-won thesis, at this particular moment in my life.

The financial support from China Scholarship Council (CSC) is gratefully acknowledged.

Abstract

The modern community is an organically assembled system of people, organizations, and infrastructures, as well as patterned interdependences and interactions. Functioning of modern communities relies on the continuous production and distribution of the essential goods and services, accomplished by large-scale, man-made, networked systems, called infrastructures. Such infrastructures are termed critical if their incapacity or malfunction could have a devastating impact on the health, security, and social well-being of community inhabitants. As exemplified by many recent occurrences, critical infrastructure systems in diverse communities across the spectrum of wealth have not been sufficiently robust and have not recovered quickly enough after severe natural disasters, with long-lasting physical damage and technical failures causing significant hardships and economic losses. Against this backdrop, it is imperative to comprehensively investigate, understand and model the disaster resilience of critical community infrastructure systems.

Among such critical infrastructure systems, the Electric Power Supply System (EPSS) stands at the core of a modern community. Among many natural hazards, the earthquake hazard stands out as potentially the most devastating and the most difficult to predict. Therefore, this thesis is focused on modeling and assessment of seismic resilience of EPSS and the community it serves.

The study begins with a review and an examination of the merits and drawbacks of the resilience modeling and assessment of current civil infrastructure system seismic resilience modeling frameworks. An important common shortcoming is the focus solely on the supply capacity of the infrastructure systems. To overcome this shortcoming, a measure of EPSS-Community system functionality and seismic resilience is formulated by comparing the service supply provided by the EPSS to the Community and the service demand generate by the Community. The supply/demand approach to quantify the seismic resilience of an EPSS-Community system is demonstrated using a virtual EPSS-Community system. A direct measure of the seismic resilience of the EPSS-Community system, the gap between the electric power supply and demand, is proposed in this thesis. This measure is tracked from the time an earthquake occurs until the EPSS-Community system has recovered to yield instantaneous and cumulative measures of resilience. One such instantaneous seismic resilience measure, the percentage of people without power (PPwoP) at any time after an earthquake, can serve as a societal measure of EPSS-Community system systemic resilience.

While the robustness of the EPSS-Community system is crucial for reducing the impact of an earthquake, the post-earthquake recovery process is critical to the seismic resilience of EPSS-Community system. This post-earthquake recovery process is case-specific, given their unique characteristics of EPSS and Community physical vulnerability, and dynamic, given the interactions among different infrastructure systems, community sectors, and the political and economic governance structures put in place after the disaster. An Agent-Based model is developed in this thesis to capture the unique dynamic characteristics of the EPSS-Community system seismic recovery process. Two individual agents, the EPSS Operator and the Administrator, are specified using a set of parameters to define their individual behavior

and interactions. The effect of agent parameters and their interactions is identified in simulations of the seismic recovery process of a virtual EPSS-Community using the supply/demand approach.

The post-earthquake restoration of a modern EPSS is contingent upon the post-earthquake serviceability of other critical infrastructure systems, in particular upon the serviceability of the transportation systems (TS) of the community. To investigate this interdependency among the community infrastructure systems, the virtual EPSS-Community system is expanded to include a transportation system, and a third agent, the TS Operator, is added to the model. The conducted case studies demonstrate that the interplay among different agents, as well as the interdependency between the civil infrastructure systems, determine the recovery path for the integrated EPSS-TS-Community system.

The community resources available for post-earthquake recovery are finite. A network-theoretical model is used to gauge the impact of the quantity of the disposable repair resources and work crews on the seismic recovery for EPSS-TS system. The case study simulation results clearly indicate the rate of EPSS-TS system recovery is affected by the amount of available resources, but, importantly, that an optimal distribution of the available resources between the EPSS and the TS can significantly reduce the system recovery time and, thus, increase its seismic resilience.

The presented scientific findings lay the foundation for a comprehensive and integrated resilience assessment on the EPSS-Community system based on the proposed agent-based network-theoretical supply/demand framework. Further work on generalizing the model by including all community infrastructure systems and refining their interactions in the model can be done using the proposed framework to investigate the interdependencies among the infrastructure systems and optimize community governance actions. Inclusion of dynamic models of community and infrastructure system post-disaster behavior, such as movement of the population, restructuring of the infrastructure and the effects on the production and consumption of goods and services, would make it possible to examine how disaster resilience of the integrated critical infrastructure systems shapes the long-term socio-economic development of the communities.

Zusammenfassung

Das moderne Gemeinwesen ist ein organisch gewachsenes System, bestehend aus Einwohnern, Organisationen und Infrastrukturen, die in gegenseitiger Abhängigkeit stehen und miteinander wechselwirken. Die heutige Gesellschaft beruht auf der ständigen Produktion und Verteilung der wesentlichen Güter und Dienstleistungen. Man bezeichnet die dafür notwendigen groß angelegten und vom Menschen geschaffenen Netzwerke als Infrastruktur. Teile diese Infrastruktur werden als kritisch bezeichnet, wenn ihr Ausfall oder Störung einen verheerenden Einfluss auf die Gesundheit, die Sicherheit und das soziale Wohlergehen der Gemeindebewohner haben könnte. Viele neuere Ereignisse haben gezeigt, dass kritische Infrastrukturen in unterschiedlich wohlhabenden Gesellschaften nicht hinreichend robust sind und sich nach schweren Naturkatastrophen nicht schnell genug erholen. Dies führt zu lang anhaltenden körperlichen Schäden und technischen Defekten, die wiederum erhebliche Schwierigkeiten und wirtschaftliche Verluste verursachen. Vor diesem Hintergrund ist es unerlässlich, die Katastrophenvorsorge kritischer Infrastruktursysteme umfassend zu untersuchen, verstehen und modellieren.

Ein kritisches Infrastruktursystem, welches im Mittelpunkt der modernen Gesellschaft steht, ist das Stromversorgungssystem (EPSS). Unter den vielen Naturgefahren ist die Erdbebengefahr möglicherweise am verheerendsten und am schwersten vorherzusagen. Daher konzentriert sich diese Doktorarbeit auf die Modellierung und Bewertung der seismischen Resilienz des EPSS und der davon versorgten Gemeinschaft.

Die Arbeit beginnt mit einer Zusammenfassung und Untersuchung der Vorzüge und Nachteile der Resilienz-Modellbildung und einer Bewertung gängiger Methoden zur Modellierung der Erdbeben-Resilienz von ziviler Infrastruktur. Der einseitige Fokus auf die Versorgungskapazität der Infrastruktursysteme stellt oft ein schwerwiegendes Manko dar. Um dieses Problem zu beheben, wird ein Maß für die Funktionalität des EPSS-Gemeinschaft-System und für die seismische Resilienz formuliert. Dies basiert auf einem Vergleich der von der EPSS angebotenen und der von der Gemeinschaft geforderten Dienstleistungen. Das Angebot/Nachfrage-Konzept zur Quantifizierung der seismischen Resilienz eines EPSS-Gemeinschaft-Systems wird anhand eines simulierten EPSS-Gemeinschaft-Systems demonstriert. In dieser Arbeit wird die Differenz zwischen dem gedeckten und dem tatsächlichen Bedarf an elektrischer Energie als direktes Maß der seismischen Widerstandsfähigkeit des EPSS-Gemeinschaft-Systems vorgeschlagen. Dieses Maß wird von dem Zeitpunkt an betrachtet, an dem ein Erdbeben auftritt, bis zu dem Punkt, an dem sich das EPSS-Gemeinschaft-System erholt hat. Dies ermöglicht eine sofortige und Einschätzung der Gesamt-Resilienz. Der Prozentsatz der Menschen ohne Strom (PPwoP) nach einem Erdbeben kann hier zum Beispiel als gesellschaftliches Maß für die systemische Resilienz des EPSS-Gemeinschaft-System verwendet werden.

Während die Robustheit des EPSS-Gemeinschaft-Systems entscheidend für die Verminderung der direkten Auswirkungen eines Erdbebens ist, ist der spätere Erholungsprozess ausschlaggebend für die seismische Resilienz des EPSS-Gemeinschaft-Systems. Dieser Nach-Erdbeben-Wiederherstellungsprozess ist fallabhängig, da es sich um

einzigartige Merkmale des EPSS und der physischen Gemeinschaftsanfälligkeit handelt, und dynamisch, angesichts der Wechselwirkungen zwischen verschiedenen Infrastruktursystemen, Gemeinschaftssektoren und den nach der Katastrophe bestehenden politischen und wirtschaftspolitischen Strukturen. In dieser Arbeit wird ein Agenten-basiertes Modell entwickelt, um die einzigartigen dynamischen Eigenschaften des seismischen Wiederherstellungsprozesses des EPSS-Gemeinschaft-System zu erfassen. Zwei einzelne Agenten, der EPSS-Betreiber und der Administrator, werden mit einer Reihe von Parametern spezifiziert, um ihr individuelles Verhalten und ihre Interaktionen zu definieren. Die Auswirkung von Agentenparametern und deren Wechselwirkungen wird in Simulationen des seismischen Wiederherstellungsprozesses eines virtuellen EPSS-Gemeinschaft-System anhand des Angebot/Nachfrage-Konzepts untersucht.

Die Nach-Erdbeben-Wiederherstellung eines modernen EPSS ist abhängig von der Nach-Erdbeben-Betriebsbereitschaft anderer kritischer Infrastruktursysteme, insbesondere der Betriebstauglichkeit der Transportsysteme (TS) der Gemeinde. Um diese Wechselbeziehung zwischen den gemeinschaftlichen Infrastruktursystemen zu untersuchen, wird das virtuelle EPSS-Gemeinschaft-System um ein Transpirationssystem erweitert und ein dritter Agent, der TS-Betreiber, wird dem Modell hinzugefügt. Die durchgeführten Fallstudien zeigen, dass der Wiederherstellungsverlauf des integrierten EPSS-TS-Gemeinschaft-System durch das Zusammenspiel verschiedener Agenten sowie durch die Wechselbeziehung zwischen den zivilen Infrastruktursystemen bestimmt wird.

Die Gemeinschaftsressourcen, die für die Wiederherstellung nach dem Erdbeben zur Verfügung stehen, sind endlich. Ein netzwerktheoretisches Modell wird verwendet, um die Auswirkungen der Menge an verfügbaren Reparaturressourcen und Arbeitsmannschaften auf die seismische Erholung des EPSS-TS-System abzuschätzen. Die Simulationsergebnisse der Fallstudien zeigen deutlich, dass die Geschwindigkeit der EPSS-TS-Systemwiederherstellung durch die Menge der verfügbaren Ressourcen beeinflusst wird, aber vor allem, dass eine optimale Verteilung der verfügbaren Ressourcen zwischen dem EPSS und dem TS die Systemwiederherstellungszeit erheblich reduzieren kann, und dadurch die seismische Resilienz erhöht.

Die präsentierten wissenschaftlichen Erkenntnisse legen den Grundstein für eine umfassende und integrierte Resilienzbewertung des EPSS-Gemeinschaft-System auf der Grundlage des vorgeschlagenen agentenbasierten und netzwerktheoretischen Angebot/Nachfrage-Konzepts. Zukünftige Verallgemeinerungen des Modells durch die Einbeziehung aller gemeinschaftlichen Infrastruktursysteme und die Verfeinerung ihrer Interaktionen im Modell können innerhalb der vorgeschlagenen Rahmen durchgeführt werden, um die Wechselwirkungen zwischen den Infrastruktursystemen zu untersuchen und Maßnahmen der Gemeinschaftssteuerung zu optimieren. Die Einbeziehung von dynamischen Modellen des Verhaltens der Gemeinschaft und des Infrastruktursystems nach einer Katastrophe, wie die Bewegung der Bevölkerung, die Umstrukturierung der Infrastruktur und die Auswirkungen auf die Produktion und den Verbrauch von Gütern und Dienstleistungen, würde es ermöglichen, zu untersuchen, wie die Katastrophen-Resilienz der gesamten kritischen Infrastruktur die langfristige sozioökonomische Entwicklung des Gemeinwesens prägen.

Content

1. Introduction

Electric Power Supply System (EPSS) is the underpinning bedrock for modern civilized societies. Its resilience is strategically important to the security and sustainability of the communities, which have become considerably more sophisticated and integrated than ever before. As indicated by the recent history, unfortunately, EPSSs were proven to be vulnerable under natural hazards like strong earthquakes, leading to negative economic and societal ramification for the entire community. Moreover, due to the influence of interdependences, the failure or malfunction of EPSS can also cascade and potentially flare up into the full-blown shutdown of the whole system of coupled infrastructure networks.

Until now, series of studies have been undertaken in order to capture the seismic behavior of the critical components across EPSS. Based on them, some pertinent mitigation strategies have been devised as the bid to harden the EPSSs. However, as revealed by the review on the state-of-the-art in Chapter 2, they are not yet strong enough to render the subtly networked modern EPSS immune to the catastrophic earthquake hazards. Hence, the resulting damage to the entire system can still be grave, even in the presence of those developed mitigation techniques.

Under this circumstance, seismic resilience has emerged, over the past decade, as a widely-accepted and viable engineering roadmap to increase the security and sustainability of modern EPSSs. Essentially, such strategy aims at realizing the sound and steady recovery of the system in the post-disaster stage, while also minimizing the initial damage inflicted by the earthquake events. A seismically resilient critical infrastructure system is the one that experiences relatively small earthquake damage and realizes a rapid post-earthquake recovery.

The seismic resilience assessment frameworks proposed to date focus solely on the functionality of the civil infrastructure networks to supply the community, while the time-varying demand from the users are usually absent. Such character renders them incapable of measuring the resilience and the associated socio-economic risk for the coupled physical network-community system subjected to natural hazards. Meanwhile, the currently employed frameworks track the recovery path for the infrastructure networks ensuing disruptions, mainly by means of the parametric Recovery Functions (RFs) on either component or the system level. The fundamental deficiency for such approach lies in the sheer difficulty to determine those parameters for every unique socio-technical system with their own case-specific characteristics. Besides, given the scarcity of the data collected across the real-world catastrophic events, it is difficult to verify and calibrate the RF parameters.

1.1. Research goals

In order to narrow the knowledge gap, the following research steps are taken:

- The review of the earthquake-caused failures of EPSS on both component and system levels will be done. The vulnerability for the collection of different kind of EPSS components under various hazards will be first summarized. The mechanism for the local damage on the specific group of components to propagate to system failure will also be identified.
- A review of the existing seismic, and broader, natural hazard, resilience assessment frameworks will be made. The roadmap to develop a new concept of CI seismic resilience will be sketched and illustrated.
- The new conceptual framework for quantifying the seismic resilience of EPSS will be put forward, and contrasted to the existing resilience assessment frameworks.
- Based on the proposed framework, a new agent-based model (ABM) that is capable of tracing the seismic recovery of EPSS considering its unique technical characters and the interplay between the participating decision makers will be devised.
- The proposed agent-based model will be further expanded to model the interdependence between EPSS and other coupled CIs, such as the transportation system (TS) in terms of the recovery of the systems.
- Based on the prosed seismic resilience quantification framework and the agent-based model, a network-theoretical model will be developed to assess the impact of the amount and distribution of the available community recovery resources on its seismic resilience.

1.2. Research Significance

As the research endeavor to help us improve the understanding on the behavioral patterns of EPSS under seismic hazards, the new conceptual assessment framework would enable the users to better evaluate the resilience behavior for the integrated physical network-community system. In order to facilitate the decision-making and the risk governance, such framework would also help to measure the systemic resilience from the socio-economic perspective, besides the purely physical functionality losses.

Meanwhile, the newly proposed agent-based model would contribute to tracking the evolving functionality trajectory of EPSS, while considering their individual technical characteristics of the EPSS and other CIs and the societal characteristics of the community.

In addition, the network-theoretical model would enable the nuanced assessment on the seismic resilience of the coupled system under varying repair resources. It would be enlightening for us to mobilize and dispense those resources in an optimized way, throughout the entire disruptive events.

Overall, the research findings in this thesis would help to cast lights on the roadmap to forge the future resilient EPSS with exposure to various disruptions, like strong earthquakes. Given the

soaring demand for electric power worldwide, the prospective improvements would contribute to increase the well-being and sustainability of the modern integrated urban communities.

1.3. Scope

This thesis is structured in six chapters：

This chapter offers the general introduction. The background and the significance for this research focusing on the seismic resilience of EPSS, are elaborated.

Chapter 2 presents the state-of-knowledge on the behavior of EPSS specifically, and CIs in general, during earthquakes. The research work to capture the seismic vulnerability of EPSS on both component and system level, are summarized first. Thereafter, development of the concept of component and system resilience explained. The efforts to apply these concepts in practice for both the real-world standalone structures and networked systems, is then reviewed.

Chapter 3 elaborates the newly proposed framework to quantify the seismic resilience of community CIs. To this end, the conceptual details for this compositional supply/demand framework, particularly its differences with respect to the existing resilience quantification frameworks, are presented first. The proposed framework is implemented using an agent-based model (ABM) and a virtual Community-EPSS example is constructed to demonstrate how to quantify seismic resilience. The ability of this model to capture the interaction between the community and CI decision makers is also illustrated.

Chapter 4 depicts how to further grow the ABM to consider the influence of the state of the other coupled networks, such as the transportation system (TS) on the seismic resilience behavior of EPSS. The findings from the comparative studies are particularly highlighted.

Chapter 5 presents the further updated model taking the time-varying configuration of the networks into the account. More importantly, the way that the available/mobilizable resources shapes the functionality trajectory for the interdependent networks, is examined and discussed.

Chapter 6 draws the most important conclusions from the work conducted in the scope of this doctoral dissertation. The outlook to prospective new studies is also suggested in the end.

Table 1.1 gives an overview of the investigated infrastructure systems and the developed/employed models.

Table 1.1. Overview on the infrastructure systems and their models

	Chapter 3	Chapter 4	Chapter 5
ABM	Operator of EPSS, Administrator	Operators of EPSS and TS, Administrator	none
Grid Topology	EPSS (IEEE 118, extracted)	EPSS (IEEE 118, extracted), TS (virtual)	TS (Lattice) EPSS (Overlaid)
Vulnerability	Fragility functions	Fragility functions	Fragility functions
Recovery	ABM (EPSS Supply) RFs (EPSS Demand)	ABM (EPSS Supply, TS) RFs (EPSS Demand)	RFs (TS, EPSS)

2. Review on state-of-the-art

2.1. The emergence of Critical Infrastructure-Urban Community Systems

Human beings have already crossed a significant milestone in history in 2009 when a majority resided in urban communities, compared to only around 34% in 1960 (Dunn 2016). Owing to the inexorable trend toward urbanization around the world, the modern communities are the preponderant engine for wealth creation and technological innovation for each nation (Bettencourt et al. 2007). In turn, this socio-economic development further incentivizes and prompts the urban sprawl (Batty 2008, Bloom et al. 2008). The advantages of booming urban communities are often offset by the recurrent urban curses of pollution, disease, and violence (Glaeser 2011). Furthermore, the ever-increasing interconnectivity and interdependence within the globally integrated modern communities have paved the way for catastrophes, such as contagious diseases, consequences of physical damage induced by natural hazards, or random or targeted technological failures, to spread rapidly and pervasively. This renders the integrated socio-technical systems of urban communities exposed to significant risks.

Modern urban communities are the organically collected system of people, organizations, and patterned relationships as well as interdependences (Alesch 2005). Most of these interactions are physically underpinned by the built environment, namely, the complex and interdependent network of engineered sub-systems and components consisting of the sector of residence, business, industry, and et al. (Batty 2012). Continuous function of a community depends on the uninterrupted inflow of necessary goods and services provided by the civil infrastructure systems. These are large-scale, man-made systems that operate synergistically and cooperatively so as to generate and distribute the services such as electric power, potable water, transportation or communication (O'Rourke 2007). In modern urban communities, such infrastructures are deemed critical, as any incapacity or malfunction would have a devastating impact on the health, security, and social well-being of the community members. Such Critical Infrastructures (CIs) are cybernetic engineered networked systems and organizations. Particularly, given the pervasive use of electric energy, the Electric Power Supply System (EPSS) has become the backbone of modern urban communities. The natural hazard resilience of EPSS is crucial for the functionality and sustainability of the entire society (Kröger and Zio 2011).

As a complex socio-technical network, the modern engineered CIs are delivering their critical functions via real-time interdependences and the interplay between the system's dynamics and changes in the underlying network topology (Gao et al. 2016). In particular, as the focus of this thesis, EPSS is a geographically distributed network to transfer power energy from the producers to the end users (Borberly and Kreider 2001). While standing at the core of the modern civilized communities, EPSS is also facing the soaring power demand stems from the consumers across the community system. The ever-increasing complexity associated with the configuration of EPSS has rendered the physical network susceptible to various disruptions, while increasing its capability to fulfil the function.

Fig. 2.1 presents the interdependencies among the CIs within a community. Primarily, it is the EPSS that provides the electric power to ensure the sustained functionality of most of the other CIs. The figure also shows that the operation of EPSS is, in turn, contingent on the operation of other CIs. Such interdependencies tend to increase the vulnerability of EPSS to service disruptions.

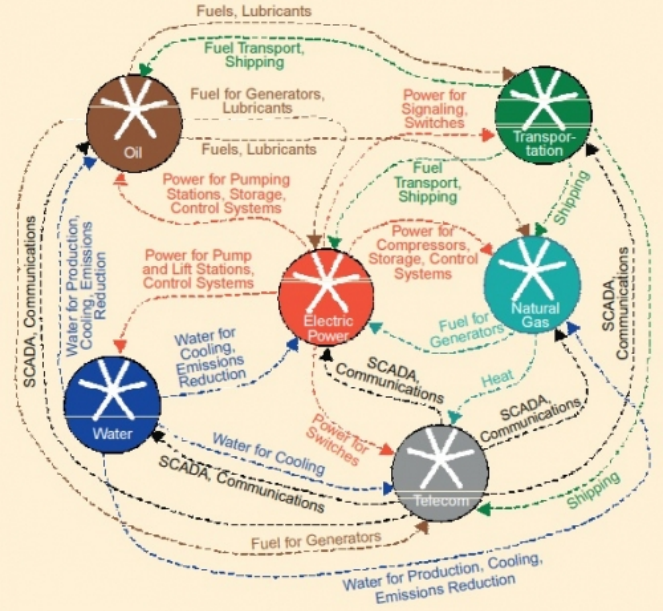

Fig. 2.1. Illustration of the interdependencies among CIs (Rinaldi et al. 2001)

Large natural hazard catastrophes, such as earthquakes, hurricanes, and floods can inflict serious damage, or even cause global failure of a community EPSS, affect other CIs and incapacitate the community itself.

For example, in the US, EPSS was revealed to be susceptible to the combination of high winds, rainfall, and storm surge brought by Hurricane Rita, in 2005. More than 500,000 people were subjected to blackout in Louisiana alone immediately after Rita's landfall. Meanwhile, more than 1.5 million customers were affected in Texas. Hurricane Rita decimated both transmission and distribution systems within the EPSS. It also became clear that massive failure of steel lattice transmission system towers can significantly hinder the post-disaster repair campaign, as most of these towers were often located in inaccessible areas. Likewise, distribution systems were also shown difficult to repair due to massive tree failures and the resulting debris (Reed et al. 2010).

Regarding China, only in 2005, the gross number of collapsed 500 kV transmission towers caused by severe storms has exceeded 18. In 2008, South China suffered a very rare freezing rain and ice disaster lasting for around 20 days, causing widespread EPSS failures. The number of collapsed and damaged towers, belonging to State Grid Corporation of China and local electrical

companies, with rating above 35 kV amounted to 7263. Consequently, the whole power system was paralyzed in that area causing very high economic losses and human suffering. In the same year, during the catastrophic 12 May 2008 Wenchuan earthquake and aftershocks, 90 substations with voltages of 110 kV and above went out of service (Fig. 2.2) while 181 power transmission lines were interrupted (Xie and Zhu 2011).

Fig. 2.2. Damaged power substation during Wenchuan Earthquake 2008 (Xie and Zhu 2011)

More recently, on 11 March 2011, the Great East Japan earthquake caused extensive damage to EPSS in a very wide region of Northeastern Japan. Approximately 4.4 million households served by the Tōhoku Electric Power Company (TEPCO) in Northeastern Japan were left without electricity because of a combination of power plant shutdowns, and earthquake and tsunami-induced electric power transmission infrastructure damage. Subsequent, the inability to repair extensive power infrastructure damage prevented immediate restoration of clean water supply and sewage services in several prefectures (Kuwata 2012). The high-speed rail power infrastructure also suffered damage (Kawashima 2012). Some support poles for catenary and power line of the JR East Shinkansen facilities fractured and collapsed. It took over two weeks to repair and replace them with the corresponding steel poles.

A summary of characteristic failure modes of EPSS components is listed in Table 2.1 (Fujisaki et al. 2014, Xie and Zhu 2011).

Table 2.1. The primary failure modes for different EPSS components under different natural hazards

	Line	Tower	Switch	Transformer-Bushing
Earthquake	Failures are very rare	Failures are very rare	**Failure modes**: Pulled down by the conductor due to the adjacent equipment interaction	**Failure modes**: Sliding or tip-over of the transformer; Breaking of the bushing
High wind	**Failure modes**: Galloping of iced conductors	**Failure modes**: Collapse due to the wind-induced coupling vibration	Failures are very rare	Failures are very rare
Ice	**Failure modes**: Ice-shedding	**Failure modes**: Collapse due to the vertical loads or the lateral unbalanced tension in conductors	Failures are very rare	Failures are very rare

EPSS was also revealed to be susceptible to technological failures. The U.S.-Canadian blackout of August 14, 2003 affected around 50 million people, in eight states of U.S. as well as two Canadian provinces. Approximately 63 GW of load was disrupted, which accounts for roughly 11% of the total load served in the Eastern Interconnection of the North American system. It was reported that a total of more than 400 transmission lines and 531 generating units at 261 power plants tripped (Andersson et al. 2005). In addition, this incident also led to 3 billion USD insurance claims (Kröger and Zio 2011).

On September 28 of the same year, due to a storm-damaged power line which supplied electricity to Italy from Switzerland, the nationwide Italy blackout was induced (Kröger and Zio 2011). It was the most serious power outage that the nation has suffered in 70 years. Note that the initial paralysis of power stations within EPSS directly led to the failure of nodes in the Internet communication network across that region, which in turn ramped up further breakdown of power stations (Kröger and Zio 2011). This event affected most of Italy (except for the islands of Sardinia and Elba) for 12 hours as well as part of Switzerland near Geneva for 3 hours. A total of 56 million people was affected. Furthermore, the rolling blackouts continued to affect about 5% of the population during the following two days as the electricity company ENEL proceeded with its effort to restore the service (https://en.wikipedia.org/wiki/2003_Italy_blackout).

2.2. Vulnerability of EPSS

The principal components of EPSS are: 1) the elements of a transmission line (the transmission towers, the transmission cables, the connections between the cables and the towers, i.e. attachments and insulators), and 2) the elements of a generation or a distribution substation (the

switches, the transformers, the bushings and other substation elements). The EPSS components function as a system, bound together by the physics principles of operation and by the EPSS operator electric power dispatch which is adopted to supply the energy at the lowest cost to consumers, considering the operational limits of the physical facilities (Kirschen 2010). Therefore, the vulnerability of an EPSS needs to be examined at both the component and the system levels.

2.2.1. Studies on the EPSS component-level vulnerability

The vulnerability of EPSS components and the corresponding retrofit strategies have been extensively investigated. The relevant results are discussed in the following sections. Note that the transmission towers and the generation substations were shown to be the EPSS components most vulnerable in earthquakes: therefore, most of this review is focused on these two components (sub-systems).

2.2.1.1. Transmission towers

The coupled transmission tower-transmission line systems are primarily employed to transit the generated electric power, and thus playing an important role inside modern EPSS. Most of the tower structures in are space trusses made of steel angle member. The stability of steel angle members is deficient because of the asymmetry of their open cross sections, eccentricities, and diverse restraints at connections. Consequently, premature failure for the tower as a whole or some tower elements has been observed during wind and ice disasters (Table 2.1.).

Regarding the wind hazard, Zhao et al. (2010) carried out the boundary layer wind tunnel test on the aeroelastic model of one practical 500 kV transmission tower-transmission line coupled system. The responses of the single tower and the corresponding tower-line coupled system model were comparatively investigated. The results showed that the magnitudes of the along-wind and the across-wind responses in turbulent flow are of the same order of magnitude. The coupling of vibration between the tower and the cables was pronounced under strong wind. The natural oscillation characteristic of the coupled system changed greatly and the vibration modes different from those of standalone tower structures were aroused. This revealed that the wind-induced vibration of transmission tower-transmission line coupled system has strong nonlinear dynamic characteristics that would remarkably influence the failure pattern of the coupled system under strong winds.

For the ice load, Xie and Sun (2012) conducted the static loading test on three pairs of transmission tower subassemblages. The failure mechanisms of the structures under simulated ice loads combined with limited wind loads were examined. It was found that the diagonal bracing members buckle and deflect significantly in their out-of-plane direction during the specimen loading process. This reduces the lateral restraint of the tower main legs in the joint area.

Meanwhile, the main legs would also be subjected to torsion caused by the deformation of the diagonal bracing members. This induces flexural-torsional buckling of the main tower legs.

In response to this failure mode, addition of a diaphragm member to the tower was proposed as a retrofit strategy. The experimental study revealed that the out-of-plane deformations of the diagonal bracing members as well as the torsional they induce in the main legs are both substantially reduced. In this case, the buckling modes of the main tower legs approach pure flexural buckling. Hence, the structural behavior could was streamlined, while the load-carrying capacity of the tower was greatly increased (Xie and Sun 2013). Although shown to be effective, it should be noted that adding diaphragms is not straightforward for many of the existing tower structures located in the inaccessible areas, given their complex configuration.

Against this backdrop, an all-steel buckling restrained brace (BRB) was designed by Trovato et al. (2015) and proposed to be another practical method to improve the resilience performance of existing high voltage transmission towers. The main feature of this BRB is that the restraining casing is built by positioning two pre-fabricated rectangular steel tube halves around the restrained member and bolting them *in situ*, by a single worker using only batter-operated tools. No filler is used to make the installation operation as simple as possible. Static loading tests were carried out on six equal-leg angle members. The test results demonstrate that, owing to the restraining steel tube, the deformation capacity of the steel angle was improved significantly, while the load carrying capacity did not increase substantially. The tested members failed in or near their gusset plate connections, while the bolts held the restraining tube together. This shows that the *in situ* installed buckling restrainer functions as expected by preventing a sudden drop in member resistance.

Considering the seismic loads, Bai et al. (2013) carried out the shaking table tests on a scaled model of the 1000 kV Ultra High Voltage (UHV) transmission tower-transmission line system. It was revealed that the dynamic response of the tower with conductors decreased significantly compared to the response of the corresponding standalone tower. This means that the conductors help to dissipate the input seismic energy and thereby increase the seismic resistance of transmission towers.

2.2.1.2. Generation substation equipment

Substations, whose function is to transform voltage and thereby connect different EPSS transmission, are another very important EPSS element. The configuration of substation itself is also quite complex. It usually consists of transformers, bushings, circuit-breakers, switches, buses and other elements such as remote switch actuation and monitoring equipment. Due to their mechanical characteristics, many substation elements were found to be quite vulnerable to strong earthquake loads. Considerable study has been conducted over the past decades in order to explain and model the seismic behavior of EPSS substation elements.

Der Kiureghian et al. (1999) analytically and numerically investigated the time history response of the stiff equipment-flexible conductor system. The dynamic interaction between the

components in this system was found to amplify the structural responses of high-frequency equipment under certain conditions. Narrowing the gap between frequencies of the two standalone pieces of substation equipment connected by a flexible conductor was proposed as one feasible method to reduce the adverse effect of such dynamic interactions. Meanwhile, reducing the stiffness of the connecting element was also found to be a practical and effective seismic damage mitigation strategy (Der Kiureghian et al. 2001).

Filliatrault and Stearns (2004) performed shaking table tests on five different pairs of simulated equipment connected by three different types of flexible connector assemblies. Two different types of dynamic response were observed. The first type involves low interaction between the two equipment items due to a large slack and/or low intensity ground motions. For this case, the large horizontal movement of the more flexible equipment was transferred almost entirely into vertical motion of the conductor with little impact on the stiffer equipment. The second type of dynamic response involves high interaction between interconnected equipment due to a small slack and/or high intensity ground motion. For this case, large vertical acceleration pulses were observed at mid-span of the conductor.

Whittaker et al. (2004) examined the seismic performance of the transformer bushings. According to their work, the poor seismic behavior of these types of bushings in the field brought in question the methods used for seismic qualification for substation equipment. In particular, the principles for fragility testing of the bushings were found to be inadequate.

Filiatrault and Matt (2005) conducted the shake table testing of a full-scale high-voltage electrical transformer-bushing system. They found that the dynamic characteristics of the bushing are greatly influenced by the flexibility of the top plate of the transformer tank. The horizontal dynamic amplification factor between the input motion at the base of transformer and the motion recorded at the base of the bushing was found to be frequency dependent. It reaches the maxima at the natural frequencies of the bushing and the transformer tank.

Considering the lesson indicating the relatively poor performance of high-voltage porcelain bushing observed in the field, Koliou et al. (2013a, b) carried out an experimental and a numerical study on the coupled transformer-bushing system to in order to capture its seismic behavior. The results showed that the high-voltage bushings mounted on the cover plates of transformers are more vulnerable to seismic load than those on a rigid base. In addition, flexural stiffeners were proposed as a measure to strengthen the base of bushings and mitigate their seismic vulnerability. The data from a shaking table test confirmed that stiffening the cover plates is beneficial to the seismic response of high-voltage bushings.

Recently, Mosalam et al. (2016) conducted the real-time hybrid simulation (RTHS) on the interconnected substation equipment using two shaking tables. A set of global and local response parameters like accelerations, forces, displacements, as well as strains, were examined to assess the effect of the tested conductor cable configuration for a wide range of support structure configurations modeled in the computer as analytical substructures. The experimental parametric

study results demonstrate that the conductor cable would significant affect the response of the interconnected equipment over the whole range of examined support structures.

2.2.2. Studies on the EPSS system-level vulnerability

The seismic vulnerability modeling and assessment of EPSS viewed at the system level, as well as all other modern CIs, involves not only the seismic vulnerability of the components, but also their complex interactions through the network they are connected by and the way that network is operated. A series of studies have been conducted over the past decades to model and explain the seismic behavior and the potential failure mechanism of EPSS under different kinds of disruptive events.

Shinozuka et al. (2007) looked into the potential of a system-wide blackout, due to the sequential failures of EPSS station components under strong earthquakes. The seismic vulnerability of the critical EPSS components (including transformers, disconnect switches, circuit breakers and buses) was considered by means of fragility curves. The possibility of progressive failures of these components could thereby be examined in a system analysis. The scenario of the component-level failures enables quantitative estimation of the direct costs of the physical damage, of the associated economic losses, as well as of the societal disruptions.

Dueñas-Osorio and Vemuru (2009) proposed a framework to examine the effect of cascading failures throughout an EPSS. The developed framework models the overloads induced by cascading failures with a tolerance parameter that measures element flow capacity relative to flow demands in the real-world EPSS. According to their findings, it was shown that improvements in the component tolerance alone will not necessarily ensure system robustness or protection against disproportionate cascading failures. Topological upgrades, at the same time, are also required to increase cascading robustness at viable tolerance levels.

Cavalieri and Franchin (2014) conducted a comparative study on five different seismic performance assessment models (of increasing complexity) of EPSS. The first two models (M1 and M2) examine the problem from a connectivity perspective, while the last three (M3 to M5) also account for power flow analysis. A case study on the well-known IEEE-118 benchmark test case, which was assumed to be located in the central United States, is carried out to investigate the utility of the five models at both system and the component levels. The outcome suggests that simpler models (M1 and M2) are suitable if only vulnerability assessment and retrofit prioritization are under consideration. The complex flow-based models (M3 to M5) are appropriate if the actual performance of the systems is of interest, as it is the case when the EPSS will be examined within a larger set of interconnected CIs.

As highlighted, the interdependence of CIs has been widely viewed as critical to the seismic vulnerability and post-earthquake functionality of EPSS. A number of studies on this topic have been conducted over the past decade.

Poljansek et al. (2012) proposed a Geographic Information System (GIS)-based probabilistic reliability model to establish network fragility curves for the spatially distributed interconnected CIs subjected to natural hazards. In this model, the geographic distributions of both the physical infrastructure and the natural hazard can be incorporated. The interconnected European gas and electricity transmission networks, where the gas-fired power plants form the physical connections between the two types of CIs, were considered. The network fragility curves measured by various performance measures, of the independent and dependent networks, were calculated. It was found that the gas network is more seismically vulnerable than the EPSS. The interdependence, however, brings an extra vulnerability to the EPSS, as its vulnerability increases with the extent of the gas network damage. Damage was also assessed at the local level in order to determine the most vulnerable CIs components.

Similarly, Omidvar et al. (2014) performed the seismic vulnerability assessment for an interdependent CI system consisting of EPSS and water distribution networks. The extended Petri net and Markov chain were employed to study the effect of interdependencies among the two systems on their vulnerability. The analyses revealed that the systemic vulnerability is substantially affected when the interdependencies are taken into account. Quantitatively, the comparative study showed that the failure probability of the water distribution network dependent on the EPSS was 1.66 that of the standalone (independent) water network.

For the hurricane natural disaster, Winkler et al. (2010) developed a new methodology incorporating hurricane damage prediction and topological assessment to characterize the impact of hurricanes upon EPSS reliability. The failure probability for standalone components within both transmission and distribution of EPSS were predicted using a fragility model. The damage model was calibrated using the component failure data of EPSS for Harris County, TX, USA caused by hurricane Ike in September of 2008, leading to a mean outage prediction error of 15.6% and low standard deviation. The hurricane reliability of three topologically distinct transmission networks was then assessed under simulated hurricane scenarios. The results demonstrated that the rate of system performance decline is contingent on its topological configuration. Meanwhile, reliability is found to correlate directly with topological features, like network meshedness, centrality, and clustering. Particularly, although it may add to the vulnerability under random failures, the compact irregular ring mesh topology is identified to be exceptionally favorable to reducing the EPSS hurricane risk.

As noted hereinbefore, EPSS was also shown to be susceptible to random technological failures as well as to intentional attacks.

Zio and Sansavini (2011) considered the viability of the component criticality indicators for a realistic-size EPSS measured by their contribution to cascading failures. Three different models of cascading failures were considered with regard to the principle for redistribution of the failure load as well as the triggering event. The rankings acquired by the different indicators were compared with the classical centrality measures. It turns out that the degree and betweenness centralities, which suggest the number of connections to a particular component and the number

of shortest paths passing through that component, respectively, play a major role in determining those network components that contribute most to the failure propagation. For the models of local propagation of a fixed amount of load and of redistribution of the failure load, the degree centrality measure becomes dominant for the cascade process, with the betweenness centrality measure presenting complementing information given the intense coupling among components. Regarding the model of cascading failures propagated by the redistribution of the shortest paths, it was found that the betweenness centrality measure can only partially identify those components contributing most to large-sized failure cascades.

2.3. The emergent concept of resilience for civil engineering structures and infrastructure systems

Natural disasters, such as earthquakes, floods and high winds, can cause severe damage to the community built environment and disrupt the social and economic functions of a community for a long time after a disaster. Against this backdrop, considerable research focus has shifted to the resilience of communities and their CIs, as it has become clear that the sound and quick recovery in the post-disaster stage is at least as critical as the disaster robustness to the disaster survival and continued post-disaster development of a modern urban community.

Resilience is a concept developed in the 1970s (Batabyal 1998). The United Nations emphasized the resilience and risk management of urban communities exposed to natural hazards (Board on Natural Disasters 1999). From a dictionary, resilience is "the ability to recover from (or to resist being affected by) some shock, insult or disturbance" (Klein et al. 2003). In 2005, community resilience was highlighted in the World Conference on Disaster Reduction (WCDR) and proposed as the new roadmap for the sustainability and security for modern communities (International Strategy for Disaster Reduction 2005). Manyena (2006) examined the connotation of resilience in terms of definition, its relationship with the notion of vulnerability, and its application to the subject of disaster management and risk reduction. According to his suggestions, resilience could be deemed as the "intrinsic capacity of a system, community or society predisposed to a shock or stress to adapt and survive by changing its non-essential attributes and rebuilding itself". Menyena (2006) also found that vulnerability is closely related to the degree of resilience, yet also complementary to system preparedness.

More recently, Cutter (2013) highlighted the significance of the strategies to build resilience as the viable roadmap to sustainability. From the political point of view, the path to disaster resilience entails the collective efforts of all the societal sectors. She further suggested that it is technically and economically imperative, to shift our focus to forging the long-term resilient community, from the disaster contingency response.

2.3.1. Development of the concept of seismic resilience

Recent earthquake disasters, e.g. the 2011 Tohoku earthquake, have re-emphasized the need for the earthquake engineering profession and the public policy makers to define earthquake disaster resilience and take measures to improve the seismic resilience of modern urban communities. Comprehensively and conceptually, Norris et al. (2008) provided the definition of community resilience as a process encompassing a set of adaptive capacities to back to the required functionality after the disruption. Community resilience would be built on four primary sets of adaptive capacities---Economic Development, Social Capital, Information and Communication, and Community Competence---that together serve as a strategy for disaster preparedness.

In earthquake engineering, Bruneau et al. (2003) proposed a broad definition of resilience to cover all actions that reduce losses from hazard, including effects of mitigation and rapid recovery. They defined the earthquake resilience of the community as "the ability of social units (e.g. organizations, communities) to mitigate hazards, contain the effects of disasters when they occur, and carry out recovery activities in ways to minimize social disruption and mitigate the effectors of future earthquakes". The authors suggested that resilience could be conceptualized along four dimensions: technical, organizational, societal and economic (TOSE). The two components, technical and economic, are related to the resilience of physical systems, such as lifeline systems and essential facilities. The other two components, organizational and social, are more related to the community. This framework was further developed to consider the operational and physical resiliency of acute care facilities (Bruneau and Reinhorn 2007). The relationship between structural seismic performance, fragility, and resilience was explored. This made possible to propose the general tool to quantify the resiliency for sociopolitical-engineering decision.

Kröger and Zio (2011) investigated the resilience of the engineered CIs. They pointed out that the CI system disaster resilience could not be considered using only traditional analytical methods of system decomposition. Instead, a new framework that incorporates a range of methods capable of examining the resiliency from perspectives of topology, functionality and others is needed.

Ouyang et al. (2012) put forward an assessment model for the disaster resilience of CI systems. To achieve this objective, the total functionality loss was considered as the measure, and was quantified throughout the disruptive events, which are classified into the "disaster prevention", "damage absorption" and "recovery" stages in the time domain.

Deco et al. (2013) put forward a probabilistic method for the assessment of seismic resilience of bridge structures. Based on such model, the initial damage induced by the seismic load was evaluated by the fragility functions. Subsequently, a probabilistic six-parameter sinusoidal-based function with considering the target level of resilience, as well as the corresponding costs, was employed to shape the recovery path of the global structure. Similarly, HAZUS (2015) also came up with a host of dataset quantifying the recovery time in terms of different desired performance level, for the damaged civil engineering facilities.

Chang et al. (2014) developed a methodological approach which can be applied to reduce risks associated with the Infrastructure Failure Interdependencies (IFIs). In order to address the range of challenging issues of IFIs---the discrepancies between infrastructures' private interests and the broader societal interests, obstacles in information sharing and the lack of chance for experience learning---this approach focused on both the development of regional risk information and the infrastructure organizations. According to the results of the case study, the importance of cross-sectoral communication to community resilience was highlighted.

Michel-Kerjan (2015) highlighted the significance of resilience, given the sheer challenge for the prediction on the extreme weather events. He further proposed a "5-C" metric, which includes physical, financial, human, social and natural capitals. Based on the collected data on those five dimensions, the policy-making can be tested with reference to the improvement on the resilience of urban systems.

Mieler et al. (2015) put forward a performance-based engineering framework for design and evaluation of the built environment to improve the overall resilience of communities under seismic hazards. The regulatory framework for nuclear power plant system was adapted for a community setting. Therefore, a consistent performance targets for the set of various subsystems as well as the community components could be established based on the seismic resilience performance goals set at the community level.

Most recently, Cimellaro et al. (2016) developed a framework to assess community resilience at different spatial and temporal scales, termed as PEOPLES. In such framework, a set of dimensions have been incorporated to enable the measurement on the systemic resilience in both emergency and the longer-term restoration phases.

2.3.2. Implication of resilience on the seismic design of structures

Owing to the comprehensive developments of earthquake engineering throughout the past decades, the currently employed design codes have enabled engineers to design structures at a host of seismic safety levels per different requirements of the users. Nevertheless, for the majority of the design codes around the world, the primary design objective is preventing the global collapse of the structural system under strong earthquakes so as to maintain life-safety of the inhabitants (ICBO 1997, GB 50011-2010 2010). In order to achieve such design objective, ductile earthquake-resistant structural systems have been widely adopted. A ductile structural system is expected to undergo large (plastic) deformations without collapsing and without a substantial loss of load-carrying capacities in response to design-level and beyond-design-level earthquake ground motion.

Such structures do not collapse but, because they dissipate the input seismic energy through large plastic deformations, tend to suffer extensive damage in large earthquakes. The functionalities associated with those structures is, therefore, significantly disrupted. Moreover, after many recent

earthquakes, the physical damage sustained by those structures was often too large to be reparable (Mitchell et al. 1996, Ye et al. 2008). Consequently, many damaged engineered structures would not effectively serve the users and can only be torn down.

Continuity and recoverability of the functionality of structures are crucial for the well-being and revitalization of modern urban communities following earthquake hazards. Against this backdrop, so-called resilient structural systems have gained widespread attention in the earthquake engineering profession and are being recognized as the powerful solution to overcome the shortcomings associated with the current design codes. As mentioned hereinbefore, resilient structures are expected to avoid the irreparable damage or collapse under strong earthquakes. Besides, such structures can bounce back after a disaster and deliver their functions without enormous monetary or technical investments and prolonged repair.

Among several newly-devised seismically resilient structural systems, base-isolated structures stand out as quite practical and feasible. As shown in Figs. 2.3 (a) and (b), compared with the traditional structures, a set of isolation bearings is placed so as to decouple the superstructure (of the base-isolated structural system) from its substructure. Hence, the integrity of the superstructure can be effectively protected. In addition, the potential seismic damage can be repaired fast, and the functionality of the structure can therefore be restored quickly (Naeim and Kelly 1999).

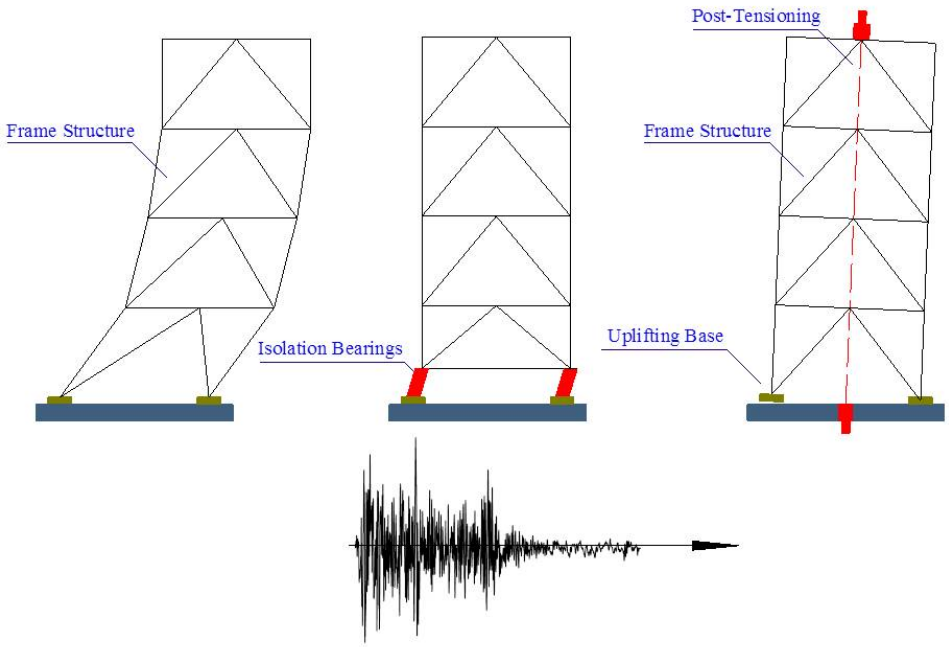

(a) Traditional (b) Base-Isolated (c) Rocking/Self-centering

Fig. 2.3. Resilient structural systems

More recently, another type of structural systems, namely, the rocking/self-centering structures, have emerged as another promising way to achieve seismic resilience. As illustrated in Fig. 2.3 (c), rocking systems allow the structure to uplift and rock (relative to its foundations) under strong earthquake ground motions, and re-center themselves after an earthquake. According to a series of experimental studies, post-tensioning tendons can be added into the structure to enhance its performance (Eatherton and Hajjar 2014, Blebo and Roke 2015). Rocking system can effectively dissipate the input seismic energy, while the serviceability of the structure can be largely maintained and continued after an earthquake making rocking a viable seismic response modification strategy for existing and newly-built structures (Midorikawa et al. 2006, Wada et al. 2009).

2.3.3. Studies on the resilience of the EPSS

Large economic losses and remarkable social disruptions after recent large earthquakes also highlight the significance of comprehensive and in-depth research into the seismic resilience for EPSS, as well as other CIs (Zio 2016). Cimellaro et al. (2014) proposed an evaluation method to gauge the resilience behavior of urban communities affected by natural disasters, considering CI interdependence. To this end, the resilience index of each CI system alone was evaluated first. The resilience indices of the set of individual lifelines were then combined by the weight coefficients that were obtained on the basis of a matrix of interdependence calculated for each region under investigation. The resilience index of that particular region could, therefore be evaluated by multiplying the resilience of each lifeline by its corresponding weight coefficient and adding the results obtained for all subregions. According to the case study conducted on the data collected after the March 11 2011 Tohoku Earthquake in Japan, it was found that the newly developed methodology is unbiased and capable of identifying the crucial CIs and their damage.

Franchin and Cavalieri (2015) put forward a probabilistic assessment paradigm for the seismic resilience of CI systems, whereby the effect of different influential factors, such as the randomness associated with seismic scenario, physical vulnerability of the examined CI system and functional consequences, can be taken into account. A case study was conducted on a representative synthetic urban system, while a corresponding sensitivity analysis was also carried out. The research results indicated that the resilience of the community system was captured well, conditioned on the initial damage.

Hu et al. (2016) investigated the disaster resilience of CIs by focusing particularly on their recovery process from localized attacks. The influence of different repair strategies on the systemic resilience was studied in comparative studies. It is well recognized that random localized attacks usually do not traumatize the CI system, as much as malicious attacks usually do (Bilis et al. 2013). When it comes to the recovery, counterintuitively, it was found even more difficult to restore the CI system after localized attacks. In this study, three different kinds of strategic repair approaches, namely, greedy recovery (GR), preferential recovery based on nodal

weight (PRNW) and periphery recovery (PR), were enumerated and considered. Specifically, GR is set to repair the damaged links in order by which the network restores the largest network functionality in every time step. Correspondingly, PRNW will preferentially repair those edges connecting the isolated nodes serving the largest population to the functional component within the network. Finally, PR will prioritize the isolated node with the largest population on the repairing list. In addition, random recovery (RR) was also examined as the baseline strategy. Based on the research outcome, it was found that strategic recovery approaches, especially PRNW and PR, were far more effective. By comparison, RR was revealed to be unable to restore the functionality of the system in a satisfying manner. The proposed PRNW exhibited a low computational complexity and a high efficiency in terms of connecting the most populated regions in a quick manner. It can be employed as the practical protocol for the resource allocation to optimally shape the recovery process, by significantly shortening the needed time to restore system function and reduce the associated losses, especially for CIs under where earthquakes induce damage similar to random localized attacks.

Mensah and Duenas-Osorio (2016) developed a resilience assessment framework as the effort to establish a computationally efficient algorithm for quantifying the response of EPSS under hurricane hazards, while reviewing its applicability to large real systems by encompassing hazards, physical responsive behavior, and the restoration processes. To this end, a Bayesian network was utilized to model the transmission system responses so the associated probabilistic dependencies can be depicted in a figurative and tractable manner. It propagated hurricane-induced damages across the power system to service customers considering the physics and the constraints of electric power flow. The framework quantified customer outages in distributed blocks liked by the radial distribution feeders throughout the entire system, and shaped system restoration based upon the resource mobilization practices and a set of prioritization sequences. The conducted case study on EPSS of Harris County, Texas, under Hurricane Ike in 2008 substantiated that the proposed framework could yield system responses that match the actual outages recorded following the event quite well. Meanwhile, the computational efficiency for this framework was increased notably compared with the previous impact assessment model. More importantly, study on the example EPSS confirmed that that resilience-driven restoration strategy can hugely improve the system-level functionality, especially in the aftermath of hurricane events.

Via *in situ* observation, Krishnamurthy et al. (2016) studied the impact of the interdependence on the resilience for EPSS during the real-world seismic events, namely, the 2011 M_W 9.0 Tohoku earthquake in Japan and the 2010 M_W 8.8 Maule offshore earthquake in Chile. The interdependences between EPSS and telecommunication network were focused on. The analysis was carried out by collating time series of the physical damage inflicted by EPSS and telecommunication system damage, outages, and service restoration as field-collected in the areas affected by the respective earthquakes. The metrics used for the comparison, namely the dependence predominance and the restoration delay index, were based on cross-correlation functions and a measure of dependence predominance based on the peak cumulative cross-correlations and dominant restoration times between the two infrastructure networks. Results

corroborated that there is indeed a strong coupling between the restoration of power and telecommunication infrastructure systems in both events. For instance, the power system outage restoration process in Japan led the restoration of mobile communication networks more quickly than that of landline telephony systems, confirming similar observations from Chile. In both Chile and Japan, the landline and mobile system restoration processes tended to occur together, likely due to infrastructure collocation in the switching centers and common transmission links. The trends from these two events provide evidence of significant and asymmetric dependence of communication systems on power supply infrastructure, indicating the need for novel technological alternatives, such as micro-grids, to improve communication networks performance during disasters and set the foundation for future disaster-resilient smart grid systems.

Nan and Sansavini (2017) proposed a quantitative framework for the assessment of resilience of CIs. Within such framework, the absorptive, adaptive, and restorative resilience capabilities were investigated. Meanwhile, different measures and phases associated with these capabilities were also considered. Two components, namely, an integrated metric for resilience quantification, and a hybrid multi-layer modeling approach to capture and quantify the system performance across interdependencies constituted the framework. Three resilience improvement strategies were proposed accordingly, each of which focuses on the improvement of a particular resilience capability, i.e. improvement of the repair efficiency, improvement of human operator performance, and improvement of remote terminal unit (RTU) battery capacity, of the considered system. In order to validate its granularity, the framework was then applied to a case study with accounting for the developed system improvement strategies. The results offered a set of revealing perceptions for decision-makers. Primarily, it indicated that the largest enhancement in the system adaptive and restorative capability would be achieved by improving repair efficiency. Correspondingly, growth of the human operator performance and RTU battery capacity would have the most significant impact on enhancing the system absorptive capability. The hybrid multi-layer approach proved to be effective in capturing the influence of interdependencies, as well as quantifying the coupling strength between interdependent CIs by modeling their functional behaviors. The simulation results also revealed that the System under Control and Supervisory Control and Data Acquisition within EPSS are closely interdependent. Besides, it was further suggested that the physical dependence has deeper impacts on the systemic resilience, compared with informational dependence. The advantage of the proposed approach was also demonstrated to be representative of different layers throughout EPSS with proper method presenting their operations and physical and functional diversities. Enhancements in different sub-systems can be measured by their effects on the performance of the global system, within this developed approach.

Fang and Sansavini (2017) established a tri-level planner-attacker-defender model to frame the optimally combined plan for the investments on capacity expansion and switch installation across EPSS. Such model integrated long-term system planning for transmission expansion, with the short-term switching operations as the response to disruptions. Essentially, the optimum investment plan was set to minimize the weighted sum of the nominal costs, i.e. investment,

operating costs, and the maximum loss of functionality due to the targeted attacks. The mixed-integer optimization was solved by decomposition via two-layer cutting plane algorithm. Numerical results on a benchmark EPSS revealed that only small amount of investments in transmission line switching can improve resilience by adapting to disruptions through system reconfiguration. Sensitivity analysis showed that the transmission planning under the assumption of small-scale attacks would result to the most robust strategy, i.e. the minimum-regret planning, if many constraints and limited investment budget affect the planning. Correspondingly, the assumption of large-scale attacks would provide the most robust strategy as the planning process is involving large flexibility and budget.

Pilot research efforts have already been carried out to examine the physical and informational behavior for micro power grid (MPG) and smart grid (SG) solutions to enhance CI system natural hazard and technological failure resilience.

Kwasinski et al. (2012) examined the operational behavior of MPG during natural hazards and their aftermath. Two strategically critical component groups, namely, the distributed generators as well as the local energy storage that ensure the availability of MPG, were particularly focused on. Both theoretical analysis and the corresponding Monte Carlo simulations demonstrated that under natural hazards, MPGs could achieve more reliable availabilities compared with the conventional EPSSs, and therefore render them a promising strategy for the development of advanced smart grids. Additionally, local energy storage and various energy sources were also needed in order to realize the higher availabilities. On the other hand, the application was found to be restrained by the huge economic as well as the technical cost.

Pournaras et al. (2014) studied the robustness of SGs which is potentially challenged by the unpredictably surging electric power peaks, or temporal demand oscillations that can cause blackouts and increase the supply costs. In this sense, planning for the demand was put forward as a practical strategy to mitigate those effects and increase the systemic robustness. Very likely, however, such operational goal might be achieved at the expense of the comfort of the consumers served by the power grid. In order to cast light on this dilemma, a decentralized agent-based model that quantified and balanced the trade-off between robustness and discomfort under demand planning was developed. Eight selection functions were experimentally assessed using real data from two operational SGs. These functions offered different quality of service levels for demand-side energy self-management that accounted for both robustness and discomfort criteria. The experimental validation with real data substantiated the load-shifting and load-adjustment potential of those various selection functions, and also their discomfort impact on the consumers.

As the follow-up and complement, Pournaras and Espejo-Uribe (2017) recently investigated the pathway to increase the performance robustness of SGs by means of maintaining the supply capacity of the system under disruptions. It was expected that the introduction of active devices, like smart transformers, driven by intelligent software and networking capabilities, would bring vital chances for the real-time online automated control and regulation. It was, however, difficult to mitigate the disruptions like cascading failures. So far, the local intelligence by itself cannot

appropriately cope with such complex collective phenomena with domino effect. The intelligently coordinated and prompt mitigation action was required. To this end, two optimization strategies for the self-repairable SGs were proposed and examined. These strategies aimed at establishing the coordination mechanism for smart transformers that runs in three healing modes and exercises collective decision making of the phase angles in the conductor of a transmission system to improve the network reliability under disruptive events. The conducted experimental assessment employing the self-reparability envelopes in different case networks, AC power flows and different number of smart transformers revealed that the self-repairing reliability and capability of the SG network would be improved proportionately to the number of deployed smart transformers participating in the coordination.

2.4. Network science-based seismic resilience of integrated critical infrastructure-community systems

As a typical geographically embedded system, CIs are entities whose networked nature renders them appropriate for mathematical analysis by means of the concepts and tools from network science (Duenas-Osorio et al. 2007). A flurry of research has been conducted on this particular subject.

Buldyrev et al. (2010) studied how the local failure inside one CI network would evolve and bolster the global collapse across the entire system of the interdependent CI networks. Illuminated by the real-world example of such concurrent malfunction, namely, the full-blown blackout that affected much of Italy on September 2003 (which has been elaborated hereinbefore in the Section 2.1.2), a framework for capturing the robustness of interacting networks under such cascading failures was established. An exact analytical approach tracking the path for how the critical fraction of nodes that, on removal, would induce a failure cascade and lead to the complete disintegration of two interdependent networks, was developed. It was demonstrated that a broader node degree distribution would increase the vulnerability of interdependent networks to random failure, which was just opposite to the behavior of a single network.

Brummitt et al. (2012) examined the effect of intertwining among CI systems in terms of the cascading behaviors for the interacting systems. Enlightened by cascades of load shedding in the integrated EPSS and other CI, the Bak-Tang-Wiesenfeld sand-pile model on modular random graphs and on graphs based on actual interdependent EPSSs were studied. Starting from two isolated networks, it was shown that adding some limited amount of connectivity between them would be conducive, on the ground of its ability to suppress the size of largest cascading events in each system. Too much interconnectivity, however, became deleterious as overly dense interconnections laid the paths for neighboring networks to inflict large cascades. Furthermore, as in real CIs, new interconnections would increase capacity as well as total possible load, and therefore contribute to even larger cascades. Ultimately, based on a multi-type branching process and simulations, it was indicated that the interconnectivity among CIs should be set on an

optimized level in order to avoid the devastating global cascade while maintaining the functionality of the integrated CI systems.

Correspondingly, follow-up research conducted by Schneider et al. (2013) further investigated the approach to determine the set of autonomous nodes so as to optimize the robustness of coupled networks. The obtained finding revealed that the betweenness and the degree distribution should be viewed as the paramount parameters for the selection of such nodes. Particularly, the former was found to be the most effective for modular networks. Considering the case of the 2003 Italian blackout event, it was demonstrated that the protection for only four communication servers with highest betweenness could reduce the chances of catastrophic failure. As this strategy was adopted, the resilience to random failures or attacks was remarkably improved. Meanwhile, the fraction of autonomous nodes necessary to change the nature of the percolation transition, from discontinuous to continuous, was notably reduced as well. Moreover, it was also shown that even for those networks with a narrow distribution of node degree, their robustness can be substantially improved by aptly choosing a small fraction of nodes to be autonomous.

Helbing (2013) looked into how components whose behavior was easily manageable or even harmless, can still pose unpredictable and uncontrollable systemic risks, when closely intertwined together. The improper design or operation of the global socio-economic system laid the foundation for the catastrophic failures. In other words, current law may not treat situations well, as the core problem did not root in the behavior of individual components, yet in the interacting mechanism among them. Meanwhile, with respect to the looming notion that ‘big data’ can potentially help to make the anthropogenic networks more predictable and controllable, in light of the capacity for the real-time management to overcome malfunction induced by the delayed feedback or miscommunication, he argued that too much data, however, can also make it more challenging to sift those reliable from the huge amount of incorrect information. Misinformed decision making can still emerge consequentially. Overall, the ever-increasing interconnections within the globally integrated modern society have created pathways for catastrophes to spread rapidly and pervasively. This renders the sophisticatedly networked socio-technical systems vulnerable on a planetary scale. A globally participatory approach, he believes, would be a strategically momentous issue to study to tame cascading effects across CI networks, and help to mobilize the collective effort needed to increase the resilience for the entire IC system.

2.5. Knowledge gap

The resilience of modern EPSS is a transdisciplinary research domain encompassing engineering, complex networks, computational science, economics, and also social sciences (Brummitt et al. 2013). The sections of this chapter present a comprehensive review of the research to model and explain the vulnerability and resilience of EPSS to catastrophic natural, technological or man-made disruptions. Owing to those endeavors, some important insights into how to increase the disaster resilience or EPSS were gained. Nonetheless, given the soaring electric power demand

around the world, and the increasing EPSS complexity and interdependence, the existing knowledge is still insufficient to enable build enduring, reliable and resilient EPSSs. To this end, it is imperative to address the following issues：

1. The resilience quantification frameworks proposed to date addresses the ability of the civil infrastructure system to function and provide service, i.e. to supply the community. The demand on the supporting civil infrastructure systems generated by the community functions is assumed to remain unchanged. This is, however, not true in many the real-world cases. Moreover, the gross functionality loss is difficult to evaluate, as the recovered system functionality level is dynamic and case-specific, and will not necessarily be the same as that at the pre-shock level. In this sense, a resilience quantification framework should be established to track both the supply of the CI service and community functionality demand for this service from the time of the disaster to the end of the recovery, so as to measure the disaster resilience of the integrated Urban Community-Critical Infrastructure system in engineering, societal and economic ways.
2. The currently employed frameworks modeling the recovery for the CI networks ensuing catastrophic disruptions are mainly based on the so-called Recovery Functions (RFs) on either the component or the system level. Such approach, although practical, involves a set of shortcomings. Specifically, some of the decisive parameters for RFs, e.g. the duration for the entire recovery or the functionality evolution trajectory, are usually pre-defined based on experience or engineering judgment. In order to make up for these deficiencies, an adaptive framework should be established, whereby the systemic recovery behavior could be modeled in a more rational way by accounting for the case-specific characteristics of the CIs and the community repair resources.
3. As already indicated by the some of the research hereinbefore, there is a significant and profound influence of the status of the other CIs on the EPSS component and system repair during the post-earthquake recovery phase. Such interdependence between different CIs should also be taken into account to examine the impact on the resilience of EPSSs.
4. In addition to the preceding point, available and mobilizable repair resources and their distribution to different repair tasks during the recovery stage also plays a large role in terms of the resilience of EPSS. The influence of this factor should also be considered and quantified.

3. Seismic Resilience Assessment of EPSS-Community System

As presented in Chapter 2, EPSS is the bedrock of modern urban communities, and its seismic resilience is critically important for the post-earthquake recovery and continued development of urban communities. It is anticipated that a resilient EPSSs reduce the effects of large disasters on a community by providing the energy resource for a quick and stable recovery (Lundberg and Johansson 2015). Unlike robustness, it has been widely consented that the systemic resilience of engineering assets should be examined as the time-varying process, rather than an instantaneous state (Michel-Kerjan 2015).

In Section 3.2 of this Chapter, the existing supply-based seismic resilience quantification frameworks are reviewed firs. A novel compositional resilience quantification framework based on simultaneously tracking the service supply from a CI and the demand for service from the served community throughout the post-earthquake recovery period, is proposed thereafter. Besides the physical functionality loss, an often-used measure of CI seismic resilience, a new resilience measure focused on gauging resilience from the socio-economic point of view is proposed.

Similar to the well-known seismic fragility/vulnerability functions (Porter 2003), probabilistic recovery functions RFs are crafted to quantify the probability that the functionality of the object under consideration will be restored after a certain recovery time, given the damage state induced by the earthquake. RFs have been employed in seismic resilience quantification frameworks developed to date to mode the functionality recovery trajectory for either the component or the global network (Deco et al. 2013). While the RFs are practical and tractable, as they generalize all the influential factors to a few dominating parameters, they conceal the underlying complexities of the post-earthquake recovery process. Recovery of EPSS components depends not only on their damage state, but also on the amount and availability of the repair resources and the repair priority plans put into effect by the CI operators and the community. Establishing a "blanket" RFs at the EPSS level is not possible because the system recovery is contingent on the component recovery as well as the EPSS network topology and the electric power dispatch strategies implemented by the EPSS operator after an earthquake. Meanwhile, there is a profound influence of the state of other CIs, e.g. the transportation system, on the EPSS component and system repair activities during the post-earthquake recovery phase. Consequently, there are remarkably few RFs available in the literature (HAZUS 2015). Finally, as opposed to seismic vulnerability functions, it is quite difficult to validate and calibrate the proposed RFs, given the meagerness of post-earthquake recovery data.

In order to address this challenge, a novel approach to develop model-based RFs is proposed in Section 3.3 of this Chapter, with the goal to dissect the complexities associated with the seismic recovery process of EPSS-Community system. This approach is based on the Agent-Based Model (ABM) paradigm (O'Sullivan and Haklay 2000). Specific agents representing the actors in the EPSS repair process, namely, the Operator of the EPSS and the Administrator of the community,

are instantiated and the rules that govern the interaction among these agents are defined. The proposed framework is then exemplified in a case study, where parameter variations are carried out to examine the influence of different agent behavior characteristics and the earthquake intensity on the EPSS supply recovery rate.

Using the ABM RFs and the compositional resilience quantification framework, the following questions can be answered:

1. How does the recovery of EPSS-Community system evolve across the post-earthquake phase?
2. How do the parameters and the interaction among different agents shape the recovery path?
3. How can the resilience of the integrated EPSS-Community system be improved?

In Section 3.3, the application of the proposed seismic resilience quantification framework and the agent-based recovery model to a virtual EPSS-Community system is presented. The topology, the parameter distributions, the seismic contingency dispatch strategies as well as the systemic resilience measures are presented. Section 3.4 discusses the resulting seismic resilience of example EPSS-Community system under different earthquake scenarios and the interaction patterns between the agents. Section 3.5 reviews the main findings and points out the possible future research topics.

3.1. Supply-Demand resilience assessment framework

3.1.1. Functionality loss framework

Following the conceptual seismic resilience assessment framework established by Bruneau et al. (2003), Ouyang et al. (2012) put forward a model for assessing the functionality loss of the affected CI.

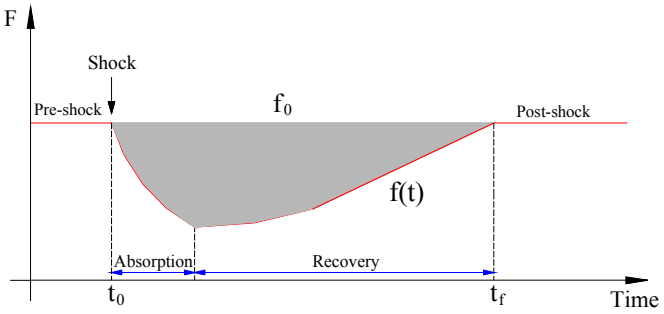

Fig. 3.1. Seismic resilience quantification based on functionality loss (Ouyang et al. 2012)

Based upon such model, the gross resulting functionality losses can be utilized as a direct measure of seismic resilience (more accurately, loss of resilience) of a CI. The time after an earthquake can be divided into three phase, namely, the absorption, the recovery and the post-shock phase, as shown in Fig. 3.1. Specifically, after a damaging earthquake, the immediate damage is, in most cases localized, but may sometime propagate further due to possible cascades within a CI or among the inter-dependent CIs. Hence, the deliverable CI functionality may take some time to reach the post-disaster minimum, indicating the end of the absorption phase. Thereafter, the CI will start to recover its functionality, until it stabilizes at a new, post-shock level. The time scales of the absorption and the recovery phases are very different (hours vs. days), especially after catastrophic earthquakes (Ge et al. 2010, Iuchi et al. 2013) when the recovery phase may take years. Based on the tracked functionality path during both the absorption and recovery phases, the gross functionality losses (GFL) can be measured as the shaded area illustrated in Fig. 3.1. Mathematically, it is realized in Equation 3.1, where f_0 and f(t) refer to the pre-shock functionality level of the CI system and its time-varying functionality throughout the absorption and the recovery phases, respectively.

$$\text{GFL} = \int_{t_0}^{t_f} (f_0 - f(t))dt \qquad 3.1$$

The functionality loss resilience quantification framework, presented above, is straightforward and feasible, in particular for standalone civil engineering structures. It might be, however, problematic for a CI system, or even a system of CIs. First, the demand for the function of the CI (the service provided by the CI) from the urban community it serves is assumed to remain unchanged, which is usually not true after natural disasters like earthquakes. Second, the gross functionality loss is difficult to evaluate as the system level, given that the boundaries of the CI and the community are difficult to define. Third, the functionality of the CI, as well as the functions of the community, in the post-shock phase may not necessarily be the same as those before the shock. For example, the functionality level of an "adaptive" system (Linkov et al. 2014) can be higher after the shock than that before the shock. In this case, the shaded area in Fig. 3.1 is not well defined, suggesting that there is a functionality gain, which can be misleading for resilience assessment and the associated decision-making. Similarly, in case of a "ductile" system (Linkov et al. 2014), whose functionality cannot be restored to the pre-shock level but still exists, Equation 3.1 results in an infinite functionality loss, which is not informative neither.

3.1.2. A supply-demand resilience quantification framework

To resolve these shortcomings, a novel compositional resilience quantification framework based on simultaneously tracking the service supply from a CI and the demand for service from the served community throughout the post-earthquake recovery period, is proposed By and large, the difference between the supply and demand for the service provided by the CI is stable under

normal operation conditions. But during and after the catastrophic earthquakes, this kind of balance will be disrupted and needs to be rebuilt through a sustainable recovery path, and then stabilized at some level.

In this framework, the supply and demand are separately tracked across their own "absorption" and "recovery" phases, respectively. It should be noted that, similar to the power supply under seismic events, the demand from the affected community will also decrease since many users, like factories, schools as well as residential buildings area also damaged or possibly destroyed. Besides, other community CIs are also affected by the earthquake. As the consequence, the lives of community inhabitants are severely disrupted, to the point that some are temporarily displaced. Therefore, a considerable part of the pre-shock demand will be lost in the absorption phase.

The recovery of the supply and the demand can follow very different paths in the recovery phase. Generally, the demand recovery rate tends to be slower than that of the supply, and can become faster only if more resources are devoted to rebuilding the buildings of the community. In addition, the business activities cannot restart until the CIs (not only EPSS) and the basic public services have been restored.

As shown in Fig. 3.2, the an equivalent of the gross functionality losses for an EPSS-Community system after an earthquake is quantified by measuring the cumulative electric power deficit *PD(t)* over the time periods when the distributed electric power supply *DP(t)*) is insufficient to cover the demand for electric power *D(t)*.

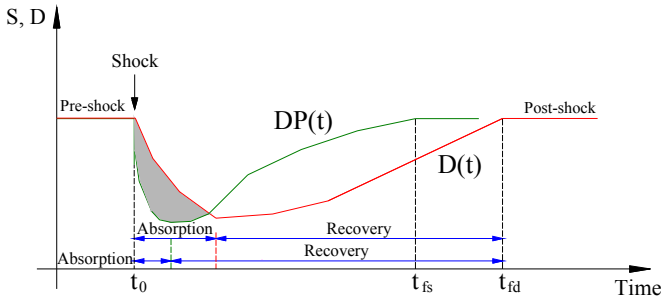

Fig. 3.2. Electric power supply and demand tracked during absorption and recovery phases

The EPSS system-level gross functionality loss is computed by adding the power deficit experienced at each of the *n* distribution nodes of the EPSS.

$$GFL = \sum_{i=1}^{n} PD_i \qquad 3.2$$

The power deficit at each EPSS distribution node is obtained by aggregating the gap between the supply and demand (when the latter is larger than the former) during both the absorption and recovery phases.

$$PD_i = \sum_{k=1}^{m} \int_{t_{k,0}}^{t_{k,f}} (D_i(t) - DP_i(t))dt \quad 3.3$$

In Equation 3.3, m is the total number of intervals where $D_i(t)$ is larger than $DP_i(t)$, throughout the entire disruptive event. Correspondingly, $t_{k,0}$ and $t_{k,f}$ refer to the start and the end points of each such interval, respectively. For each distribution node i, $D_i(t)$ quantifies the gross power needed from all the user across all the communities severed by it.

Meanwhile, following the operational constraints of the EPSS, $DP_i(t)$ refers to the sum of the available power from all reachable generation substations (the red squares in Fig. 3.3). It should be noted that the produced power in those generation substation is delivered to cover the demand from the reachable distribution nodes (the hollow blue circles in Fig. 3.3) based on the adopted power dispatch strategy, and may not be available to cover the demand at distribution node i.

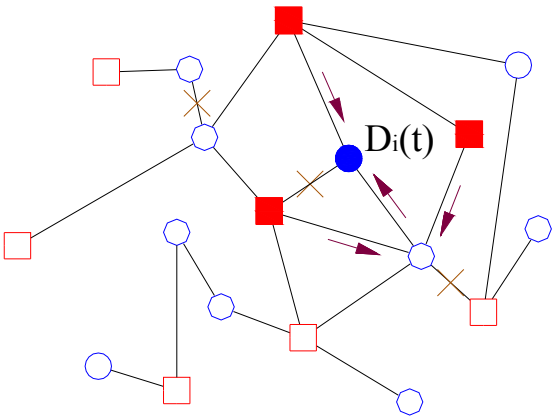

Fig. 3.3. Illustration for the deliverable power and power demand

3.2. Realization of the proposed supply-demand EPSS seismic resilience quantification framework

For an EPSS in normal operations, the total electric power supply capacity is designed to cover the community demand. A strategy for distributing the generated electric power to the consumers with the goal of minimizing the costs, maximizing the profits, and minimizing the risks to the network infrastructure while minimizing the risks of disrupting the balance of supply and demand (i.e. brown- and black-outs) is called the electric power dispatch (Morsali et al. 2014). The

balance between the supply and the demand can be disrupted due to damage from strong earthquakes.

The functionality of the EPSS-Community system is assessed by disaggregating this large-scale heterogeneous system into a set of supply and demand nodes while preserving their connectivity. The earthquake ground motion intensity measures (IMs) at the nodes differ and depend on their geographic location with respect to the earthquake epicenter. The geographic distribution of IMs at the EPSS-Community system node sites, and the earthquake scenario, is determined using ground motion prediction equations for a given earthquake magnitude and location of its epicenter.

3.2.1. EPSS-Community system functionality assessment in the absorption phase

Given an earthquake scenario, seismic fragility functions are used to evaluate the Damage State (DS) of each EPSS-Community system component conditioned on the earthquake ground motion intensity the component experienced. Specific fragility functions are adopted for each component of EPSS (e.g. transformers, switches, and circuit breakers) and communities (e.g. office and apartment buildings, factories, schools, hospitals) to represent their unique physical and societal behavior (Déle and Didier 2014). For simplicity, three damage states are considered, i.e. no damage (DS1), moderate damage (DS2) and extensive damage (DS3). Vulnerability of each component is then assessed by computing its remaining degree of functionality. In particular, no loss of functionality is assumed if a component is in damage state DS1, complete loss of functionality is assumed if the component is in DS3, and an intermediate interpolated degree of function loss is assumed for components in DS2. One such loss of functionality damage-state-based assignment is adopted in Sun et al. (2015a).

Decreased functionality of each node, on the supply or on the demand side, is determined individually, as specified above. Decreased functionality the EPSS-Community system at the end of the seismic damage absorption phase is computed by aggregating the functionality of the nodes using a model of EPSS operation, the seismic contingency electric power dispatch.

3.2.2. Recovery of the Community power demand

Once the earthquake damage is absorbed, the Community and the EPSS enter a relatively long recovery period. The post-earthquake recovery path of the electric power demand generated by the Community is affected many factors, e.g. the efficiency of the reconstruction of buildings and industrial facilities , the restoration of public services, as well as the societal norms and conventions. In the compositional resilience quantification framework, RFs are used to model the post-earthquake recovery path. As shown in Fig. 3.4, $RP_{DS2}(t)$ and $RP_{DS3}(t)$ RFs are sigmoidal functions of time in the recovery phase, formulated as lognormal probability distribution functions to satisfy the bounds and the monotonicity requirements. Following (Yang et al., 2012),

a random number $r \in [0, 1]$ is generated at any time point in time t during the recovery simulation process. If a component is in DS2, it is considered as fully recovered at time t if $r < RP_{DS2}(t)$. If a component is in DS3, it can recovery partially (to DS2) or fully (to DS1). Thus, the state of a component in DS3 is determined as follows: it recovers fully if $r < RP_{DS3}(t)$, it recovers partially, to DS2, if $RP_{DS3}(t) < r < RP_{DS2}(t)$, and it does not recovery if $r > RP_{DS2}(t)$. Once a damage state is determined, the functionality of a component is evaluated using a deterministic relation between the damage state and the functionality loss outlined in Section 3.3.1. Finally, the demand for electric power by a component of a Community is assumed to be directly proportional to its degree of functionality.

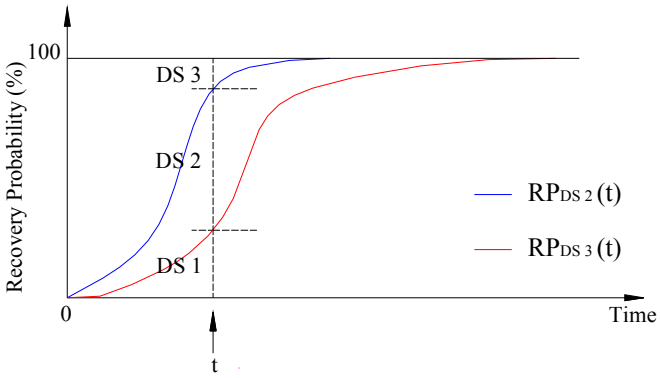

Fig. 3.4. Recovery functions for the EPSS-Community system components

To facilitate quantification of the seismic resilience of EPSS-Community system, the power deficit for different sectors of the society is tracked separately. To this aim, the community built inventory associated with the population through permanent or high intermittent occupancy, namely the residential buildings, the schools and the critical facilities such as hospitals, are combined into the *Population* sector, while the portion of the built inventory associated with production, such as industrial facilities and office buildings, are grouped into the *Factory* sector. The total demand at a distribution node i is:

$$D_i(t) = D_{p,i}(t) + D_{f,i}(t) \tag{3.4}$$

where $D_{p,i}(t)$ and $D_{f,i}(t)$ are the instantaneous demands from the *Population* and *Factory* sectors connected to the EPSS at distribution node i, respectively, at time t in the recovery process. Instantaneous demand depends on the initial damage and the rate of the recovery process of each component of the community built inventory, as well as on the occupancy type and quantity associated with that component. The initial damage state is determined as stated in Section 3.3.1, and the recovery process is modeled as stated in Section 3.3.2. The electric power demand is

computed considering the loss of functionality damage-state-based assignment proposed in Sun et al. (2015b).

The power delivered to the distribution node *i* is determined by the electric power dispatch strategy adopted by the EPSS operator. In normal operating conditions, the delivered power $DP_i(t)$ matches the demand $D_i(t)$ at each distribution node *i*. Further, when a distribution node supplies both the *Population* and the *Factory* sectors of the community, the supply is distributed to the two sectors proportionally to their demand. In emergency situations, such as after an earthquake, the power deliverable to a distribution node may be smaller than the demand at that node because of loss of power generation substations and transformers due to earthquake-induced damage and possible inability to transmit the available power through the damaged EPSS network because of transmission line capacity limits. Consequentially, the power deficit at the distribution node *i* is:

$$PD_i(t) = D_i(t) - DP_i(t) \geq 0 \quad (3.5)$$

If the distribution node *k* failed and is has not recovered at time *t* the power deficit is equal to the node demand, i.e. $PD_i(t) = D_i(t)$. The power deficit at node *i* is equal to zero when the delivered power equals the demand. For distribution nodes that supply both the *Population* and the *Factory* sectors of the community the power deficit is proportioned in the same proportion as the demand, namely:

$$PD_{p,i}(t) = PD_i(t) \times (D_{p,i}(t)/D_i(t)) \quad (3.6)$$
$$PD_{f,i}(t) = PD_i(t) \times (D_{f,i}(t)/D_i(t)) \quad (3.7)$$

At the level of the EPSS-Community system, the power deficit $PD(t)$, $PD_p(t)$ and $PD_f(t)$ are computed by summing up the corresponding distribution node power deficits (Equation 3.1).

3.2.3. Resilience Measure

Resilience of the EPSS-Community system in the proposed framework is quantified by counting the number of people without power at time *t* during the post-disaster recovery process. This is an instantaneous resilience measure.

At the distribution node *i*, the number of people without power $PwoP_i(t)$ is directly related to the power deficit of the *Population* sector of the community. However, the actual number of people without power after a strong earthquake is contingent on many different factors (e.g. casualties, rescue and evacuation of the population, post-earthquake aid and temporary housing, long-term post-disaster organization of the community) that are not contained explicitly in the proposed

framework. To estimate number of people directly affected by a power deficit at distribution node *i*, the following is assumed: a) if the transformers in the distribution substation failed, the entire population P_i served by this node is considered affected; b) otherwise, the number of people without power is proportional to the ratio of the power deficit $PD_i(t)$ and the power demand $D_i(t)$ associated with the population. It is further assumed that 65% of the power demand is directly consumed by the residents (Eurostat 2015) and the remaining 35% is consumed by other activities in the *Population* sector (e.g. transportation, food safety and preparation, heating or cooling, etc.). Therefore, for every operating distribution node *i* the percentage of population without power is:

$$PwoP_i(t) = (PD_{p,i}(t)/(0.65 \times D_{p,i}(t))) \times P_i \leq P_i \quad 3.8$$

where P_i is the number of people served with distribution node *i*. This number corresponds to the number of the built inventory components served by the distribution node *i* and the occupancy of these buildings. It is assumed that P_i remains constant during the entire recovery process, i.e. changes in the population (injuries, deaths, outflows and inflows due to evacuations, etc.) are not modeled.

At the EPSS-Community level, the number of people without power in the entire community is evaluated as $PPwoP(t)$, the percentage of population without power, calculated by summing the distribution node $PwoP_i(t)$ values at time *t* after an earthquake and normalizing by the total community population served by the EPSS.

3.2.4. Agent-based seismic recovery model of the EPSS supply

The post-earthquake recovery process of EPSS is stochastic and case-specific. This is due to the uncertainties in the earthquake magnitude and in the intensity of ground motion excitation at the locations of EPSS and community components, the vulnerability of these components, the preparedness of the EPSS and the community to affect the post-disaster recovery, the interconnections among different community and infrastructure systems, and the interaction among community administrators and infrastructure operators during the recovery process.

The extent of the EPSS-Community system functionality loss is assessed in terms of electric power deficit. The information about the system state and component condition is assumed to reach the EPSS operator in the immediate aftermath of the earthquake. The operator assess situation and, after a short period of time, the repair teams are dispatched to repair EPSS components and restore power supply following a certain prioritization strategy. The rate of EPSS component repair depends on the functionality of other civil infrastructure systems, namely the telecommunication and the transportation systems, which is, in turn, affected by the lack of

electric power, thereby inducing additional dynamics in the already complex EPSS-Community system.

For an EPSS in normal operations, the total electric power supply capacity is designed to cover the community demand, and the electric power dispatch is designed to minimize electricity costs and risk to the network infrastructure, as well as to maximize the EPSS profit. However, after strong earthquakes, it is likely that power generation and supply capacity cannot cover the demand from the served community. Therefore, the EPSS operator devises a Seismic Contingency Dispatch Strategy (SCDS) to distribute the available power resources to the consumers that can use electric power. Restrained by the inadequate power supply capacities, the operators first have to develop a "ranking list" (which can evolve over time) to decide which consumers should be prioritized, and which would be "sacrificed". This prioritization strategy is case-specific and it is established by making trade-off among societal, economic, political and sometimes even ethical considerations.

The EPSS recovery priorities and the SCDS might not necessarily reflect the needs of the community it serves. Therefore, the EPSS recovery process may need to be steered externally, by local community leaders, to ensure that community priorities are addressed. The actual recovery path results from the interplay between the EPSS and the community recovery priorities. In order to account for different priorities and behavior patterns of the involved player, the functionality restoration path of EPSS-Community system is modeled using an Agent-Based Model (ABM).

For simplicity and with no loss of generality, two principal players, the EPSS operator (hereafter Operator) and the local community leadership (hereinafter Administrator) are considered in this framework. The two-player framework can be easily extended to a multi-player one if the actions of additional entities that affect the recovery process are to be accounted for in the recovery process. The two featured agents act as follows:

Operator: The behavior of this agent is described by three attributes, namely Velocity, Efficiency and Tenacity, denoted as V, E and T_o, respectively. Specifically, V describes the average travelling speed of the repair team between two repair locations using the available roads, E quantifies the repair rate as the percentage of component functionality restored per day, and T_o refers to the degree with which the Operator agent is capable of executing its own repair plan priorities.

Administrator: The behavior of this agent is described by one attribute, the Tenacity (denoted as T_a) that quantifies the ability of the community leaders to enforce community repair priorities, and one (or more) community resilience measure threshold values.

Following an earthquake that disrupts the EPSS-Community system, the Operator agent starts the repair actions after an idle period needed for the emergency actions, EPSS state acquisition, and planning that includes the information about the state of other community infrastructure systems. The EPSS recovery plan reflects the balance of income and expenses deemed optimal from the business perspective of the EPSS owners. In this ABM, the tempo of the restoration is governed

by the Operator agent's V and E parameter values that can be considered as directly proportional to the cost of recovery.

Simultaneously, the recovery of the community power demand proceeds (modeled as described in Section 3.3.2). However, the recovery priorities of the community may be different than those of the EPSS. For example, the need for electric power in the most damaged regions may be essential for emergency rescue, medical care, water and food supply, and for sanitation, making a prolonged lack of electricity supply in certain areas undesirable. The community may have its own recovery performance objectives (SPUR 2009, Smith 2013) that quantify the state of the built environment and civil infrastructure systems, as well as high-level functions of the community (Mieler et al., 2015), during the recovery process and set a recovery timeline and milestones.

A periodic check of the community recovery milestones is implemented in the ABM through a comparison of one or more resilience measures to their threshold values at certain instances during the recovery process. If the rate of recovery is satisfactory, the EPSS operator is allowed to continue the recovery process following their own priorities. However, if the rate of recovery is too slow, the community may be able to enforce its recovery priorities by making the EPSS operator change its recovery plan. In this ABM, this process is implemented through the interaction between the Administrator and the Operator agents. Namely, if the rate of community recovery is not fast enough, the Tenacity T_a parameter of the Administrator is increased to make it more likely that the Operator will be forced to address the community recovery priorities. If this is the case, not only is the Operator recovery plan changed to address the community priorities, but the V and E parameters of the Operator agent are also incremented to model the increase in EPSS operator resources invested in community recovery.

In the framework proposed in this Chapter, the recovery of the EPSS-Community system is evaluated using the percentage of people without power *PPwoP(t)* described in Section 3.3.3. The rate of recovery is evaluated only once, at t=72 hours (three days) after the earthquake disaster (SPUR 2009, Smith 2013). This point in the recovery process is assumed to be critical for the success of the recovery process and is termed *Resilience Check Time* (Cimellaro et al. 2016). However, other resilience measures can be checked at one or more other instances during the recovery process to make sure that the recovery process is meeting the community performance objectives.

The value of *PPwoP(t=72 hours)* is compared to the community recovery threshold value to check the recovery progress. If the progress is satisfactory, the Operator agent continues with the recovery process following its original repair priority plan. Otherwise, the Tenacity parameter of the Administrator agent, is incremented relative to the initial Tenacity of the Operator. The values of the Tenacity attributes of the two agents determine whose priorities are going to be addressed first during the recovery process, as shown in Fig. 3.5.

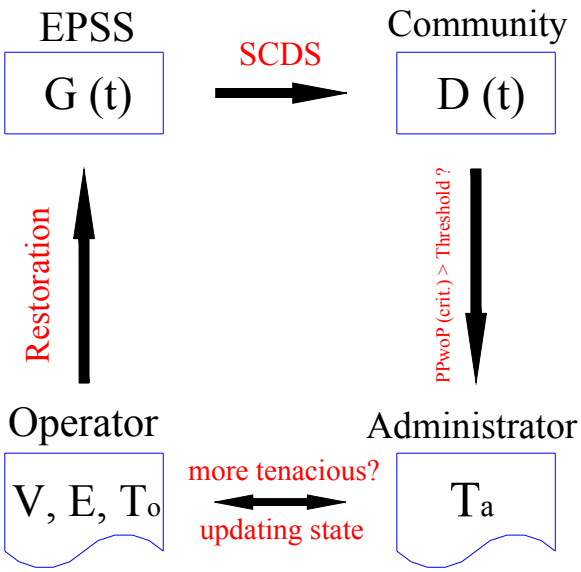

Fig. 3.5. Illustration of the interactions among the Administrator and Operator agents

Namely, if $T_a < T_o$ there are no changes, but if $T_a \geq T_o$ the priorities of the community take precedence. As a result, it is likely that the Operator will be forced to embrace the Administrator's recovery priorities. For example, the Operator may need to repair the most seriously damaged substations first, and only thereafter proceed in the descending order of damage for the remaining damaged EPSS components. If the repair plan change is triggered, the speed V and the efficiency E attributes of the Operator are increased in order to increase the rate of the recovery process. The agents' state update also reflects the ability of the Administrator to prioritize the EPSS Operator vehicles on the available roads while coordinating the restoration campaign. The EPSS restoration proceeds using the plan selected after the check of the recovery process progress until all damaged EPSS components are fully repaired.

3.3. Application of the Proposed Framework

The proposed ABM framework was implemented in Matlab and is demonstrated using a virtual EPSS-Community system. The EPSS is extracted from the IEEE 118-node Benchmark System (Christie 1993). As illustrated in Fig. 3.6, the EPSS consists of 15 generation substations (red squares) and 19 distribution substations (blue circles). Generation substations inject electric power into the network and transfer the electric power using the interconnecting power lines. Distribution substations supply the low-voltage power grids, i.e. extract electric power from the network and transfer it to the consumers in the community.

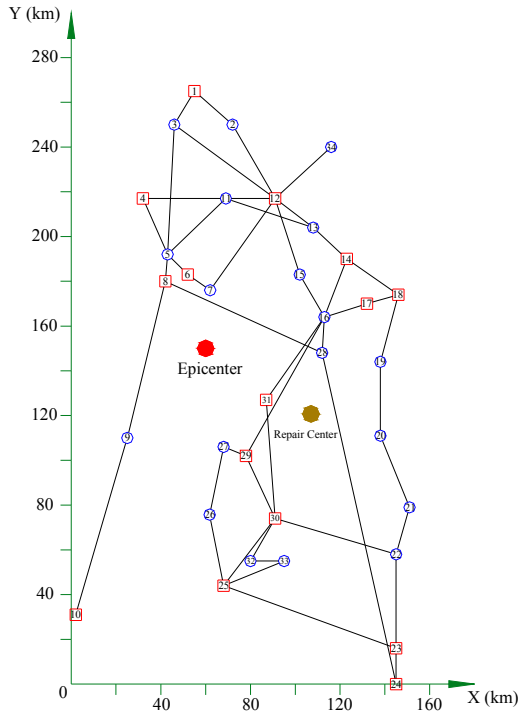

Fig. 3.6. Topology of the virtual EPSS-Community system

As shown, the generation substation (Fig. 3.7) consists of two main and one reserved 220 kV bus bars (81, 82 and 83). They are connected with a circuit breaker on each side, respectively. Generators (61 and 62) are attached to each main bar. The reserved bus bar can serve as the backup for either the input or the output bus bar employing a workable configuration of the circuit breakers.

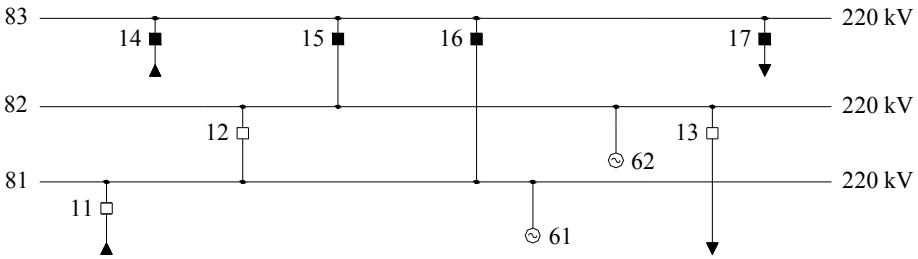

Fig. 3.7. The configuration of generation substation

Similarly, the distribution substation (Fig. 3.8) also consists of two main bus bars (81 and 82) and one reserved bus bar (83). Transformers (61, 62 and 63) are used to transform the 220 kV input power voltage to the 35 kV output power voltages. The circuit breakers (11 through 21) are set to facilitate the safe operation of the substation and the engagement of the reserve bus bar when

necessary. Besides transferring high-voltage into low-voltage power, the distribution substations should also transit high-voltage power within EPSS.

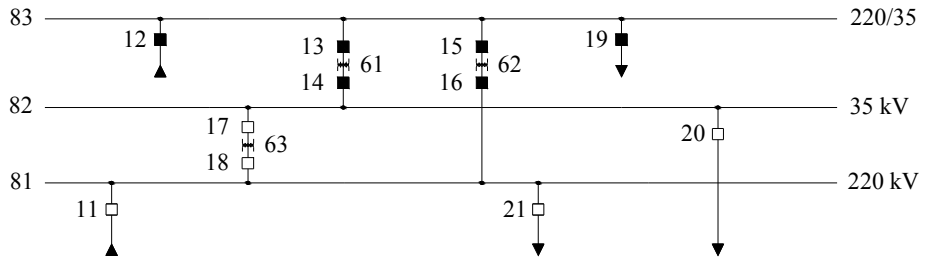

Fig. 3.8. The configuration of distribution substation

The nominal electric power supply capacity of the 15 generation substations and the electric power demand of the 19 distribution substations are presented in Table 3.1, respectively. Also listed is the assumed population served by each distribution substation. For simplicity, only the distribution and the generation substations are considered, while the other components of the EPSS as not modeled.

Table 3.1. Characteristics of the generation and distribution substations of the virtual EPSS

Generation		Distribution			
Generation Substation	Power Generation (MW)	Distribution Substation	Power Demand (MW)	Population Served P_i (10^3)	Sector Served
1	150	2	41.6162	76	*Population+Factory*
4	50	3	61.7809	66	*Population+Factory*
6	50	5	69.6968	96	*Population+Factory*
8	100	7	16.1609	66	*Population*
10	50	9	52.9856	32	*Population+Factory*
12	100	11	34.3699	134	*Population*
14	25	13	53.3392	224	*Population*
17	50	15	60.0792	224	*Population*
18	50	16	64.6848	256	*Population*
23	25	19	4.1300	24	*Population*
24	50	20	26.9800	24	*Population+Factory*
25	50	21	6.1100	24	*Population*
29	50	22	4.1300	24	*Population*
30	50	26	29.2884	76	*Population+Factory*
31	50	27	51.3934	72	*Population+Factory*
		28	16.6912	64	*Population*
		32	16.0809	66	*Population*
		33	9.4406	44	*Population*
		34	114.1500	0	*Factory*

The topology and the societal structure of modern communities are complex and heterogeneous. In order to reduce the complexity of this example, the community served by the virtual EPSS described above is disaggregated into two sectors, i.e. the *Population* sector comprising the residential buildings and the critical facility, and the *Factory* section, comprising the industrial facilities. The built inventory in each of these sectors is further divided into sub-categories listed in Table 3.2.

Table 3.2. Community built inventory types in the two power demand sectors

Sector	Use	Type of Structure
Population	Residential	Reinforced concrete apartment building
		Masonry apartment building
		Masonry single-family house
	Critical Facility	Hospital
		School
Factory	Industrial	Heavy industrial building
		Light industrial building
		Office building

The EPSS and the served community are made geographically denser by scaling the length scale of the IEEE 118 EPSS down by a factor of 5, resulting is a roughly 32x50km area of the virtual EPSS-Community system (Fig. 3.6 scaled down by 5). Thus, significant ground shaking due to earthquakes with a magnitude between 4 and 7 could be expected on most of the EPSS of community component sites.

The seismic hazard environment is modeled by locating the earthquake hypocenter close to the geographic center of the EPSS system, as shown in Fig. 3.6. This hypocenter location is not changed in this study to control the computational effort. The intensity of shaking at each EPSS or community component site, measured using peak ground motion displacement, velocity and acceleration values is computed using the ground motion attenuation relations proposed by Campbell and Bozorgnia (2008). The magnitude of the earthquake (M) is associated to the occurrence probability using the bounded Gutenberg-Richter law (the seismic hazard curve) with parameters a=4.4 and b=1 (Kramer 1996).

3.3.1. Vulnerability analysis

Libraries of seismic fragility functions are available for the components of the community built environment (Rossetto and Elnashai 2003, Kwon and Elnashai 2006, Jeong and Elnashai 2007, Senel and Kayhan 2009, ATC-58 2015, OpenQuake 2015, Syner-G 2015) and civil infrastructure systems (HAZUS 2015, Syner-G 2015) including the EPSS components. Fragility functions suitable for the built inventory (Table 3.2) and the components of the EPSS generation and distribution substations (Table 3.1), such the transformers, circuit-breakers and busses, are

selected from these documents. The VFs are obtained as described in Section 3.3.1. For simplicity but with loss of generality, only DS1 and DS3 are considered for the EPSS components with the exception of the generators. Three damage states were used to describe the earthquake damage to the built inventory components and to evaluate the resulting electric power demand as described in Section 3.3.1. The power demand of schools and hospitals in DS1 and DS2 was kept at the pre-disaster level regardless of the incurred damage to reflect their role as emergent shelters.

3.3.2. Parameters of the power demand Recovery Functions

Power demand stems from the community requirements, i.e. from the electric power needed to support the functions of the components of the community built inventory (Table 3.2). Therefore, the power demand depends on the ability to restore the functions within the buildings, which, in turn, depends on the level of the incurred earthquake damage. The RFs are lognormal probability distribution functions with the parameters defined in Table 3.3. Different RFs are defined for damage states DS2 and DS3. It is assumed that no recovery is needed if the component is in damage state DS1. Given the component damage state, the probability of its full function recovery at time t in the recovery process is computed using the RF appropriate to the specific building inventory. The resulting electric power demand is computed as outlined in Section 3.3.2.

Table 3.3. Parameters for the RFs of the community built inventory components

Type of Structure	Damage State	Mean (Days)	Std. (Days)
RC apartment building	DS2	14	12
	DS3	210	60
Masonry apartment building	DS2	14	12
	DS3	210	60
Masonry single-family house	DS2	10	9
	DS3	150	54
Hospital	DS2	12	10
	DS3	150	30
School	DS2	25	20
	DS3	240	90
Light industry building	DS2	45	40
	DS3	270	180
Heavy industry building	DS2	45	40
	DS3	300	180
Office building	DS2	25	20
	DS3	240	72

The recovery of the residential building and hospital functions is assumed to be the fastest among all community built environment components. Assuming that the population is not evacuated, the focus of the recovery is restoring shelter. Once the people are in their homes, or temporary shelters, their demand for electricity will recover quickly. The recovery of multi-story apartment

buildings is assumed to take more time than the recovery of single-family homes. The durations of the recovery of light and heavy industry is the longest but is also affected by a larger uncertainty, because their operation cannot fully recover, or even restart, unless the community population (not only EPSS) is on its way to recovery. The schools and high-rise buildings can recover moderately fast, compared to the other built environment components mentioned above. The recovered power demand *D(t)* at the EPSS-Community system level is tracked by integrating the recovered demand of every component of the community built inventory.

3.3.3. Parameters of ABM agents

The parameters of the ABM Operator and Administrator agents are defined as random variables with probability distributions shown in Table 3.4. The velocity of the Operator agent repair crew vehicle V_i is scaled down by the length scale factor to match the size of the scaled-down EPSS-Community system (Fig. 3.6), and it also accounts for the damage to the road network that may hamper the repair efforts. The initial repair efficiency E_i quantifies the initial recovery efficiency of the generation substations. To simplify the simulations, the recovery of the distribution substations was modeled in parallel by assuming that all of them will fully restore their functionalities at a specific period of time, the Recovery Threshold, after the earthquake event because of their proximity to the inhabited areas and the availability of additional repair crews. The Recovery Threshold for distribution substations is defined by a uniform distribution with limits set as a function of the earthquake magnitude (Table 3.4).

Table 3.4. Probability distributions of the Operator and Administrator agent parameter values

Parameter	Distribution Type	Lower Limit	Upper Limit
Operator			
V_i (km/h)	Uniform	6	8
E_i (1/day)	Uniform	20%	30%
Recovery Threshold (day)	Uniform	*M*-2	*M*+4
$T_{o,i}$	Uniform	0.4	0.5
Administrator			
$T_{a,i}$	Uniform	0.3	0.4

* *M* is the seismic magnitude obtained from the hazard curve.

3.3.4. Monte Carlo simulation of the recovery of the EPSS-Community system

The uncertainties related to the earthquake scenarios, the EPSS and the community component damage states, the disaster preparedness of the EPSS operator and the community, and the

interaction between the recovery governance structures are represented by probability distributions and propagated via Monte Carlo simulations of individual earthquake-damage-recovery realizations.

Each simulation starts by assuming an earthquake of a certain magnitude M occurred with the hypocenter located as shown in Fig. 3.6. The probability of occurrence of this earthquake is obtained from the seismic hazard curve. The ground motion intensities are computed using the Campbell & Bozorgnia (2008) attenuation relations for the rock site. The VFs (Section 3.3.1) are used to establish the state of the EPSS-Community system at the beginning of the recovery phase. This state description comprises of the damage state of each EPSS and community component. Before the recovery time t counter is initiated, the SCDS of the EPSS Operator is selected (Table 3.5) and the attributes of the Operator and the Administrator agents V_i, E_i, $T_{o,i}$ and $T_{a,i}$ are randomly generated from the distributions as detailed in Section 3.4.3. The Operator's initial tenacity $T_{o,i}$ is always larger than the Administrator's initial tenacity $T_{a,i}$ allowing the Operator to plan the EPSS restoration without interference. As a result, the repair crew will focus on the least seriously damaged substation, and then travels to fix the other substations following the ascending damage severity order. Such prioritization is justified on two grounds: 1) repairing slightly damaged components tends to be fast and the access to them is, most likely, not hampered by the damage to the transportation systems, enabling prompt restoration of electric power to some customers; and 2) heavily damaged substations may need replacement rather than repair, which requires additional planning, design, financing, equipment acquisition, and transport.

The damage severity S_n of a damaged generation substation n is quantified as the functionality loss normalized by the original functionality level, i.e.:

$$S_n = 100*(1-f_{d,n}/f_{o,n}) \tag{3.9}$$

where $f_{o,n}$ and $f_{d,n}$ are the levels of functionality (the power generation capacity) before and after the earthquake, respectively. The repair time r_n for each generation substation n is:

$$r_n = S_n/E_i \tag{3.10}$$

Given the repair priority order, the travel time t_n between the damaged substations n-1 and n for $n \in [2, N]$, can be calculated based on the road distance D_n between substation n-1 and n as $t_n = D_n/V_i$. For any damaged substation n in the repair list, the traveling time to it and the time to repair it is:

$$\begin{cases} t_1 = t_0 + d_0/V_i & \\ t_n = r_{n-1} + D_n/V_i & if\ T_{a,i} < T_{o,i} \\ r_n = t_n + S_n/E_i & if\ T_{a,i} < T_{o,i} \\ t_n = r_{n-1} + D_n/V & if\ T_a \geq T_{o,i} \\ r_n = t_n + S_n/E & if\ T_a \geq T_{o,i} \end{cases} \quad 3.11$$

where t_0 is the emergency action and restoration planning period right after the earthquake (set to equal 36 hours in this study) and d_0 is the distance between the repair center and the first-generation substation to be restored. The attributes V_i and E_i in Eq. (8) are updated if the state of the Operator is updated after the recovery performance check at the *Resilience Check Time* as described in Section 3.3.4. Specifically, the Tenacity parameter $T_{a,i}$ of the Administrator agent is incremented by 0.1, i.e. $T_a = T_{a,\,i} + 0.1$, at the *Resilience Check Time*, and compared to the Tenacity parameter $T_{o,i}$ of the Operator agent. The magnitude of the increment value is selected considering the values of the Tenacity Parameter distribution bounds in Table 3.4. If the community concerns prevail $T_a \geq T_{o,i}$ the EPSS component repair priority list is reversed (i.e. the most damaged substation will be repair first), and the Velocity and the Efficiency parameters of the Operator agent are increased (in this study $V = 1.1*V_i$ and $E = 2*E_i$) to increase the rate of the recovery process.

The seismic restoration campaign evolves though the discrete time steps t_n and r_n. The generation capacity *G (t)* at the level of the EPSS-Community system at time *t* is:

$$G(t) = \begin{cases} \sum_{j=1}^{n-1} f_{o,j} + f_{d,n} + \frac{t - t_n}{r_n - t_n} \times (f_{o,n} - f_{d,n}) & t_n \leq t < r_n \\ \sum_{j=1}^{n-1} f_{o,j} + f_{d,n} & r_{n-1} \leq t < t_n \end{cases} \quad 3.12$$

During a time step t_n, power supply capacity *G(t)* remains unchanged while the repair crew is travelling because no substation is under repair. Once the repair crew arrives at the generation substation *n* and starts the repair process, its functionality follows a linear recovery with slope equal to E_{ini}, if $t_n \leq t < r_n$ and $T_a < T_{o,\,ini}$, or with slope equal to E, if $t_n \leq t < r_n$ and $T_a \geq T_{o,\,ini}$.

The transmission lines are considered to remain undamaged in this model. The distribution substations are considered to be fully functional after the Recovery Threshold time (Table 3.4). Therefore, the power demand at the level of the EPSS-Community system *D(t)* is computed as stated in Section 3.4.2.

3.3.5. Seismic Contingency Dispatch Strategies

In this case study, five different SCDSs listed in Table 3.5 are proposed. Strategy 1 prioritizes the supply to communities which have the largest post-earthquake demand. This strategy reflects the EPSS operator preference to supply first their largest users during the restoration process. Such strategy assumes that electric power can be produced in sufficient quantities.

Table 3.5. Prioritization Strategies for Seismic Contingency Dispatch

Strategy	Criterion
1	Maximum demand
2	Minimum demand
3	Largest Population
4	Maximum normalized demand
5	Minimum normalized demand

On the other hand, distribution substations with small power demand might be prioritized because the ability to generate electric power may be limited after an earthquake (SCDS 2). Similarly, SCDSs 4 and 5 prioritize distribution substations according to the maximum and minimum power demand normalized by the pre-earthquake demand, respectively. Finally, Strategy 3 prioritizes distribution substations serving large populations.

In order to supply the communities following the priority list established by the SCDS, the distribution substation nodes are ranked in the descending order according to the prioritization criterion, e.g. the instantaneous power demand for SCDS 1. The capability of the EPSS to transmit power to distribution substation k=1, 2,…, 19 after the disruption, is assessed by evaluating the shortest paths between a distribution substation k and any generation substation l=1, 2,…, 15. In order to allocate the available transferable power, the demand of the distribution substation is assigned to the closest generation substation following the dispatch priority ranking. The power allocation terminates if the total demand of the distribution substations is satisfied, or if the EPSS generation capacity is reached. In the latter case, distribution substation i cannot be supplied and is affected by an electric power deficit $PD_i(t)$. The power allocation procedure and the available transferable power are updated during the recovery process based on the updated status of supply and demand side EPSS and community components.

3.4. Results of the Virtual EPSS-Community System Resilience Assessment

The recovery of the virtual EPSS-Community system is simulated using the Monte Carlo simulation technique. Two case studies are investigated. In Section 3.5.1, only the Operator agent

guides system recovery, and its repair priorities are always enforced. The influence of the five SCDSs on the EPSS-Community system resilience is assessed in Section 3.5.2. In Section 3.5.3, the Administrator agent is introduced and its influence on the recovery path is assessed by the comparison with the results of Section 3.5.1. The comparison is done for the SCDS 1. Each case study involves 2000 earthquake events where damage is induced and the resulting recovery paths are tracked until pre-earthquake conditions are restored.

3.4.1. Operator Agent Recovery Process

Fig. 3.9 shows the medians of the electric power generation capacity, the delivered electric power, the electric power demand and the electric power deficit in a scenario with an earthquakes of magnitude *M*=7.5 and SCDS 1.

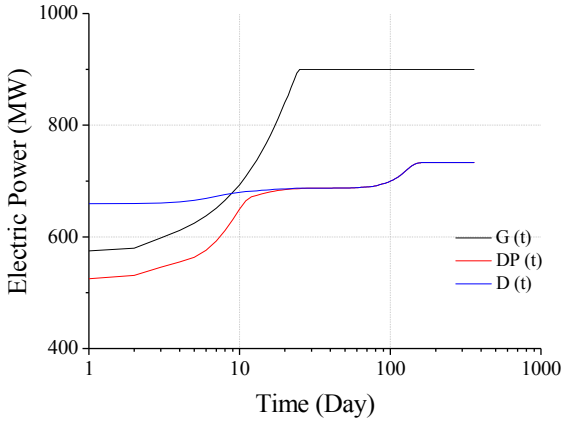

Fig. 3.9. Evolution of the generation capacity, deliverable power, and power demand in the EPSS-Community system for a Magnitude 7.5 earthquake scenario and SCDS 1 (median values)

Before the event, the EPSS supplies 900 MW of the electric power and covers the 733 MW of community demand. Immediately after the event, the median electric power demand drops to 660 MW and the median power generation capacity drops to 575 MW. Further, the median deliverable power drops to 528 WM due to low-voltage power transformer failures and high-voltage power transmission line capacity insufficiencies. After the recovery starts, it takes 25 days to restore the median EPSS generation capacity to the pre-earthquake level, whereas it takes 165 days for the community demand to recover.

The evolution of the *PPwoP* EPSS-Community system resilience measure is plotted in Fig. 3.10 for the *M*=7.5 earthquake scenario and SCDS 1. Immediately after the strong earthquake, 34% of the community population is likely to be without electric power, as indicated by the median *PPwoP*. The median duration to complete recovery, i.e. the time required for all people in the

community that can use electric power to receive it, is 11 days. The 20% and 80% quantile curves in Fig. 3.10 indicate the uncertainty associated with the seismic recovery of the EPPS-Community systems, and show that the median *PPwoP* is symmetric with respect to the quantiles.

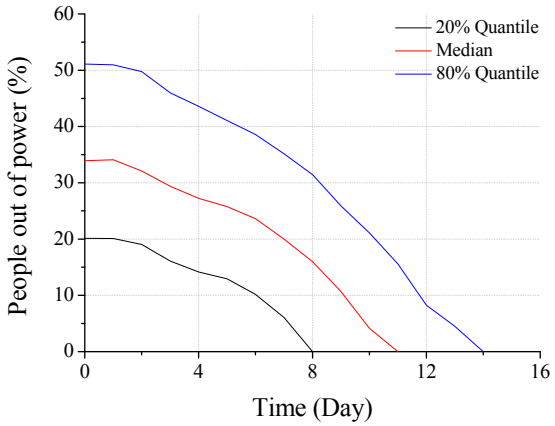

Fig. 3.10. Evolution of PPwoP for a Magnitude 7.5 earthquake scenario and SCDS 1

The influence of the earthquake magnitude on the EPSS-Community system resilience is assessed in Fig. 3.11, which shows the *PPwoP* for *M*=6, 6.5, 7 and 7.5 earthquake scenarios with SCDS 1.

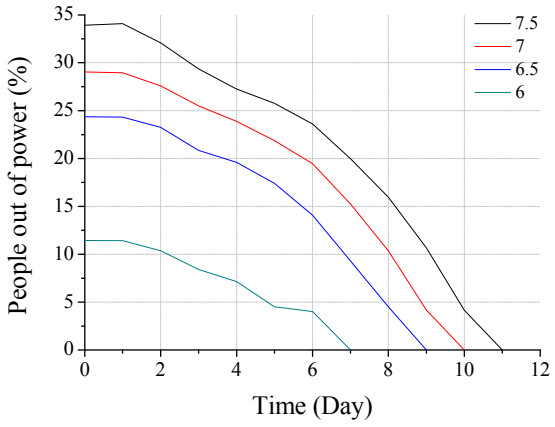

Fig. 3.11. The evolution of the median *PPwoP* for different earthquake magnitude scenarios for SCDS 1

The resilience of the EPSS-Community system is significantly affected by the earthquake magnitude. The post-earthquake median *PPwoP* values are 34%, 29%, 24% and 11% for magnitudes 7.5, 7, 6.5 and 6, respectively. Fig. 3.11 reveals a remarkable gap between the

consequences of *M*=6 earthquake and the three stronger earthquakes. The median duration to complete recovery is 7, 9, 10 and 11 days for the four seismic scenarios, respectively.

Fig. 3.11 shows that the electric power restoration process can be roughly divided into three stages after the EPSS repair starts (36 hours after the earthquake in this study). Specifically, in the first stage (between 36 and 72 hours after the earthquake) the *PPwoP* decreases quickly although the EPSS restoration strategy targets the least seriously damaged stations first. The explanation can be found if the demand-side is taken into account: the recovery probability for all the component of the built environment is rather small before the third day (see Table 3.2) and therefore the gap between the deliverable and the demanded power can narrow relatively fast. In the second recovery stage between day 3 and day 5 (or day 6 for the *M*=6 earthquake scenario), the *PPwoP* keeps decreasing, but at a smaller rate, because buildings are restored and the power demand increases. In the third stage after day 5 (or day 6 for the *M*=6 earthquake scenario), the generation capacity is restored quickly because the repair crew focuses on more severely damaged generation substations, and the *PPwoP* decreases at a faster rate again.

3.4.2. Impact of the SCDSs

The resilience of different community sectors, the *Population* and the *Factory* sectors specified in Table 3.1, is affected by the SCDS implemented by the EPSS operator. In order to quantitatively examine this influence, the seismic resilience of EPSS-Community system is evaluated for the two sectors separately for the five SCDSs listed in Table 3.5.

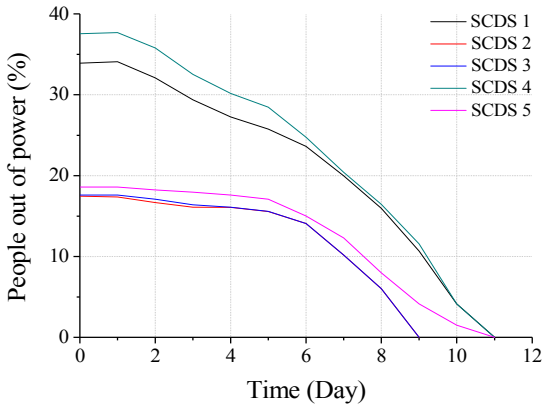

Fig. 3.12. Evolution of the *Population* sector recovery for the M=7.5 earthquake scenario and the five SCDSs (median values)

The main function of the *Population* sector is to support the basic livelihood of community dwellers. Its seismic resilience is measured by the *PPwoP* resilience measure defined in Section

3.3.3. The evolution the *PPwoP* median during the recovery process in the *M*=7.5 earthquake scenario is presented in Fig. 3.12 for the five SCDSs. The five curves in Fig. 3.12 form two clusters. The first cluster results from SCDSs 1 and 4, which prioritize the power supply to communities having large demand and large normalized demand. They result in *PPwoP* of 34% and 38% immediately after the earthquake, respectively. It takes 11 days to fully restore the power to *the Population* sector under these two strategies. Conversely, SCDSs 2, 3 and 5 lead to much smaller *PPwoP* (less than 20%) immediately after the earthquake, and a faster recovery of the *Population* sector. Therefore, the seismic resilience of the *Population* sector is significantly improving if SCDSs 2, 3 (and to some extent 5) are employed by the EPSS operator.

On the other hand, the choice of the SCDSs has an opposite effect on the recovery of the *Factory* sector. This recovery process is tracked using the evolution of the power deficit of the Factory sector, $D_f(t)$ defined in Eq. 3.7, shown in Fig. 3.13., for the five SCDSs. In particular, the Factory sector power deficit after the earthquake is 19% for SCDS 1 and 21% for SCDS 4. The SCDSs 2, 3 and 5 result in over 80% power deficit of the Factory sector. Furthermore, using SCDS 1 fully satisfies the demand of the Factory sector in just 4 days, compared to between 9 and 10 needed when using other strategies.

SCDS 5 offers a balance between relatively high resilience and speedy recovery of the *Population* sector and somewhat shorter recovery of the *Factory* sector.

These results can be explained in terms of the interplay among the earthquake scenario, the topology of EPSS-Community system, and the recovery pattern of different community sectors. First, the distribution stations with large power demand, e.g. node 34 in Table 3.1, which is a purely *Factory* sector distribution node, and nodes 13, 15 and 16, which are mixed, will be prioritized in SCDS 1 and SCDS 4. Distribution node 34 is much farther away from the epicenter compared to distribution nodes 13, 15 or 16, making the expected damage to node 34 much smaller. Therefore, it is likely to recover significantly faster.

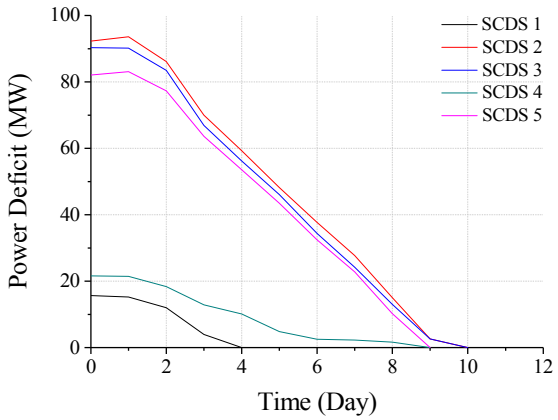

Fig. 3.13. Evolution of the *Factory* sector recovery for the M=7.5 earthquake scenario and the five SCDSs (median values)

3.4.3. Operator and Administrator Agent Recovery Process

The effects of the interaction between the Operator and the Administrator agents on the recovery of the EPSS-Community system are examined by re-running the magnitude *M*=7.5 earthquake scenario and SCDS 1 simulations with both agents. As explained in Sections 3.3.4 and 3.4.4, a check of the rate of recovery is performed at the *Resilience Check Time* set to be 72 hours after the earthquake in this study. The value of the *PPwoP* EPSS-Community system resilience measure is compared to a threshold. Three threshold values, 10%, 20% and 30%, are used in this study. If the *PPwoP* exceeds the threshold at the *Resilience Check Time*, the Tenacity Parameter of the Administrator agent is incremented and compared to the Tenacity Parameter value of the Operator agent, as outlined in Section 3.4.4. In the conducted simulations, the probabilities that the recovery plan of the Operator agent is changed were 41.7%, 33.7% and 26.0% for the 10%, 20% and 30% *PPwoP* threshold, respectively. For comparison, the case without activation threshold, i.e. no Administrator agent, is also reported.

Fig. 3.14 shows that the involvement of the Administrator agent increases the rate of power generation recovery and shortens the recovery process. In the case of a strict *PPwoP* threshold equal to 10%, the change of repair priorities induced by the Administrator agent resulted in complete recovery after 19 days as compared to 25 days that it takes without the Administrator agent. The effects of the Administrator agent on the recovered generation capacity decrease for larger *PPwoP* thresholds, and the recovery path approaches the case without interaction as the Administrator became "weaker".

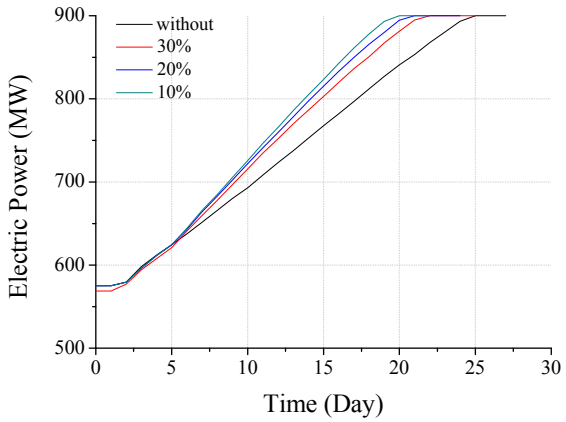

Fig. 3.14. Evolution of the electric power generation recovery for the M=7.5 earthquake scenario and the SCDS 1 (median values)

The effects of the Administrator agent is also evident in the rates of decrease of *PPwoP* during the recovery process, as shown in Fig. 3.15 for the M=7.5 earthquake scenario and the SCDS 1. The change in the recovery rate does not occur immediately at the Recovery Check Time (3 days in this study), but somewhat later, on day 5. This change then results in shortening of the time to full recovery from 11 to 9 days for the 10% *PPwoP* threshold level.

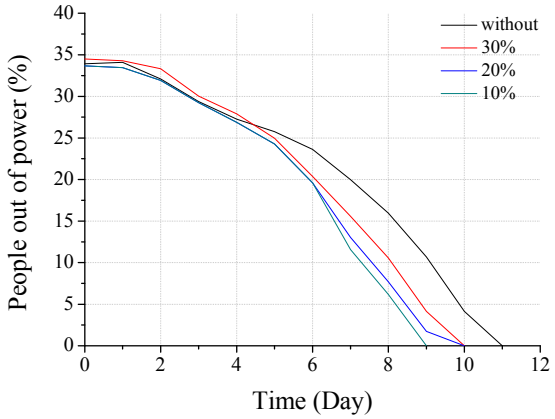

Fig. 3.15. Evolution of the *PPwoP* EPSS-Community resilience measure for the M=7.5 earthquake scenario and the SCDS 1 (median values)

3.5. Conclusions and Outlook

In this Chapter, a conceptual supply-demand framework was first proposed. Instead of quantifying the evolution of the seismic response of EPSS in the aftermath of an earthquake using a single parameter to measure system functionality, the proposed framework tracks the post-earthquake evolution of the supply provided by the EPSS and the demand generated by the customers in the community. The difference between the electricity supply, representing the ability of the EPSS to function, and demand, representing the ability of the community to function, is a direct measure of EPSS resilience. The evolution of the supply/demand difference is tracked through time after the occurrence of the earthquake, divided into the Absorption and the Recovery phases. Clearly, failure of the EPSS occurs when it supplies less electricity than the community needs: thus, the EPSS may provide sufficient power, even if it functions below its capacity, compared to the diminished ability of the damaged community to use the power.

Resilience of an EPSS is computed using a compositional approach. During the (relatively short) Absorption phase, the loss of EPSS supply and the community demand is assessed using component vulnerability functions (probability of loss of function, directly related to incurred damage, conditioned on the earthquake intensity measure) and integrating at the EPSS and community levels. The restoration of the community electric power demand is evaluated using the seismic recovery functions. With reference to the supply, however, an agent-based approach

was devised in this Chapter to model the post-earthquake EPSS power generation and deliverability behavior.

Namely, two agents, the EPSS Operator and the Community Administrator, are used to represent the recovery priorities, planning and actions of the EPSS operators and the community as they strive to recover from a disaster. The agent-based framework enables nuanced modeling of the recovery process, emphasizes the need to consider the supply and the demand occurring in the EPSS-Community system to understand the recovery process, and highlights the effects of EPSS system repair and electric power dispatch strategies and community demand recovery on the resilience of different sectors of the community and the community as a whole. Remarkably, the agent-based model reveals the emergency of possibly conflicting interests of the community and the EPSS operator and models the effect of the resolution of these conflicts on the recovery process and the resulting EPSS-Community system resilience.

In particular, the proposed agent-based seismic resilience quantification framework provides the following answers to the questions posed in the introductory section of this Chapter. The EPSS-system-related electric power deficit and the community-related resilience metrics are computable and can be tracked during the damage absorption and recovery processes to indicate the resilience (or lack thereof) of the EPSS-Community system. Clearly, the larger the earthquake hazard, the more challenged the EPSS-Community system will be. However, increasing the robustness to reduce the vulnerability of the EPSS and Community components, as well as increasing the rate of their repair results in an EPSS-Community system that recovers faster. Remarkably, the rate of electric power demand recovery is at least as important for the EPSS-Community system resilience as the rate of electric power supply recovery. The community can monitor the rate of the EPSS-Community recovery process using the proposed resilience measures and intervene effectively early on in the recovery process to change its rate or priorities. More importantly, the conducted simulations reveal the remarkable role contingency electric power dispatch strategies have on the resilience of different community sectors. This points to the need to plan a dynamic post-disaster interaction between the community and the civil infrastructure system operators and develop contingency service dispatch strategies as well as consistent contingency demand regulation measures to shape the recovery process and maximize community resilience. The proposed agent-based seismic resilience quantification framework can be used to model and test such strategies and measures and thus contribute to improving community risk governance.

The proposed seismic resilience-quantification model can be improved. First, it can be enriched by modeling and monitoring a larger array of resilience metrics, some specific to community sectors and infrastructure systems components, others aggregated at the system level. Second, it can be generalized to model more complex repair planning and execution strategies (e.g. multiple repair crews), as well as to include the influence of other community infrastructure systems (e.g. transportation and communication) in the recovery modeling and simulation. Third, it can be expanded to include agent-based models of how disasters affect the population, such as casualties,

evacuations and permanent or temporary relocations. Fourth, it can be made more sophisticated by refining the behavior of agents and modeling the interactions between them based on the instantaneous values of the monitored resilience metrics. Such a model could, with reasonable expectations, be calibrated against the damage absorption and recovery data collected after the past earthquake disasters.

4. Seismic Resilience Assessment of an Integrated CI-Community System

As indicated by the literature review in Chapter 2, modern CIs have been more integrated and interdependent through sharing and exchange of the operation resources and information (Kröger and Zio 2011, Helbing 2013). Such interdependency underlies the efficient functioning of the CIs. However, it simultaneously renders them more vulnerable to disruptive events that could be natural hazards, terrorist attacks, and random technical errors (Albert et al. 2004, Zhao et al. 2010, Kawashima 2012). The inflicted local damage can be exacerbated by cascading through one or more CIs and lead to the severe global failure of the system of CIs (Dueñas-Osorio and Vemuru 2009, Buldyrev et al. 2010, Zio and Sansavini 2011). According to the filed observations from the recent catastrophic earthquake disasters around the world, the damaged CIs are usually struggling to recover from the initial seismic damage they suffered (Hollnagel and Fujita 2013, Hwang et al. 2015). Moreover, the stagnant recovery of one standalone CI often hinders the restoration of many other CIs, as well as the rescue and evacuation of people in the affected areas (Kawashima et al. 2009, Lekkas et al. 2012).

Many studies have been carried out over the past decades on the seismic behavior of integrated CIs in urban communities. Based on those findings, increasing robustness and reparability, two basic elements of resilience, improves the seismic behavior of coupled CIs (Farr et al. 2014). Considerable research efforts have been put on CI robustness. Bashan et al. (2013) pointed out that the failure of a tiny fraction of the nodes of any sub-system can potentially fragment the globally integrated CI system. Against that backdrop, Brummitt et al. (2012) indicated that the interdependence among CIs should be set on an optimal level in order to avoid a devastating global cascade in interconnected CI system. Correspondingly, the research conducted by Schneider et al. (2013) also revealed that the nodes with high betweenness are significant to the reduction of cascades within coupled networks. A small amount of research has been conducted on the repair and recovery for CIs so far. Given the dense interdependence and the vulnerability, study on the post-disaster recovery of modern integrated CI system has been significant and timely.

Starting from the compositional supply/demand framework for quantifying the seismic resilience of a system comprising the community and a single CI, and the RFs computed using the agent-based model (Chapter 3), a framework to model the recovery behavior of an integrated CI-Community system is developed in this Chapter. Specifically, the Electric Power Supply System (EPSS), the Transportation System (TS), and the corresponding Urban Community they serve, are examined. The ABM proposed in Chapter 3 is further upgraded so as to capture the recovery path of the intertwined EPSS and TS after an earthquake. Three individual agents, the operators of EPSS and TS, and the community Administrator, are defined by attributes that model their behaviors during the post-earthquake recovery process. More importantly, the rules for the interaction among the set of agents are also specified. The proposed framework is exemplified

using a virtual EPSS-TS-Community system. The recovery trajectory of the system is computed for different earthquake scenarios. The influence of the interdependence between EPSS and TS on the systemic resilience of the community they serve is highlighted. The impact of different agent behavior characteristics on the systemic resilience is also investigated and discussed.

4.1. The Agent-Based Modelling Framework

Modern CI-Community system is a heterogeneous and intertwined socio-technical network. Its resilience after catastrophic natural hazards is dynamic and dependent on many influential factors (Cimellaro et al. 2016). In a typical seismic event, the components of both EPSS and TS, and the elements of the built environment of the urban community will be damaged to some degree. Note that unlike biological or financial systems, the physical damage of CIs (induced by the earthquake) usually cannot recover spontaneously (Majdandzic et al. 2013). Instead, their functionality can only be restored if apt external recovery measures are executed.

As (some) information about the damage status of a CI is collected, the recovery process starts, with the CI operator dispatching repair teams to restore the damaged facilities. In most cases, CI operators act independently, following their own repair prioritization plans. Nevertheless, due to the interdependence among different CIs, the recovery process of single CI would affect, and in turn, be influenced by, the restoration of the other CIs, as well as by the recovery of the community.

The compositional supply/demand framework, elaborated in Chapter 3, is employed to analyze the interdependencies emerging during the post-disaster recovery process of a coupled EPSS-TS-Community system. To achieve this goal, the ABM proposed in Chapter 3 will be further developed by including the Operator of TS. The recovery paths of the integrated CIs can therefore be modeled with accounting for the different strategies and capabilities of all players involved in the recovery process. Similar to the ABM in Chapter 3, it was assumed that the post-disaster recovery priorities of EPSS and TS are governed by their own business needs and repair costs and effort, not necessarily by the recovery requirements of the community. Therefore, the recovery process may need to be overseen and coordinated externally. A community administrator, typically an emergency management coordination entity, assumes such a role.

4.1.1. Agent-Based seismic recovery model of the integrated CI-Community system

In this Chapter, without loss of generality, only EPSS and TS are included in the proposed model. Accordingly, three principal players, the **EPSS Operator**, the **TS Operator** and the community **Administrator** are defined as separate agents. The **EPSS Operator** and **TS Operator** agents follow predefined recovery plans based on independently-derived repair priority schemes constrained by their own resources. Crucially, a successful implementation of the EPSS recovery plan depends on the availability of roads: EPSS repair crews can only go to the substations by

driving along the instantaneously available roads and bridges, which are simultaneously undergoing a repair process. Therefore, the most efficient path for the EPSS repair crews along the available roads is computed using the state of the TS in each new time step. Finally, it is likely that the repair priorities for the Community and the CIs will differ during the post-disaster recovery process. The **Administrator** agent is, therefore, defined to coordinate the CI recovery campaign and optimize the outcome with respect to predefined community priories. The behavior of the agents is defined using random variables called attributes and pre-defined repair plans as follows:

EPSS Operator: an agent whose behavior is described by three attributes: V_e, E_{eg}, and E_{ed}. Specifically, V_e describes the average travelling speed of the EPSS repair team among the repair locations. Meanwhile, E_{eg}, E_{ed} quantifies the repair rate as the percentage of functionality restoration per day for generation substations and distribution substations within EPSS, respectively.

TS Operators: an agent whose behavior is defined by two attributes V_t, and E_b. Very similar to EPSS Operator, V_t refers to the travelling speed of its repair team, while E_b quantifies the efficiency for this team to restore the functionality for the damaged components of the TS.

Administrator: In this model**,** the agent is assumed to have only two states: "*active*" or "*inactive*". The state indicates whether it will enforce its own repair plan and override the CI agent repair plans at a decision point. The state will be determined according to the preset Community performance objectives for the post-disaster recovery process.

In a CI-Community system post-earthquake recovery simulation, following the assumption made in Chapter 3, the **EPSS Operator** agent was set to start the repair of the damaged EPSS components one and half days after the seismic event. This is done to provide some time for life-saving emergency actions, acquisition of the damaged state of the EPSS, and repair crew and equipment mobilization. Inside EPSS, the generation substations were ordered by their damage grade, from least to most seriously damaged ones. As mentioned in Chapter 3, such repair sequence enables quick recovery of the last damaged portions of the EPSS system, provides more options for power dispatch management early on, and maximizes the amount of supplied power, thus potentially maximizing the profit of the EPSS. Correspondingly, the distribution substations were ranked according to the population from the communities they serve, from largest to the smallest.

In order to facilitate model calibration two EPSS repair crew were defined and made responsible for repairs of the generation and the distribution substations, respectively. Thus, at the beginning of the post-disaster recovery process simulation, the two EPSS repair crews were sent from the repair center to restore the seismically damaged EPSS facilities. The crew calculates the time needed to reach the location of the substation that is at the top of the repair list, starting from the EPSS repair center, taking into account the current state of the TS functionality to compute the shortest path between the origin and the destination and the **EPSS Operator** V_e attribute. Once at

the EPSS component sites, the crew repairs it to fully restore its functionality. The required repair time is calculated based on the component damage state using with the E_{eg} and E_{ed} attributes. Once this repair is completed, the **EPSS Operator** agent is at a decision point. It selects the next EPSS component on its current repair priority list, and repeats the process starting from the current location of the repair crew and taking into account the state of the TS at that time in the simulation.

Correspondingly, in this model, the **TS Operator** agent was set to start the repair of the damaged TS components two days after the earthquake. A single TS repair crew, initially located at the TS repair center, was considered in this simulation. In this model, only the bridges of the transportation network were assumed to be damaged, while the links (roads) are assumed to remain undamaged. The importance of any single seismically damaged TS bridge was measured by its betweenness within the transportation network. Betweenness is defined as a centrality measure of a vertex within a graph (Brandes 2001). Betweenness centrality quantifies the number of times this bridge acts as one link along the shortest path between any other two nodes inside the TS (Freeman 1977). The TS repair group ranks the damaged bridges based upon betweeness centrality in a descending order. Such repair strategy is adopted on the grounds that the bridge with higher betweenness is more prone to become the bottleneck for the traffic flow within the TS. In addition, it is also assumed that the TS repair crew does not depend on the electric power provided by the EPSS.

The **Administrator** agent monitors the Community recovery process using a set of resilience measures. The community recovery performance objectives are formulated in terms of exceeding threshold values of selected community resilience measures at certain intervals after the earthquake. In this simulation, the **Administrator** agent determines if the rate of community recovery is satisfactory or not by comparing a community resilience measure to a threshold value at one point in time after the earthquake, called the *Resilience Check Time*.

In each simulation, the state of **Administrator** is always set as “inactive” until this time point. If the rate of recovery is not satisfactory at this moment, the **Administrator** agent state is switched to “activate”, which means that Administrator will intervene and, depending on the comparison of agent attributes, force EPSS Operator and TS Operator to perform a one-time adjustment their attributes and repair schedules. In such case, the travelling speed and the repair efficiency attributes of both **EPSS Operator** and the **TS Operator** are incremented (to speed up the recovery process), and the repair schedules are updated to prioritize the recovery of the community at the expense of the costs and profit of the CI system operators.

4.1.2. Simulation of the recovery path for integrated CI-Community system

For an integrated EPSS-TS-Community system in one earthquake scenario, assume N_g damaged generation substations and N_d distribution substations inside the EPSS. Meanwhile, N_b bridges

are also damaged within the TS. The set of five attributes V_e, E_{eg}, E_{ed}, V_t and E_b are randomly generated from uniform distributions as discussed in Section 4.1.1.

Similar to Chapter 3, the generation substation repair crew focuses on the least seriously damaged one, and then travels to fix the other substations following the ascending damage severity order. For any damaged generation substation n, its performance after and before the seismic event is denoted as $f_{d,n}$ and $f_{o,n}$, respectively. Thus, its damage severity S_n is quantified as the functionality loss normalized by its original level, as $S_n = 100 \times (1 - f_{d,n}/f_{o,n})$ (%). The repair time for each substation n is quantified as S_n / E_{eg}.

Given the priority order of the repair list, the travelling time t_n among the damaged generation substations n-1 and n for $n \in [2, N]$, can be calculated based on the shortest travelling distance SD_n between substation n-1 and n, as SD_n/V_e. Note that shortest distance is determined according to the instantaneously available TS, whose state is also time-varying. Hence, for any damaged substation n on the restoration list, the traveling time to it t_n and the time to repair it r_n can be quantified as (in case that the state of the Administrator is still "inactivate"):

$$\begin{cases} t_1 = t_0 + SD_0/V_e \\ t_n = r_{n-1} + SD_n/V_e \\ r_n = t_n + S_n/E_{eg} \end{cases} \quad 4.1$$

where t_0 is the "idle" period right after the seismic event and SD_0 is the shortest distance between the repair center and the first generation substation to be restored.

The seismic restoration campaign evolves though the discrete time steps t_n and r_n. The evolution of the power supply capacity for the considered EPSS $G(t)$ is quantified by Equation 3.12. The recovery for distribution substations is modeled in the same way. The only difference is that the performance for every considered distribution substation (out of the N_d ones) is either *fully functional* again or still *failed*. Numerically, the damage severity in Equation 4.1 is always 100 (%) for any of the *failed* substation.

This model is also employed for formulating the restoration of the TS. Similar to distribution substations, the damaged bridge is available again to the traffic only if it is fully repaired. In the developed model, for each bridge v among the N_b damaged ones, its betweeness $C_B(v)$ is quantified as:

$$C_B(v) = \sum_{s \neq v \neq t \in V} \frac{\sigma_{st}(v)}{\sigma_{st}} \quad 4.2$$

where σ_{st} is the total number of shortest paths from node to node and $\sigma_{st}(v)$ is the number of those paths that pass through bridge v. In addition, V refers to the total number of the nodes (vertices) within the entire TS.

In this Chapter, the power demand from the Community was still modeled using conventional recovery functions, which quantifies the probability that the component functionality exceeds a threshold after a set number of recovery days conditioned on its initial functionality loss.

In any time points of the recovery process, given the status of the power generation capacity (provided by the generation substations), transition capacity (provided by the distribution substations) and the power demand from the community, the CI-Community system resilience is examined using the supply/demand approach. In this Chapter, percentage of people without power (*PPwoP*) is also employed as the measure of societal resilience of the CI-Community system.

4.1.3. Updating the states for the agents

As discussed hereinbefore, the **Administrator** agent is assumed to examine whether the recovery jointly carried out by **EPSS** and **TS Operators** is satisfactory at the Resilience Check Time. The **Administrator** agent is "inactivate" from the beginning of the simulation until this time. This examination is conducted by comparing *PPwoP* to a threshold value at this specific point in time after the earthquake. If *PPwoP* is larger than the pre-defined threshold, the **Administrator** state will be switched to "activate" and have the states of **EPSS** and **TS Operators** updated accordingly. (In other words, the paradigm used in the Section 3.2.4 of Chapter 3, was simplified by removing the tenacity parameter of the agents and making the Administrator intervention deterministic if a recovery performance threshold is exceeded at Recovery Check Time). It means that EPSS repair crews will address the repair of the most seriously damaged substations first, and thereafter proceed in the descending order of damage for the remaining damaged substations. Besides, the speed and the efficiency attributes of the two Operator agents are increased in order to increase the rate of the recovery process. Hence, the attributes of V_e and E_{eg} in Equation (4.1) will be increased to speed up the recovery process on EPSS generation substations. The set of time points (t_n, r_n) in Equation (3.12) will also be updated. This update mechanism will be applied on the distribution substation and the TS in parallel. The agents' state update in the model refers to the ability of the Administrator to offer the incentive to the Operator of CIs so that they can expedite the restoration campaign. The EPSS and TS restoration continues until the all damaged components within the two CIs are fully restored, typically 360 days in the conducted simulations.

4.2. Case Study

In this case study, both the EPSS and the Community are the same as the ones used in Chapter 3. Thus, the road network of the TS was designed to serve the Community, and has a configuration similar to that of the EPSS (Fig. 4.1(b)). It has 32 bridges shown by red dots. The individual roads were modeled only as links between the TS nodes. The EPSS repair center is located near node 42 while the TS repair center is located near node 35, as shown in Fig. 4.1(a) and Fig. 4.1(b).

The size of the case study region was modified by reducing the length scale of the IEEE 118 Benchmark System 5 times to simulate the effect of moderate earthquakes in dense population settings. The seismic hazard environment was modeled by fixing the locating the earthquake hypocenter close to the geographic center of the case study region (Fig. 4.1(a)). Given that an earthquake of magnitude M occurs, the intensity of shaking at each EPSS, TS and Community component site was computed using the ground motion attenuation relations for a rock site (Campbell & Bozorgnia 2008).

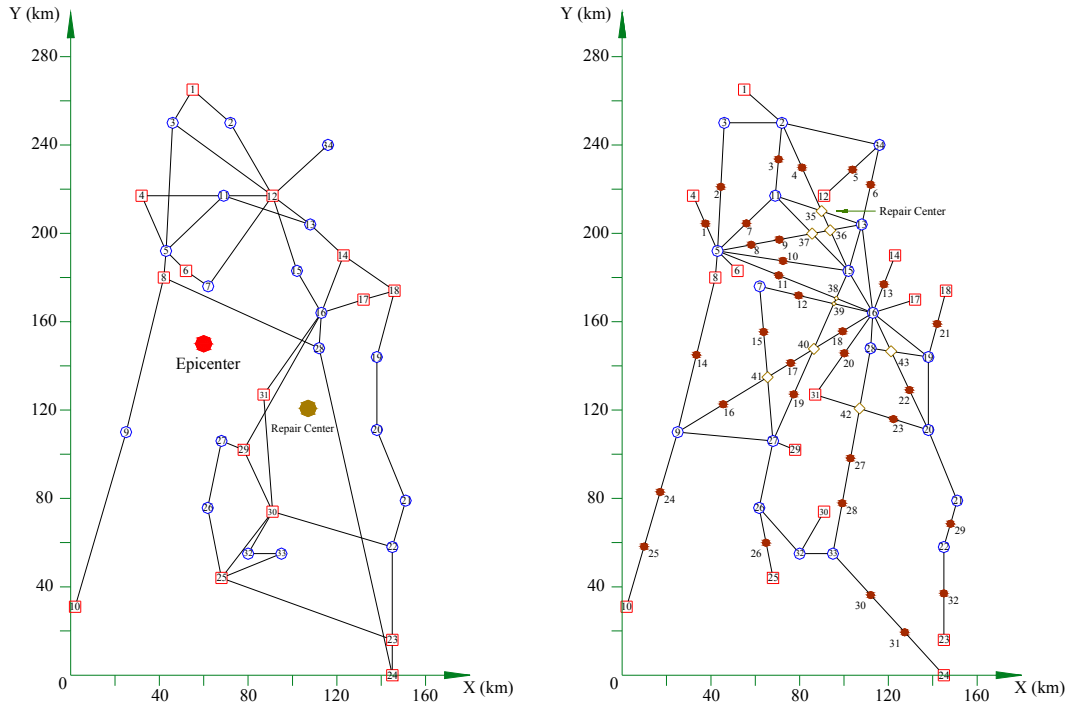

(a) EPSS (b) TS

Fig. 4.1. Topology of the virtual EPSS-TS-Community system

4.2.1. Community Resilience Simulation

The resilience of the EPSS-TS-Community system is modeled using the compositional supply/demand framework. The state of the electric power supply and demand is modeled through the earthquake damage Absorption and Recovery phases. The Absorption phase is a

relatively short period immediately following the earthquake when the EPSS-TS-Community systems is accumulating damage (direct and cascading) and finding a new equilibrium at a substantially lower functionality level.

Damage to the EPSS components and the Community built environment components is computed using seismic vulnerability functions, expressing the probability that each component will retain a certain portion of its functionality conditioned on the intensity of the earthquake ground motion at its location. The decrease of power supplied by the EPSS and the decrease of the power consumed by the Community was assessed in proportion to the loss of component functionality using a model of EPSS operation, a so-called power dispatch model.

In this Chapter, only the bridges within the TS were considered to be vulnerable to earthquakes. Earthquake-induced damage to the bridges was classified into three damage states (DS1: no damage; DS2: slight to moderate damage; and DS3: extensive damage or collapse) using the fragility function developed by Zheng et al. (2013). Bridges in both damages states DS2 and DS3 were considered to be closed to all traffic immediately after the earthquake.

After the Absorption phase, the EPSS-TS-Community system enters a considerably longer Recovery phase. Resumption of function of the EPSS was modeled by the developed ABM while the Community components were done using recovery functions (RFs). The ability of the EPSS to deliver power was computed at each decision point considering the current state of the EPSS components (improved by the repairs) and a seismic contingency dispatch strategy to balance the EPSS and prioritize the supply to communities that have the largest post-earthquake demand (SCDS 1 in Section 3.4.5). The ability of the Community to consume electric power is determined at each decision point considering the current state of the Community built environment components (improved by the repairs).

Recovery of the traffic function of the damaged bridges was modeled as follows. For bridges in DS2, the rate of function recovery was assumed to be presented by the Efficiency attribute of the TS Operator agent. Nevertheless, the recovery process for the severely damaged bridges that are in DS3 was modeled using recovery functions to take into account that the repair or, perhaps, rebuilding of such bridges may take a significantly longer time. The parameters of the recovery functions for TS bridges in DS3 are shown in Table 4.1. Note that two recovery functions are used to express different probability distributions of time to full restoration of bridge traffic in cases when the Administrator agent is inactive or active.

Table 4.1. Parameters for the recovery function of severely damaged bridges in DS3

Administrator	Mean (Days)	Std. (Days)
Does not intervene	150	90
Intervenes	90	60

4.2.2. Agent Parameters

The attributes of the EPSS and TS Operators and Administrator agents are random variables. The probability distribution function types and the value bounds of these attributes are listed in Table 4.2. The specific values of the agent attributes are determined once, at the beginning of each post-earthquake recovery simulation.

For instance, the V_e attribute of the EPSS Operator has a uniform probability distribution and takes values between 8 and 10 km/h. Note that at every decision point, the EPSS Operator computes the shortest path for the repair crew to travel from the current to the next repair location using the current traffic function state of the TS. This is the point where the EPSS and TS interact. Similarly, the V_t attribute of the TS Operator is randomly set to between 7 and 8 km/h and the next repair location is computed as the nearest one given the current function state of the TS.

Table 4.2. Attributes of the **EPSS Operator**, **TS Operator** and **Administrator** agents

	Distribution	Lower Limit	Upper Limit
EPSS Operator			
V_e (km/h)	Uniform	8 km/h	10 km/h
E_{eg} (per day)	Uniform	20%	40%
E_{ed} (per day)	Uniform	50%	100%
TS Operator			
V_t (km/h)	Uniform	7 km/h	8 km/h
E_b (per day)	Uniform	40%	80%

* M is the earthquake magnitude.
** Speed attributes for both the EPSS and TS Operator agents are reduced by length scale of 5.

A constant repair rate is specified using the E_{eg} and E_{ed} attributes in terms of the portion of functionality of a component repaired per day. In this simulation, duration of repair the EPSS supply substations to full functionality is computed using such constant repair rate. For example, E_b is uniformly generated as 50% (as the lower and upper bound are 40% and 80%, respectively) in one simulation. The needed time to restore the functionality of one damaged bridge should be 2 days, as the seismically damaged distribution substations and bridges are set to be in the failed state (i.e. the loss is 100%).

The repair rates and durations assumed here refer to the assumption that there is only one single repair crew for the generation substations, distribution substations, and the bridges, respectively. While additional simulations need to be conducted with multiple repair crews, the obtained results can be calibrated and adapted.

4.2.3. Community Recovery Performance Check

Resilience of the EPSS-TS-Community system is quantified by tracking the difference between the electric power delivered by the EPSS and the electric power consumed by the Community at each decision point during a post-earthquake recovery process simulation.

In this Chapter, the community **Administrator** is assumed to perform a Resilience Check by comparing the *PPwoP* 72 hours after the earthquake to a pre-defined threshold (SPUR 2009). In the following case studies, the threshold values of PPwoP for Administrator to assess the restoration are set as 10%, 20% and 30%, respectively. As mentioned in Section 4.1.3, the recovery process is deemed unsatisfactory, and thus the Administrator agent will intervene to speed it up if the attained *PPwoP* value is larger than the set thresholds. In those cases, the EPSS Operator repair schedule is changed such that the most severely damaged EPSS components are repaired first, its Speed attribute is increased by 10% and its Efficiency attribute was doubled. The TS Operator repair schedule is not changed, but its two attributes will also be updated in the same way. In addition, the estimated repair time for bridges in DS3 is shortened (Table 4.1).

4.3. EPSS-TS-Community System Behavior

The post-earthquake damage absorption and recovery process of the case study EPSS-TS-Community system was investigated by conducting simulations in a Monte Carlo (MC) setting. Two cases are investigated separately. First, the simulations were conducted without the Administrator agent, in order to observe the behavior of the system where Community performance objectives are neglected and the only interaction is between the EPSS and the TS Operators that impacts the travel time of the EPSS repair crews. Second, the simulations were conducted with the Administrator agent, allowing the Community to interact with the EPSS and TS Operators and assert its post-earthquake recovery performance objectives. The effects of agent attribute values and earthquake magnitude were investigated in each case. The duration of the post-earthquake recovery process was set to 360 days. In each analysis, the statistics of the resilience indicators are derived from 2,000 Monte Carlo simulations.

4.3.1. The case without the Administrator agent

The medians of the EPSS electric power generation capacity for four earthquake magnitude levels M equal to 6, 6.5, 7, and 7.5 are shown in Fig. 4.2.

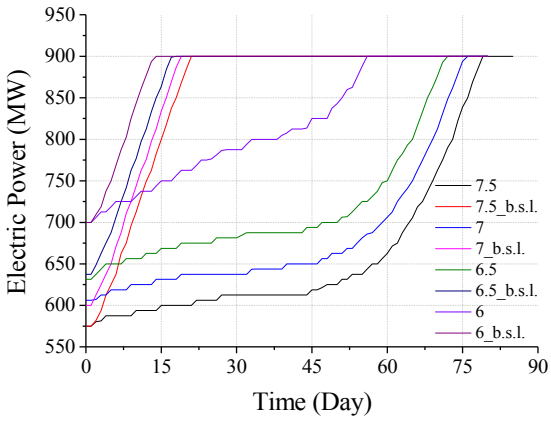

Fig. 4.2. Median generation capacity curves in the "baseline" and "intertwined" scenarios

Two scenarios are examined: the "baseline" scenario, computed assuming that there is no damage to the TS, and the "intertwined" scenario, where damage to the TS is considered in the simulations. The difference is found to be significant. The "intertwined" system takes much longer to recover (56, 72, 76 and 79 days, respectively) than the "baseline" system (14, 18, 19 and 21 days, respectively). This result indicates that post-earthquake recovery simulations without considering the interaction among the community CI systems may produce unconservative estimates of the community recovery times, more so for more intense earthquakes.

The reason for a significant prolongation of the post-earthquake recovery in the "intertwined" scenario is the idling of the EPSS repair crew while it is waiting for the TS repair crew to complete various bridge repairs. In more intense earthquake simulations (M>6), there is a change in the rate of generation capacity increase about 50 days after the earthquake, when the bridges critical for EPSS repair were repaired and open for traffic. Conversely, given the assumed agent parameters, the TS Operator seems to be the bottleneck for recovery after strong earthquakes. Simulations at lower intensities (M<6.5) indicate that TS damage and recovery affects the EPSS recovery to a lesser extent.

In order to investigate the evolution of the randomness of the recovered functionality of EPSS during the entire recovery process, the probability distribution of the results from the MC simulation at every time points also needs to be considered. To be representative, the histograms of the result attained immediately after, and on the 60th day after the earthquake, are presented in Fig. 4.3. The blue curves in both Fig. 4.3 (a) and (b) present the normal distribution derived from the mean and the standard deviation of the corresponding MC dataset. It can be found from Fig. 4.3 (a) that the power generation capacity of EPSS immediately after the earthquake follows the normal distribution, although it is contingent on many stochastic influential factors. However, as the restoration proceeds, the system will be fully recover in many individual MC simulations. The resulting histogram in Fig. 4.3 (b) deviates from the normal distribution because the system-

level generation capacity reaches 900 MW in these full-recovery cases. Mathematically, the median will be larger than the mean due to the truncation effect.

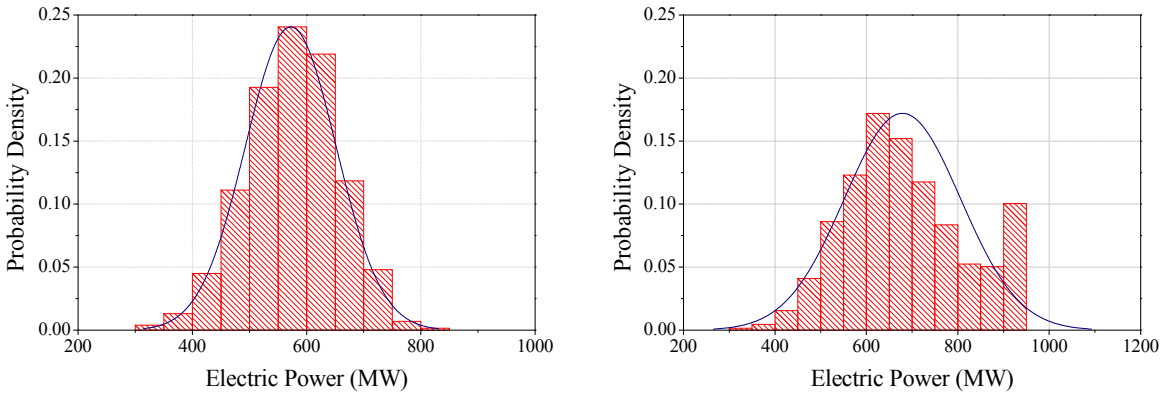

(a) First day (b) 60th day

Fig. 4.3. Histogram of EPSS generation capacity in the "intertwined" scenario

The evolving power deficit *PD(t)* of the EPSS in the M=7.5 "intertwined" scenario (*Section 3.3.2*), tracked as the gap between the time-varying Deliverable Power *DP(t)*, and the power Demand *D(t)*, is shown in Fig. 4.4. Before the earthquake, the EPSS supplies 900 MW of electric power and covers the 733 MW of community demand.

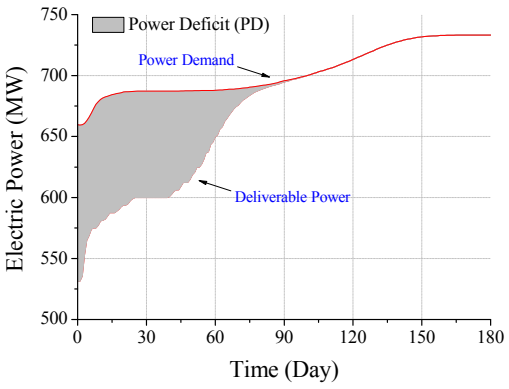

Fig. 4.4. Median of the deliverable power (*DP*) and power demand (*D*) for a M=7.5 earthquake in the "intertwined" scenario

Immediately after the earthquake, the median demand *D(t)* decreased to around 660 MW as the earthquake damage is absorbed in the community. Meanwhile, the median power generation capacity drops to 575 MW. Further, due to failure of transformers and losses of transit capacity, the median of deliverable power *DP(t)* decreased to 531 MW. Thus, the EPSS is not able to

satisfy the demand anymore. The shaded area in the figure refers to the period of power deficit (*PD*) and is termed "lack of resilience". Similar to Fig. 4.2, the *DP(t)* remains almost unchanged over the first three days and then start to increase. The gap between the *DP(t)* and *D(t)* reduces, and disappears on the 102th day after the earthquake. However, it took 165 days for the community power demand to be restored to the pre-disaster level. The supply delivered by the EPSS was able to follow this increase in demand without problems.

The evolving functionality of TS under in the "intertwined" scenarios is shown in Fig. 4.5 for the four earthquake intensities. The number of operational bridges (DS1) was 7, 8, 9 and 12 for magnitude 7.5, 7, 6.5 and 6 earthquakes. The bridges in DS3 delay the recovery process, evident in the change of slope of the functionality curves. The duration to full TS recovery (all bridge repaired) is quite similar for the four earthquake magnitudes (78 days for M=7.5 and 76 days for M=6).

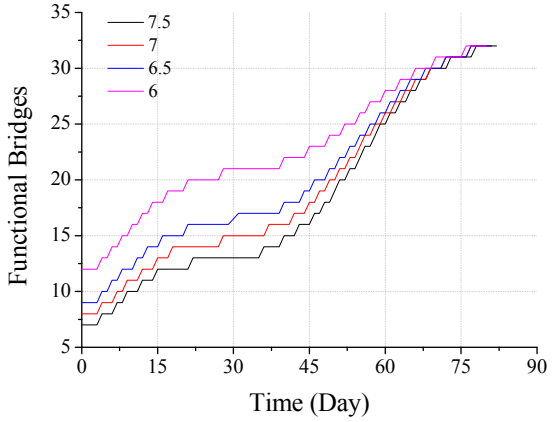

Fig. 4.5. Median of the TS function recovery of TS in four "intertwined" earthquake scenarios

Fig. 4.6 illustrates the evolution of the median values of the *PPwoP* system resilience measure. The "baseline" and the "intertwined" scenarios are compared in Fig. 4.6 (a), indicated significant difference. For more intense earthquakes (M=7.5, 7, 6.5) it took 64, 61 and 54 days to provide electric power to the entire population in the "intertwined" scenario and only 9, 8 and 7 days in the "baseline" scenario, indicating again a very critical role the TS plays in the recovery of the EPSS. However, for the M=6 earthquake, it only took 13 and 4 days, respectively, to supply the entire population, principally because that the initial functionality loss at this earthquake intensity was much smaller than in the stronger earthquakes, while the damage to the community built environment (i.e. demand) was still significant. Therefore, the EPSS can cover the power demand much sooner, even though it still took more than 50 days for the "intertwined" EPSS-TS to fully restore the power generation capacity (Fig. 4.2).

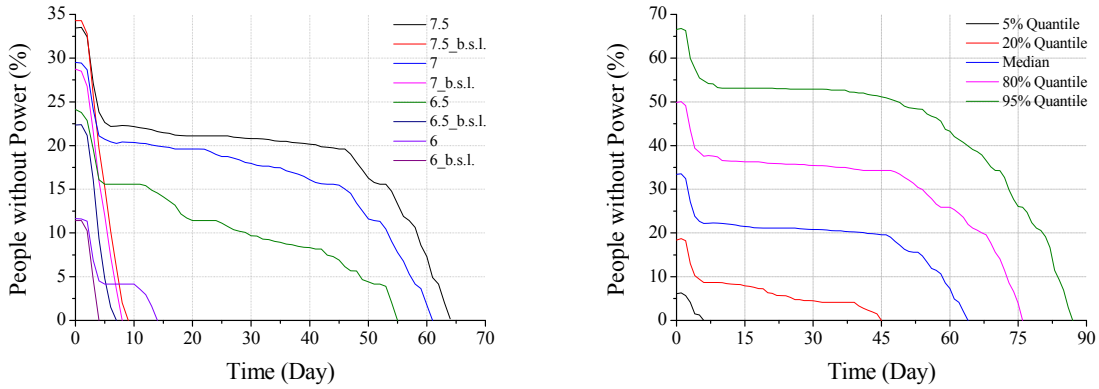

(a) Comparison of different scenarios (b) Randomness in the M=7.5 "intertwined"

Fig. 4.6. Evolution of the PPwoP system resilience measure

In Fig. 4.6 (b), the evolution of the randomness associated with the *PPwoP* system resilience measure for the M=7.5 earthquake and the "intertwined" scenario, was plotted. Note that the median *PPwoP* remained virtually constant (at about 20%) from day 7 until day 45 after the earthquake. This can be very demanding for the population. The 5%, 20%, 80% and 95% quantile curves indicate that the randomness is large, and that it affects the *PPwoP* measure equally across the entire time period of observation.

4.3.2. The case with the Administrator agent

The effects of the interaction between the Community and the EPSS and TS are shown by comparing the simulations conducted with and without the Administrator agent. As discussed hereinbefore, four scenarios are investigated. Namely, in simulations with the Administrator, at the Resilience Check Time, set at 72 hours after the earthquake, the attained *PPwoP* value is compared to 10% (most demanding), 20% and 30% (least demanding) thresholds to determine if the post-earthquake recovery process is satisfactory or not form the community standpoint. If the attained *PPwoP* in a simulation exceeds the threshold, the repair plan of the EPSS Operator is inverted and the attributes of the CI agents updated to increase the rate of recovery, as specified in Section 4.1.3.

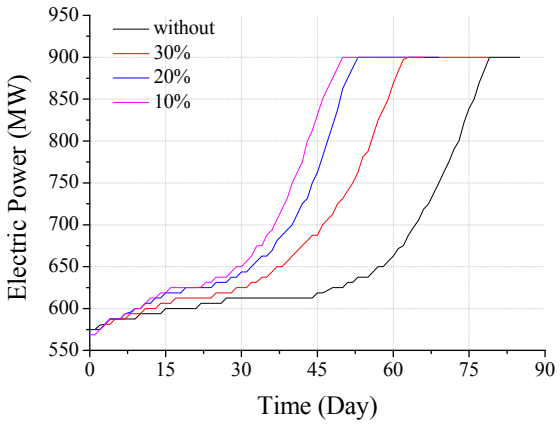

Fig. 4.7. Median of recovery of the power generation capacity for three PPwoP threshold values for the M=7.5 earthquake

Fig. 4.7 presents the median of the generation capacity of intertwined EPSS-TS-Community system after earthquakes of magnitude M=7.5 for the three threshold values of *PPwoP*=10%, 20% and 30%. For comparison, the case without the activation threshold, i.e. without the Administrator agent, is also plotted. The effect of intervention to speed up the post-earthquake recovery process is significant, particularly in the case of the 10% *PPwoP* threshold, when it took 50 instead of 79 days (Fig. 4.2) for the EPSS to fully recover the power generation capacity. The effect of the interference from the Administrator is also evident at higher *PPwoP* decision thresholds, but was not as strong.

Similar to Fig. 4.3, Fig. 4.8 presents the histograms of the data from the conducted 2000 MC simulations (and the fitted normal distribution) for the gross generation capacity of EPSS immediately, and on the 60th day after the earthquake. It reveals that the probability distribution of the gross generation EPSS capacity is almost the same as that shown in Fig. 4.3(a), which matches the assumption that the Administrator will only check the resilience behavior of the CIs system 72 hours after the seismic event.

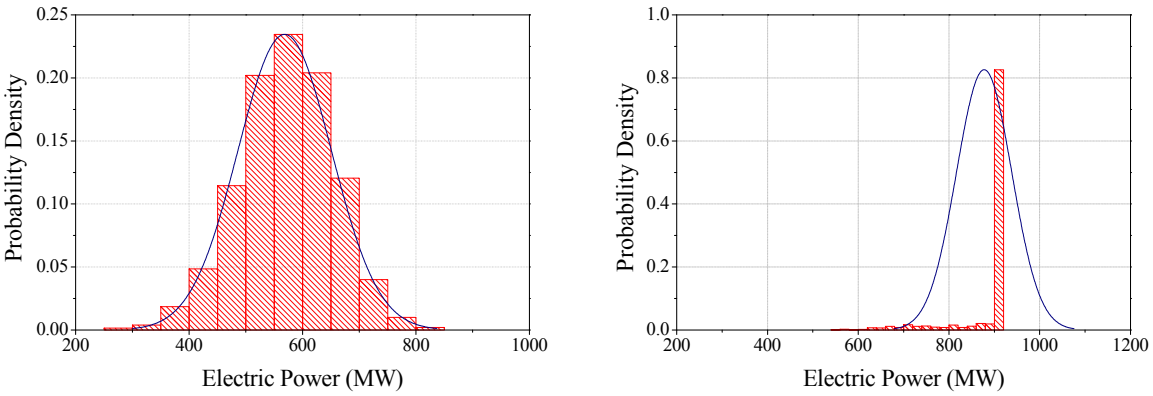

(a) First day (b) 60th day

Fig. 4.8. Histogram of EPSS generation capacity with intervention of the Administrator

The overwhelming majority of the system-level functionality has been fully recovered after 60 days, as shown in Fig. 4.8 (b). Thus, the normal distribution fit is poor. By comparison with Fig. 4.3(b), the favorable effect of the intervening Administrator is clear.

The effect of Administrator intervention is similar for the TS. As shown in Fig. 4.9, the full recovery of TS is shortened by 26 days for the *PPwoP* threshold value of 10%. The recovery trajectory is roughly the same as this value is set to be 20%. However, as the Administrator becomes more tolerable and defines the *PPwoP* threshold at 30%, the effect of its intervention becomes less pronounced. It indicates that the community recovery performance threshold can have a significant impact on the recovery path of the CI-Community system. The recovery performance objective should be set low enough so that the Community can intervene and speed-up the recovery process, but not too low such that the recovery priorities of the CIs are completely neglected.

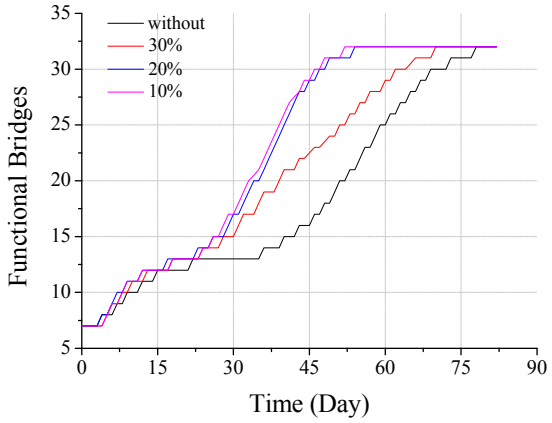

Fig. 4.9. Median of recovery of the TS for three PPwoP threshold values for the M=7.5 earthquake scenario with Administrator intervention

The data on the rate of *PPwoP* reduction shown in Fig. 4.10 also indicates that the intervention of the Administrator to speed up the recovery process can be very effective. The resulting *PPwoP* evolution trajectories are significantly different compared to the case without intervention. Most importantly, the long horizontal "plateau" shown in Fig. 4.6 did not appear anymore, revealing that the Administrator fulfilled its task. For the threshold of 10%, it only takes 38 days to lift all the people out of power outage, which is 40% shorter than the case without intervention.

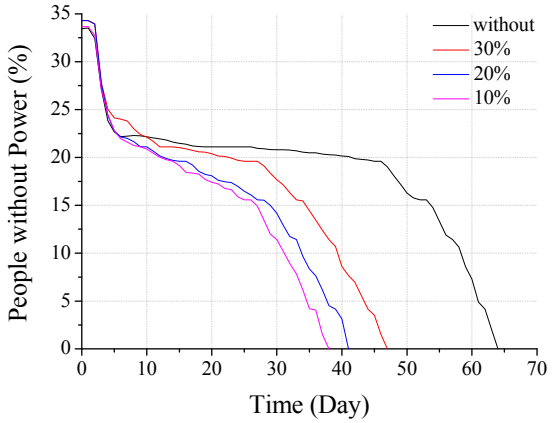

Fig. 4.10. The evolution of *PPwoP* median for different *PPwoP* threshold values for the M=7.5 earthquake scenario

4.4. Conclusions

The modern CI-Community system is a dynamic and integrated socio-technical network. The compositional supply/demand framework with agent-based recovery models for computing the post-earthquake recovery path of single CI was extended in this Chapter to include multiple interdependent CIs. The interdependence between different CIs was taken into account, and its impact on the resilience behavior of the integrated system was examined. The recovery trajectories of the CIs were shaped employing an Agent-Based Modeling paradigm to account for the different strategies and capabilities of the entities involved in the recovery campaign.

The case study based on the IEEE-118 Benchmark System was established and **EPSS Operator, TS Operator,** and **Administrator** agents were defined. A set of Monte Carlo simulations was run to test the proposed ABM framework and to examine the influence of different earthquake scenarios and agents' behavioral attributes on the resilience of the integrated CI-Community system.

According to the simulation results, it was found that:

1. The developed framework could be employed to capture the seismic resilience behavior of the integrated CI system;
2. The agent-based approach was revealed to be flexible and representative of the dynamic behavior of the involved players during the seismic recovery process;
3. The interdependence among the infrastructure systems, as well as the interplay with the community post-earthquake recovery performance objectives, was demonstrated to remarkably influence the CI-Community system recovery path.

For the real-world cases, the interdependence mechanisms between EPSS and different CIs are varied and can be even much more complicated than the ones modeled in this Chapter. Their recovery paths would therefore be more closely entangled, and thus more challenging to comprehend. The proposed framework in this Chapter should be further advanced to rationally account for such realistic CI and Community interdependencies during the post-earthquake recovery period.

5. Network-theoretical model for the recovery of EPSS

The case study carried out in Chapter 4 has already revealed that the recovery of the community EPSS depends remarkably upon the status (and the recovery) of the community TS after an earthquake. Meanwhile, as indicated by the review on the state-of-the-art in Chapter 2, the efficient and timely recovery of these two CI systems depends on the available repair resources and crews (Chang et al. 2012, Cimellaro et al. 2016, Zhao et al. 2016).

In this Chapter, a network-theoretical model is proposed to gauge the impact of the amount of the available community repair resources, on the post-earthquake recovery of the EPSS and the TS and the resilience of the coupled EPSS-TS system.

5.1. The network-theoretical model

For the sake of simplicity and without loss of generality, two interdependent CI systems, namely, the TS and EPSS are considered in the model. The gross number of the unit repair resources disposable by the entire community is denoted as R (The value of R will always be set as even integer, to facilitate the simulations in the case study hereinafter). The initial amount of the available resources for the repair of EPSS is set to γR ($0<\gamma<1$). Correspondingly, the amount of resources for the repair of TS is therefore $(1-\gamma)R$. Both are rounded to the nearest integer.

Post-earthquake resilience of the coupled EPSS-TS systems will be examined separately in the "absorption" and "recovery" periods, using the compositional supply/demand framework presented in Chapter 3.

5.1.1. Configuration of the physical networks

In this model, the two systems were configured as overlaid (Andersen et al. 2001). The TS is represented as a rectangular grid spanning the 160x280km region (similar to the region spanned by the virtual EPSS-TS-Community system used in Chapters 3 and 4), as shown in Fig. 5.1. The EPSS is constructed by randomly placing its substations (pink dots) at the same coordinates where the crossings of the road of the TS are. Meanwhile, the TS bridges (green dots) are always located in the mid points between road crossings. Under earthquake hazard, as presumed in Chapter 4, both EPSS substations and TS bridges can be damaged, whereas roads are assumed immune to earthquakes. However, note that any single road (between two grid nodes) can be removed from the TS network if a bridge on it is damaged and remain in this state until the bridge is reached by a repair crew and repaired.

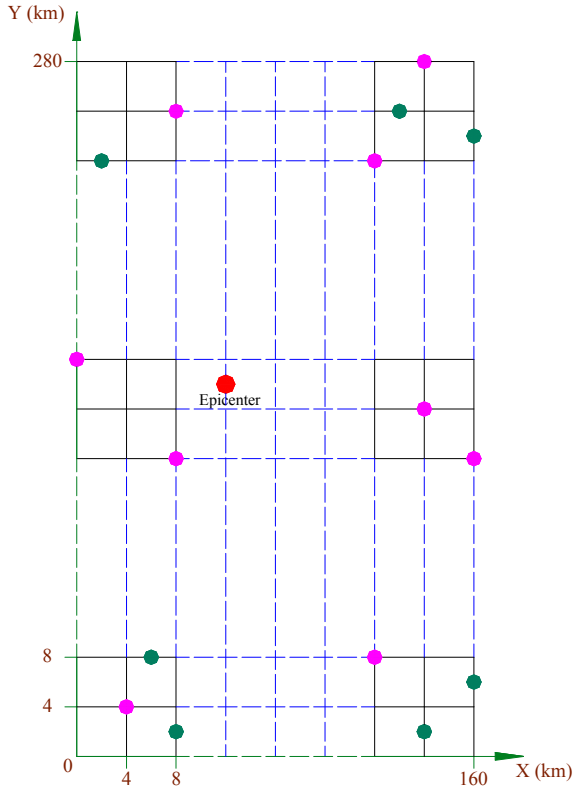

Fig. 5.1. The topology of the overlaid EPSS-TS system

5.1.2. Absorption stage

For both CI systems, similar to Chapters 3 and 4, the damage states (DSs) of all the components are determined by means of vulnerability functions (VFs). In particular, only two seismic DSs, namely, fully functional and non-functional, will be considered for the nodes (substations) of the EPSS.

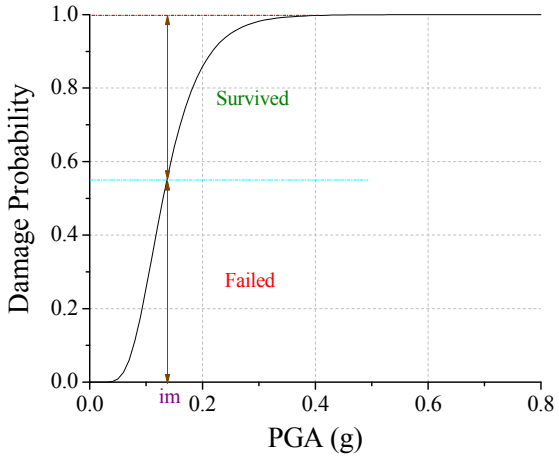

Fig. 5.2. Fragility model of EPSS substations

Specifically, the fragility model of the high-voltage substations with unanchored EPSS components (Syner-G 2015) was adopted. It should be noted that four seismic damage states (minor, moderate, extensive and complete) were considered, and that the EPSS component can lose its functionality if it is in either extensive or complete damage state. Therefore, the fragility functions associated with the moderate damage states were employed in this Chapter to determine the post-earthquake functionality of the EPSS nodes (Fig. 5.2). By contrast, three DSs were taken into account for the bridges in the TS. Besides the fully functional (DS1) and the collapse (DS3), moderate damage (DS2) was also considered. The corresponding seismic fragility models were the same as those adopted in Chapter 4. In addition, like Chapters 3 and 4, the NGA model was still employed as the earthquake intensity attenuation function.

The selected vulnerability functions simplify the simulations and are not meant to represent the seismic vulnerability of bridges in real TS. Meanwhile, note that the functionality of the two networks is assumed not to be dependent upon each other during the post-earthquake absorption stage.

5.1.3. Recovery stage

In this model, both EPSS and TS are assumed to enter the recovery stage immediately after the "absorption" stage, i.e. no time is set aside for damage assessment and recovery planning. As extensively discussed in Chapter 3, the post-earthquake recovery of CIs is dynamic and stochastic. More importantly, unlike in the "absorption" stage, the recovery path is contingent on the decision-making in terms of the repair strategy and the distribution of the available repair resources, both involving CI Operators and the community Administrator. Only the "random repair" strategy (Hu et al. 2016) will be employed in this model.

Throughout the entire recovery stage, the time-varying number of damaged TS nodes and the available repair unit resources are denoted and tracked as $D_t(t)$ and $R_t(t)$. Note that these are also integers with $R_t(0) = (1-\gamma)R$. It is further assumed that a single unit of recovery resources is sufficient to affect repairs on a single damaged element of the EPSS (substation) or the TS (bridge). In every time step of the recovery simulation, in order to determine the recovery priority for the set of the remaining damage nodes of the TS, $D_t(t)$ is computed first and compared with $R_t(t)$. In case when $D_t(t) > R_t(t)$, which means the available repair resources are not able to cover all the damaged bridges, $R_t(t)$ will be zero in the next step, and $R_t(t)$ bridges out of $D_t(t)$ will be randomly selected and repaired. If, on the other hand, $R_t(t) \geq D_t(t)$, repair is started on all of the damaged bridges and lasts until the bridges are again fully functional.

The repair duration for every single damaged bridge in either DS2 or DS3, is model in a "black−and-white" way. Taking the bridge in DS2 as the example, it can be restored and become fully functional again 3 days after the repair has been started. Note that the starting time point is not necessarily the time when the recovery process starts after an earthquake, but it is the date

when a repair resource has become available. The repair time for a bridge in DS3 (collapse) is set to 150 days.

The unit repair resource dispatched to repair any single bridge will be available again (and can be mobilized to repair the other failed bridges) when the bridge becomes functional again, and the R (t) will therefore be updated correspondingly.

The recovery path for an EPSS substation is defined in a different way. Since only two damage states are considered, functional or no-functional, for an EPSS substation, the recovery probability is quantified by the cumulative distribution function of the exponential distribution type with the mean value of 6 days:

$$P(t) = 1 - exp(-\frac{t}{6}) \quad 5.1$$

As shown in Fig. 5.3, in every time step t of the simulation, a randomly generated number is compared with the corresponding value of Equation 5.1. As in Section 3.2.2, the EPSS substation is considered to be repaired when the generated number is smaller than the value computed from Equation 5.1. As for bridge, the unit repair resource becomes available again when the repair of an EPSS substation is completed.

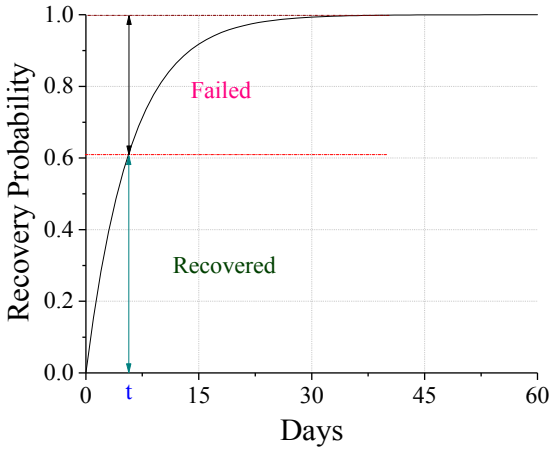

Fig. 5.3. The recovery for single damaged substation

5.1.4. Dependency between two systems

The dependency between TS and EPSS emerges in the recovery stage (Chapter 4). In this model, it is assumed that the starting time step for the repair of a damaged EPSS substation is the time step when the needed unit repair resource is available and when this EPSS substation is within

the Largest Component (LC) of the TS (Di Muro et al. 2016), i.e. when the damaged EPSS substation is considered to be reachable by a repair unit using the available TS. This represents the physical link between the two CIs.

Immediately after an earthquake, the topology of the TS network will change significantly as many of the links (Fig. 5.4) are removed due to damage incurred by bridges on these links. Specifically, the TS network will be fragmented into a set of clusters (nodes connected by remaining links) of different sizes (number of nodes in the cluster). LC is the cluster with the largest number of nodes (Newman et al. 2001), as shown in Fig. 5.4. In this illustration, only the substations on green nodes will be reachable by repair crews and repairable, whereas the repair of all others damaged substations (isolated or in smaller clusters) can start only when the TS bridges are repaired such that they become a part of the LC and, thus, become reachable by a repair crew. Thus, the evolution of the repair resources for EPSS substations R_e (t) is the same that for R_t (t) (Equation 5.4) with the additional dependency on the repair process of the TS network established through the LC concept. The EPSS and TS recovery continues until the all damaged components within the two CIs are fully restored, typically 3600 days in the conducted simulations.

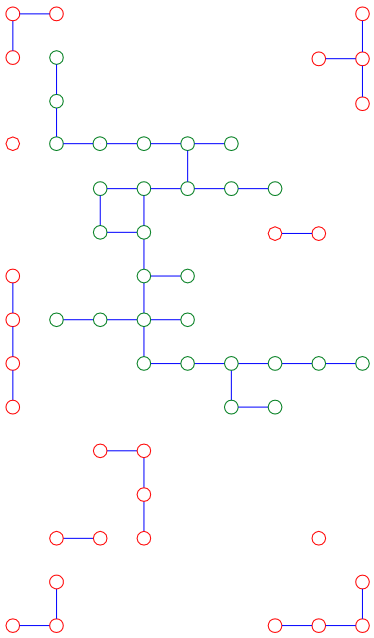

Fig. 5.4. An illustration of the Largest Component (blue links and green nodes) of the TS

5.2. Application of the model

The model was applied on a virtual coupled EPSS-TS system, shown in Fig. 5.1. A regular lattice is constructed over a 160x280km area, by dividing it into the set of squares with the side length of 4 km. A total 2911 (41×71) nodes are thus created. Those 2911 nodes, and the corresponding

(41×70+71×40) 5710 links constitute the TS. 800 EPSS "substations" are randomly placed on the lattice nodes, while 3200 bridges are randomly located on (the middle points of) the links, respectively. As introduce hereinbefore, the EPSS and TS are generated by the randomly placed nodes at the very beginning of every single MC simulation. An earthquake scenario is created by selecting an earthquake magnitude. In all simulations, the epicenter was assumed to be at node (60, 150) km and did not change. A total of 100 MC simulations are conducted for each earthquake scenario. The size of the network area will be reduced by 5, like in Chapters 3 and 4.

For the sake of simplicity, the functionality level for both TS and EPSS was measured by the total number of functional nodes within the system, in each simulation time step.

5.2.1. Recovery of the coupled EPSS-TS system under constant amount of repair resources

Fig. 5.5 presents the EPSS recovery time for earthquake scenarios with different magnitudes. Bound by the NGA earthquake intensity attenuation model, only magnitudes from 4.5 to 7.5 were considered. The amount of available repair resources R was set to 200 and the ratio γ specifying the distribution of these resources between the EPSS and the TS was set to 0.5. Meanwhile, as the demand from the community is not modeled here, three different recovery targets, namely 95%, 93.75% and 90% of the pre-earthquake electric power supply level were considered in order to examine the systemic resilience given different functionality requirements.

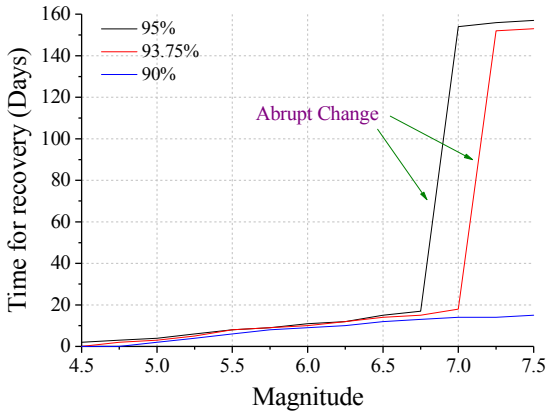

Fig. 5.5. Recovery time for the median EPSS functionality for different earthquake magnitude scenarios

Abrupt changes in recovery time, indicating a recovery regime change and substantially longer time for the recovery, was observed for the 95% and 93.75% recovery targets. They occurred at different earthquake magnitudes. Considering the case of 95% recovery target, the recovery time for the EPSS was always below 20 days and increased very slightly for earthquake magnitude 4.5

to 6.75 scenarios. Note, however, a dramatic increase in the recovery time as the earthquake scenario magnitude increased to 7.0 and above. Specifically, the recovery time increased from 17 days for M=6.75 scenario to 154 days for the M=7.0 scenario. The rate of recovery time increase becomes much slower as the magnitudes reach up to 7.25 and 7.5. For the earthquake magnitudes considered, the recovery time was shorter than 15 days for the 90% recovery threshold.

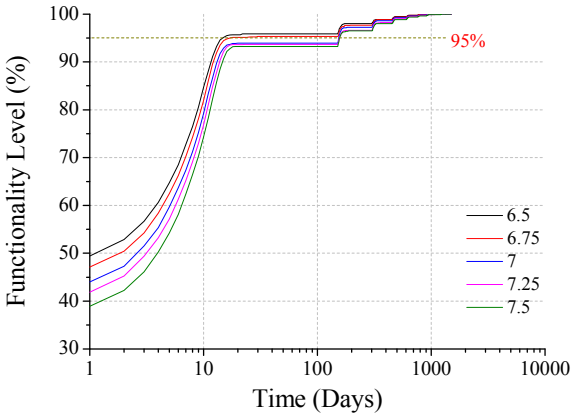

Fig. 5.6. The median of the EPSS functionality for different earthquake magnitude scenarios

The functionality level of the EPSS was tracked for different earthquake magnitude scenarios and is presented in Fig. 5.6 (scenarios with magnitudes lower than 6.5 are not shown). The recovery trajectories comprise a set of horizontal lines, indicating constant functionality over a prolonged period of time, and a set of sudden increases of functionality over relatively short periods of time. It can be further observed that all EPPS functionality curves for magnitudes larger than 7 are below the pre-defined threshold level (e.g. 95% of pre-earthquake functionality) until the 150th day of the simulation, which also matches the result in Fig 5.5. This day signifies the recovery of many of the collapsed (DS3) bridges, and thus a significant increase of the LC of the TS network.

Fig. 5.7 shows the time-varying portion of inaccessible EPSS substations in different earthquake magnitude scenarios. In simulations with the 95% recovery target, the critical inaccessibility threshold is 5% (i.e. this is the portion of EPSS substations not in the TS LC). For earthquake scenarios with magnitudes larger than 7, the portion of inaccessible substations stayed above 5% until the 150th day when a set of collapsed bridges was restored, and the TS LC dramatically increase. In comparison, for the 6.75 earthquake magnitude scenario, less than 5% substations are outside the LC on the 10th day, meaning that the recovery target was achieved.

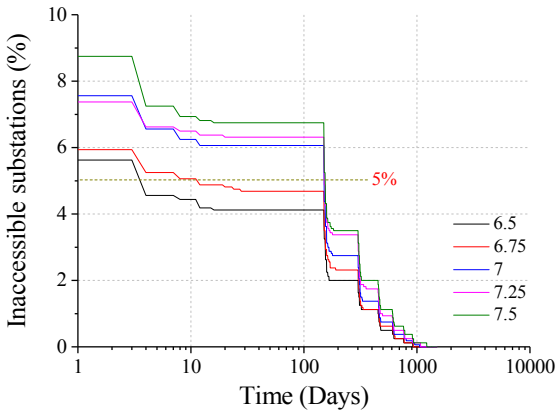

Fig. 5.7. The median portion of inaccessible substations under different earthquake magnitude scenarios

Fig. 5.7 shows the time-varying portion of inaccessible EPSS substations in different earthquake magnitude scenarios. In simulations with the 95% recovery target, the critical inaccessibility threshold is 5% (i.e. this is the portion of EPSS substations not in the TS LC). For earthquake scenarios with magnitudes larger than 7, the portion of inaccessible substations stayed above 5% until the 150th day when a set of collapsed bridges was restored, and the TS LC dramatically increase. In comparison, for the 6.75 earthquake magnitude scenario, less than 5% substations are outside the LC on the 10th day, meaning that the recovery target was achieved.

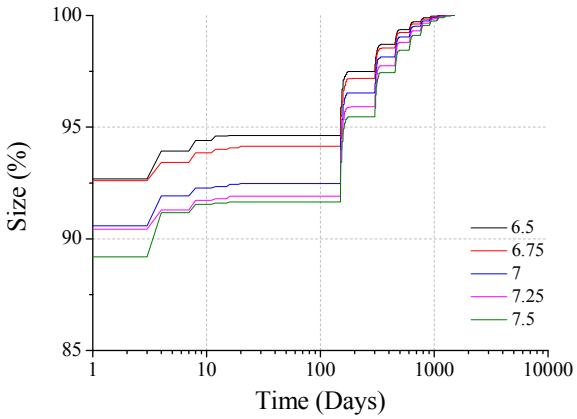

Fig. 5.8. The median of the LC size for different earthquake magnitude scenarios

As explained in Section 5.1.4, the number of inaccessible substations was contingent on the total amount of the initially damaged ones and the size of the LC. Fig. 5.8 shows how the size of the LC changes with simulation time. In all earthquake scenarios, it takes more than 1000 days for

the LC to be restored to the full TS network size. It is also evident that the trends in Figs. 5.7 and 5.8 are well-synchronized. The LC size (normalized by its full size in the pre-earthquake stage) in earthquake scenarios with magnitudes of 7, 7.25 and 7.5 are all considerably lower than in the other two scenarios, which indicates that substantially more substations are outside the LC, and thus unreachable by the repair crews.

Fig. 5.9 tracks the recovery of TS under different earthquake scenarios. The initial percentage of functional bridges (excluding the bridges in DS2 and DS3) decreases as the scenario magnitude increases. For the magnitude 7.5 scenario, only 30% of the bridges are operational immediately after the earthquake, whereas 40% of the bridges remained intact in the magnitude 6.5 scenario. The rebuilding duration was shorter by about 35% in the magnitude 6.5 scenario, compared to the magnitude 7.5 scenario.

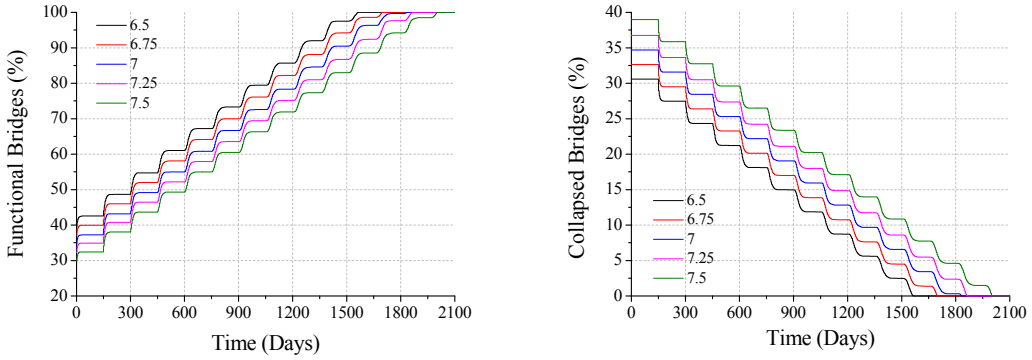

(a) TS network (b) Bridges in DS3

Fig. 5.9. The median restoration paths of bridges for different earthquake magnitude scenarios

Fig. 5.9 (b) examines the restoration trajectory of the collapsed bridges (DS3) that cause the bottleneck effect for the EPSS recovery, under different earthquake scenarios. Similar to Fig. 5.9 (a), nearly 40% of the bridges of TS were seriously damaged in the magnitude 7.5 earthquake scenario. It will then take more than 2000 days to fully restore all bridges. Given the same amount of resources, the repair rate was similar under all the earthquake magnitude scenarios. Hence, it will take 1561 days to rebuild all the collapsed bridges in the magnitude 6.5 scenario, proportional to the smaller number of damaged bridges compared to the magnitude 7.5 scenario.

5.2.2. Recovery of the coupled EPSS-TS system under varying amount of repair resources

The varying EPSS recovery times in a magnitude M=7.5 scenario given different repair resource amounts R are presented in Fig. 5.10. Following Section 5.2.1, the repair resources R is still distributed equally between EPSS and TS. As expected, the recovery of the EPSS is faster if the amount of resources R increases. Without loss of generality, only 95% recovery threshold was

considered hereinafter. Similar to Fig. 5.5, abrupt changes were observed while the total amount of the repair resources went higher. Specifically, the EPSS recovery duration decreased very slightly from 157 days to 153 days as the amount of the (unit) repair resources R increased from 200 to 450. However, EPSS recovery duration decreases abruptly to 23 days as the amount of the available repair resources reached 550. Thereafter, the EPSS recovery time stabilizes and continues to decrease slowly as the amount of repair resource increases.

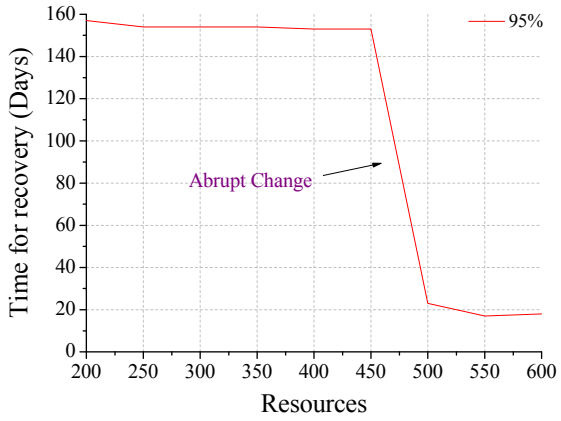

Fig. 5.10. Median EPSS recovery duration for different amounts of repair resources in a M=7.5 scenario

The recovery of the EPSS functionality in the magnitude 7.5 scenario was tracked for different amounts of repair resources and is presented in Fig. 5.11 (in order to be more informative, trajectories for repair resource amounts of 300 and 400 are not shown).

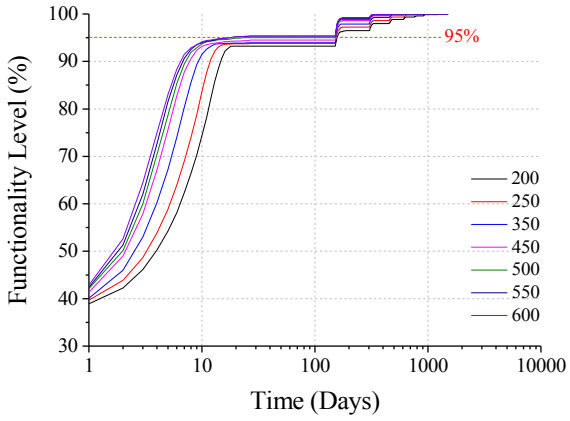

Fig. 5.11. The median of the EPSS functionality for different repair resource amounts in a M=7.5 scenario

The restoration of EPSS function is expedited with more repair resources. The recovery process enters the first "plateau" after 19 days in all examined cases, indicating that the EPSS repair crews are waiting for the inaccessible substations to be reachable again owing to the repair of the TS. Nonetheless, the functionality level of the EPSS system has already reached 95% for the cases where the amount of repair resources is higher than 500.

Fig. 5.12 tracks the evolution of the size of the TS LC in the magnitude 7.5 scenario with different repair resource amounts. The size of the TS LC undergoes a series of sudden increases, between which only minor changes occur. On the other hand, the TS LC size is recovering much faster a few days after the seismic event, owing to more available repair resources. In particular, the TS LC will be restored to about 98% after the first batch of collapsed bridges have been rebuilt in the 600 repair resource case. By comparison, this value is approximately 94% in the 200 repair resource case. This difference can significantly affect the number of the unreachable EPSS substations (waiting for the repair).

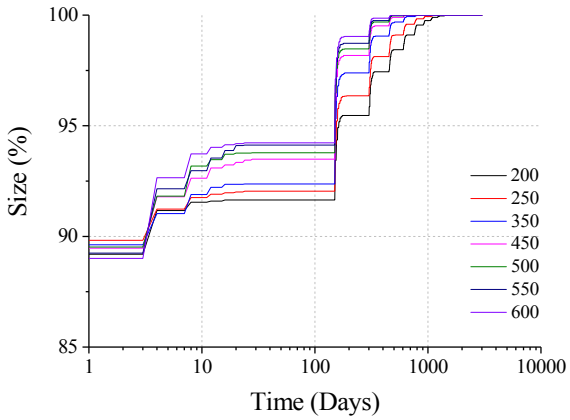

Fig. 5.12. The median of the TS LC size for different repair resources in a M=7.5 scenario

Fig. 5.13 tracks the evolution of the portion of inaccessible substations for different repair resource amount cases: the portion of inaccessible substations decreases as the TS bridges are being restored. In particular, the percentage of substations decreases to less than 5% only if the amount of repair resources is larger or equal to 500, before the first "plateau" that starts about the 20th day after the earthquake. Such observation matches well the results shown in Figs. 5.10 and 5.11.

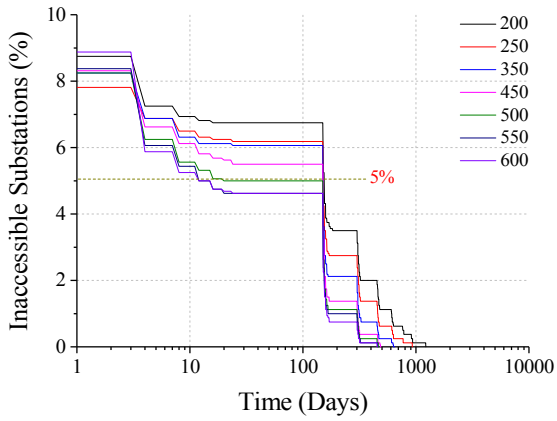

Fig. 5.13. The median portion of inaccessible substations for different repair resources in a M=7.5 scenario

5.2.3. Recovery of the coupled EPSS-TS system under varying distribution of constant repair resources

The restoration trajectories of the EPSS system in the magnitude M=7.5 scenario with R=200 repair resources and different values of the repair resource distribution factor γ are shown in Fig. 5.14.

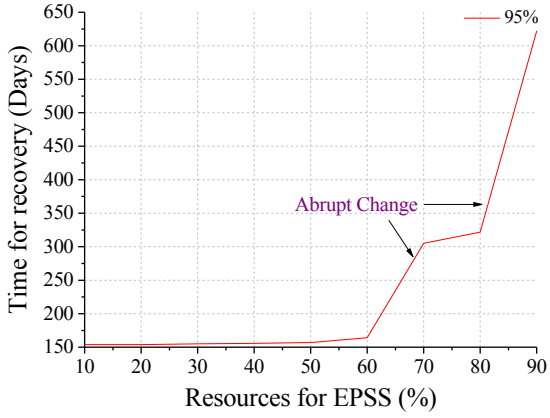

Fig. 5.14. Median EPSS recovery duration for different repair resource distribution ratios in a M=7.5 scenario

Counterintuitively, overall, it can be found that the more resources invested on EPSS, the slower the restoration will be. Meanwhile, for the 95% recovery thresholds, the abrupt changes of the repair duration are observed as a result of varying γ. specifically, the repair time suddenly

increases from 164 days to 305 days when γ changes from 60% to 70%. More importantly, the repair time continues to undergo another sharp increase, when γ reaches 80%. Note that the repair time remains almost unchanged when γ is less than 60%.

The functionality level of the EPSS was examined for different γ values, and is presented in Fig. 5.15. The EPSS functionality level reaches above 95% at the end of the first "plateau" (indicating the reconstruction of the first batch of collapsed bridges) if no more than 60% of the resources are invested on EPSS. In addition, the restoration will be significantly prolonged if the resources for EPSS recovery are above 70%: it will take 622 days for the EPSS system to reach 95% of its pre-earthquake functionality level if 90% of the resources are mobilized for EPSS repair, whereas only 154 days when only 10% of the resources are devoted to the EPSS.

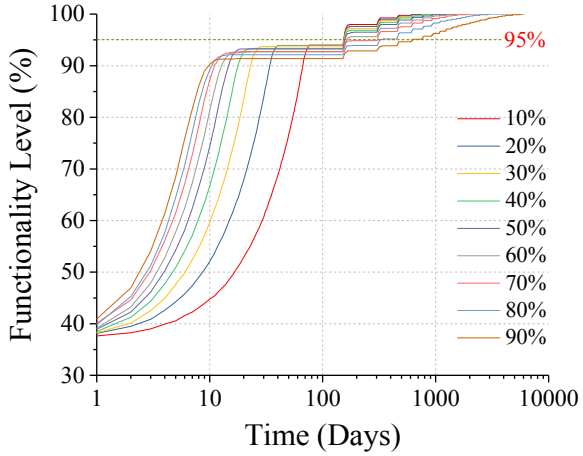

Fig. 5.15. The median of the EPSS functionality for different repair resource distribution ratios in a M=7.5 scenario

On the other hand, per Fig 5.15, it should also be noted that the more resources are helpful, but only in the earlier stages of the recovery process. In particular, the more resources are invested in EPSS, the earlier its functionality can reach the 90% level. With reference to the real-world cases, such observation indicates that the available repair resources could initially be invested in EPSS repair, especially if the emergency power supply is needed. However, later in the recovery process, the focus should shift to the TS in order to optimize and synchronize the entire restoration campaign.

Fig. 5.16 compares the recovery paths of the TS's LC for different γ values. The resources invested in the TS repair will decrease as γ is increasing. Thus, the resulting restoration of the TS LC will also be slower. In particular, for the case of when γ is 80% or 90%, it will take more than 3400 days for the TS LC to be fully restored.

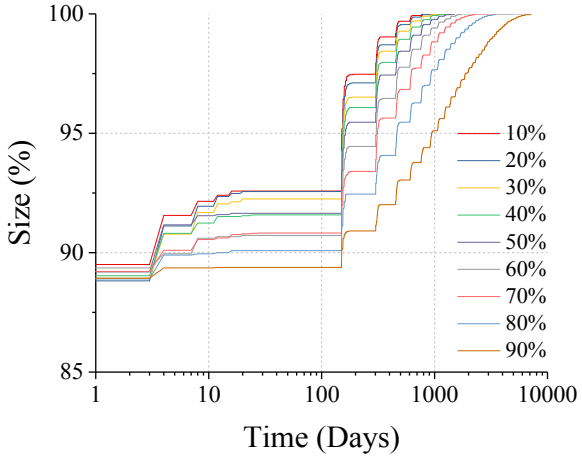

Fig. 5.16. The median of the LC size for different repair resource distribution ratios in a M=7.5 scenario

The evolution of the portion of inaccessible substations is tracked in Fig. 5.17. Similarly, it can be found that the time for the percentage of damaged inaccessible EPSS substations to decrease below 5% is similar for the γ values of 70% (301 days) and 80% (321 days), but is significantly longer compared to other cases with lower γ values. In addition, the time to reach the 5% inaccessible EPSS substation threshold is yet longer (619 days) in case of γ=90%.

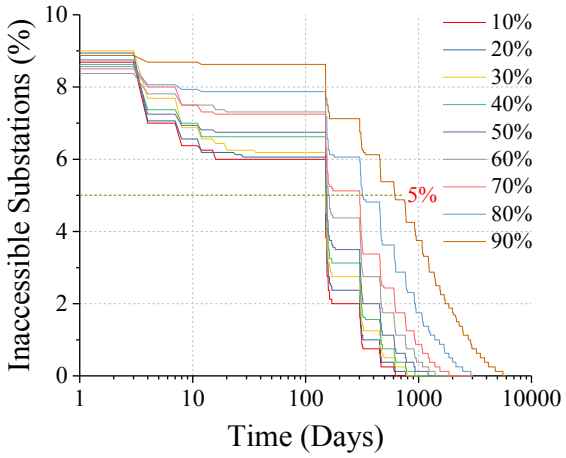

Fig. 5.17. The median portion of inaccessible substations for different repair resource distribution ratios in a M=7.5 scenario

5.2.4. Discussion

The case study simulation results revealed that the EPSS-TS recovery can undergo abrupt changes under different earthquake magnitude scenarios. As the fraction of the damaged links

and nodes crosses critical thresholds, EPSS repair time will be sharply longer (an abrupt change) as the LC of the TS is small and it takes some time for it to enlarge enough to encompass all damaged substations. The cases with varying repair resources are similar. Under strong earthquakes, meager resources will notably prolong the EPSS-TS system recovery process. However, providing repair resources above a critical threshold (proportional to the extent of network damage, and thus earthquake magnitude) can significantly reduce the EPSS-TS system recovery time.

Most importantly, an optimal amount and distribution of the available repair resources between the EPSS and TS can notably reshape the EPSS-TS system recovery path. The simulations indicate that it is detrimental to invest an overwhelming majority of the repair resources on the EPSS as an effort to restore the power supply. These resources remain barely used until as considerable part of TS is repaired enough to make a large number of EPSS substations reachable by road. As indicated by the observed abrupt changes, critical thresholds for the amount and the distribution of repair resources exist, and should be targeted to plan a fast coupled EPSS-TS system recovery.

5.3. Conclusions and suggestions

In this Chapter, in order to capture the behavior patterns during the post-earthquake recovery for the coupled EPSS-TS systems in earthquake scenarios with different amounts and distributions of the repair resources, a network-theoretical model was developed and applied on a virtual system. The main conclusions are:

1. The case study results revealed that the restoration of the coupled CI system would be substantially different under seismic scenarios with varying magnitudes. In particular, the abrupt change can be observed as the magnitude reaches some particular threshold.
2. The gross amount of the repair resources were found to profoundly shape the recovery process of the coupled EPSS-TS system. An abrupt change was also found.
3. Different repair resource distribution strategies also remarkably influence the recovery of the coupled EPSS-TS system, given the same gross amount of repair resources. The restoration of EPSS was found not to be expedited even if more repair resource are invested in it. On the contrary, the EPSS can be repaired much faster when the TS recovers smoothly and efficiently. Abrupt changes emerge in these simulations, too, indicating that repair resource distribution thresholds exist.

The results indicate that the post-earthquake recovery of coupled CI systems under different earthquake scenarios can be planned ahead of time by accumulating and correctly distributing the repair resources. Optimization of these two processes, as well as considerations of dynamic resource amount and resource distribution policies, are obvious possible extension of the proposed model.

6. Conclusions and outlook

Seismic resilience of Electric Power Supply System (EPSS) is strategically consequential to the well-being of modern Urban Communities (UCs). This issue has therefore gained the attention worldwide, and the engineering research in seismic resilience of Critical Infrastructures (CIs) has intensified remarkably in the past few decades. The findings of these studies, along with the corresponding field observations, have already unveiled that the inadequate seismic resilience of EPSS is rooted in their inherent physical vulnerabilities as well as the complex system-level operation of modern CIs and their interdependences, both physically and through a set of information and communication technologies. Due to this ever-increasing interconnectivity, the initially localized damage incurred in any single CI tends to cascade into the other ones. Additionally, the post-earthquake recovery process for EPSS and other CIs is often sluggish, mainly due to the insufficient preparedness of the system of CIs.

As a research endeavor to improve the understanding of seismic resilience of EPSS, three conceptual and numerical studies have been carried out in this thesis. First, a novel framework to quantify the seismic resilience of EPSS by tracking both the supply and the demand for electric power throughout the damage absorption and the post-earthquake recovery phases is proposed. An Agent-Based model (ABM) was then used to model the recovery of the electric power supply delivered by the EPSS to the community it serves and to capture the unique and dynamic characteristics of the seismic recovery process for the EPSS-Community system. Two individual agents, the EPSS Operator and the Administrator, are specified using a set of parameters to define their individual behavior and interactions. The effect of agent parameters and their interactions is examined by Monte Carlo simulations on the seismic recovery process of a virtual EPSS-Community system. To enhance the EPSS-Community system model, the ABM is further developed by including the third agent, namely the Operator of the transportation system (TS), to study the influence of the status of TS on the resilience of the EPSS. Third, in order to gauge how the available repair resources would shape the recovery path of the integrated EPSS and TS, a network-theoretical model was developed and applied on a virtual coupled EPSS-TS system. Occurrence of abrupt changes in the EPSS recovery rate when the amount or the distribution of the available repair resources is varied, was noted.

The most important conclusions from those conducted studies, and the corresponding outlooks will be presented in the following sections of this Chapter.

6.1. Main conclusions

Based on the studies presented in this thesis, the most important findings and the conclusions are:

- A compositional supply/demand assessment framework for the seismic resilience of EPSS was established. Besides the physical functionality loss that is usually examined as the only

measure for the seismic resilience of CIs, the newly proposed framework also enables the investigation of the resilience of an EPSS-Community system from the socio-economic perspective.

- An agent-based model (ABM) was developed in order to model the trajectory of the power supply recovery process, so as to gauge the systemic seismic resilience of the EPSS-Community system. The conducted case study revealed that the ABM enables the nuanced modeling of the recovery process following the seismic events that includes the CI and the community decision makers and their interactions. The EPSS-related electric power deficit and the community-related resilience metrics are computable and can be tracked during both the damage absorption and recovery phases to indicate the resilience (or lack thereof) of the EPSS-Community system. The communities and the CIs should set up their post-earthquake recovery performance objectives using such tractable resilience metrics.
- A set of seismic contingency electric power dispatch strategies (SCDSs) were proposed, whereby the potentially insufficient electric power in the EPSS can be delivered to the users following particular priority schemes. The case study revealed that the resilience behavior for different sectors across the coupled EPSS-Community system can be remarkably influenced by the pre-set SCDS. The communities can also help by setting up and enforcing electric power conservation efforts in the less or undamaged portions of the community immediately after an earthquake.
- The emergency of the potentially conflicting interests of the community and the EPSS operator was also demonstrated in the proposed Agent-Based model. The case study results revealed that the resolution of such conflicts would profoundly influence the recovery process of the EPSS-Community system. The communities could enforce post-earthquake recovery performance objectives by intervening, if the recovery is slow, through changing the recovery priorities of the CI operators. Such interactions among the decision makers are found to have a significant effect on the rate of the EPSS-Community system recovery.
- The dependence of the EPSS post-earthquake recovery upon the recovery of the Transportation System (TS) was successfully demonstrated. The interplay among different CI operator agents, as well as the physical interdependence between the CI system components and the sequencing of repairs, were found to collectively determine the recovery path of the integrated EPSS-TS-Community system. The recovery plans of individual CIs must be coordinated to identify the crucial interdependencies and speed up the recovery by conducting strategic repairs first.
- A network-theoretical model was developed to examine the impact of the amount and distribution of the available repair resources and work crews on the seismic recovery behavior for the coupled EPSS-TS system. The case study simulation results suggested that the rate of EPSS-TS system recovery is affected by the amount of available resources, and, significantly, that an optimal distribution of the available resources between the EPSS and TS can notably

reshape the recovery path, thus, increase the seismic resilience. The occurrence of abrupt changes, however, indicates that planning of repair resource amounts and distribution strategies must be done considering the network effects.

6.2. Prospective research issues

Based on the knowledge gap identified in Chapter 2, and the three contributions made in this dissertation, the following prospective new research issues are:

1. The interdependence among different CIs, especially in the post-earthquake recovery stage have to be studied further. The key issue is how the repair of different CIs can be conducted and coordinated by their operators and the community administrators, and how the partially restored functionality of one CI affects the others. For instance, owing to the partially restored availability of information given the repair of the telecommunication system, how will the repair of the damaged EPSS be expedited? In turn, how will the recovered power supply capacity facilitate the full repair of the telecommunication networks? This issue can be particularly important in the coming decades, given the flourishing decentralized smart grids, whose functionality is contingent on instantaneous and continuous exchange of information.

2. A topology optimization model to improve the systemic resilience of the integrated CIs systems should be proposed. As the simulations in Chapter 5 and the research presented in Chapter 2 indicate, there is an optimal interconnectivity level between CIs that minimizes the systemic risk of cascading failures. However, for many of the real-world cases, cascade-avoidance strategies tend to isolate the highly-connected elements or sub-systems within a CI system, even though such interconnectivity is potentially very beneficial during the post-earthquake recovery stage. The optimization model should also consider the provisioning and the distribution of the repair resources, as well, on a community scale, the investment balance between increasing the robustness of the built infrastructure (to reduce the initial damage) and increasing the preparedness for effective post-earthquake recovery.

3. The more nuanced Agent-Based Model (ABM) that involves the operators of other CIs (e.g. the Telecommunication, Water Systems besides EPSS and TS) and the administrator of the community, should be studied. In order to be representative of the real-world cases, the states (attributes) of the agents should be updated in the more continuous way given different instantaneous restoration behavior of the physical functionality of the set of CIs and the demand by users from different societal sectors. A dynamic game-theoretical model can be incorporated into the ABM, whereupon the complex interplay among the involved agents with different interests can be modeled. More importantly, the effect of those dynamic interactions, with reference to the entangled recovery paths of the coupled CIs-Community system following an earthquake, can be examined.

4. The model for the time-varying functionality demand for the service provided by CI systems should be established, based on the migration behavior of the community inhabitants after an earthquake. According to the collected data about the real-world mobility of the inhabitants, together with the established "herding" social behavioral patterns (Helbing et al. 2000), the model would quantify the outflow of people triggered by the widespread damage of CI systems and the community built environment following strong earthquakes. Such migration will lead to a reduction of the CI service demand in the affected areas, but also cause an increase of demand in the neighborhoods and communities accommodating the migrating inhabitants. The cascade model established by Zio and Sansavini (2011) can be employed to investigate the potential cascading failures of CIs (in those neighborhoods) induced by the abrupt overload, particularly in case of a "herding" inflow. The cascading failures will also then reconfigure the migration of the inhabitants, forming a complex coupled socio-technical system. The seismic resilience quantification model proposed in Chapter 3 and further developed in Chapter 4 could be used as a basis to develop more complex models to study such complex systems CI-Community systems after natural disasters.

Literature

1. Albert, R., Albert, I., and Nakarado, G. L. (2004). Structural vulnerability of the North American power grid. *Physical Review E* 69(2): 025103.
2. Alesch, D. J. (2005). Complex urban systems and extreme events: Toward a theory of disaster recovery. *1st International Conference on Urban Disaster Reduction, Kobe, Japan, January 18-20.*
3. Andersen, D., Balakrishnan, H., Kaashoek, F., and Morris, R. (2001). Resilient overlay networks. *Proceedings of the eighteenth ACM symposium on Operating systems principles, Banff, Canada, October 21-24*.
4. Andersson, G., Donalek, P., Farmer, R., Hatziargyriou, N., Kamwa, I., Kundur, P., Martins, N., Paserba, J., Pourbeik, P., Sanchez-Gasca, J., Schulz, R., Stankovic, A., Taylor, C., and Vittal, V. (2005). Causes of the 2003 major grid blackouts in North America and Europe, and recommended means to improve system dynamic performance. *IEEE Transactions on Power Systems* 20(4): 1922-1928.
5. ATC-58 Project web page: *https://www.atcouncil.org/36-projects/projects/85-atc-58-project* (accessed 01.05.2015).
6. Bai, J., Xie, Q., and Xue, S. T. (2013). Shaking table test on UHV single circuit cup type transmission tower-line coupling system. *Engineering Mechanics* 30(4): 472-480 (in Chinese).
7. Bashan, A., Berezin, Y., Buldyrev, S. V., and Havlin, S. (2013). The extreme vulnerability of interdependent spatially embedded networks. *Nature Physics* 9(10): 667-672.
8. Batabyal, A. A. (1998). The concept of resilience: retrospect and prospect. *Environment and Development Economics* 3(2): 235-239.
9. Batty, M. (2008). The size, scale, and shape of cities. *Science* 319(5864): 769-771.
10. Batty, M. (2012). Building a science of cities. *Cities* 29: S9-S16.
11. Bettencourt, L. M. A., Lobo, J., Helbing, D., Kuhnert, C., and West, G. B. (2007). Growth, innovation, scaling, and the pace of life in cities. *Proceedings of the National Academy of Sciences* 104(17): 7301-7306.
12. Bilis, E. I., Kröger, W., and Nan, C. (2013). Performance of electric power systems under physical malicious attacks. *IEEE Systems Journal* 7(4): 854-865.
13. Blebo, F. C., and Roke, D. A. (2015). Seismic-resistant self-centering rocking core system. *Engineering Structures* 101: 193-204.
14. Bloom, D. E., Canning, D., and Fink, G. (2008). Urbanization and the wealth of nations. *Science* 319(5864): 772-775.

15. Board on Natural Disasters. (1999). Mitigation emerges as major strategy for reducing losses caused by natural disasters. *Science* 284: 1943-1947.

16. Borberly, A. and Kreider, J. F. (2001). *Distributed generation: The power paradigm for the new millennium*. CRC Press.

17. Brandes, U. (2001). A faster algorithm for betweenness centrality. *Journal of Mathematical Sociology* 25(2): 163-177.

18. Brummitt, C. D., D'Souza, R. M., Leicht, E. A. (2012). Suppressing cascades of load in interdependent networks. *Proceedings of the National Academy of Sciences of the United States of America* 109(12): E680-E689.

19. Brummitt, C. D., Hines, P. D. H., Dobson, I., Moore, C., and D'Souza, R. M. (2013). Transdisciplinary electric power grid science. *Proceedings of the National Academy of Sciences* 110(3): 12159.

20. Bruneau, M., Chang, S. E., and Eguchi, R. T. et al. (2003). A framework to quantitatively assess and enhance the seismic resilience of communities. *Earthquake Spectra* 19(4): 733-752.

21. Bruneau, M., and Reinhorn, A. (2007). Exploring the concept of seismic resilience for acute care facilities. *Earthquake Spectra* 23(1): 41-62.

22. Buldyrev, S. V., Parshani, R., Paul, G., Stanley, H. E., and Havlin, S. (2010). Catastrophic cascade of failures in interdependent networks. *Nature* 464(7291): 1025-1028.

23. Campbell, K. W., and Bozorgnia, Y. (2008). NGA ground motion model for the geometric mean horizontal component of PGA, PGV, PGD and 5% damped linear elastic response spectra for periods ranging from 0.01 to 10 s. *Earthquake Spectra* 24(1): 139-171.

24. Cavalieri, F., and Franchin, P. (2014). Models for seismic vulnerability analysis of power networks: comparative assessment. *Computer-Aided Civil and Infrastructure Engineering* 29: 590-607.

25. Chang, S. E., McDaniels, T., and Fox, J. et al. (2014). Toward disaster-resilient cities: Characterizing resilience of infrastructure systems with expert judgments. *Risk Analysis* 34(3): 416-434.

26. Chang, L., Peng, F., Ouyang, Y., Elnashai, A. S., and Spencer, B. F. (2012). Bridge seismic retrofit program planning to maximize postearthquake transportation network capacity. *Journal of Infrastructure Systems* 18(2): 75-88.

27. Christie, R. D. (1993). Power systems test case archive. *http://www.ee.washington.edu/research/pstca/pf118/pg_tca118bus.htm*.

28. Cimellaro, G. P., Renschler, C., Reinhorn, A. M., and Arendt, L. (2016). PEOPLES: A framework for evaluating resilience. *ASCE Journal of Structural Engineering* 142(10): 04016063.

29. Cimellaro, G. P., Solari, D., and Bruneau, M. (2014). Physical infrastructure interdependency and regional resilience index after the 2011 Tohoku Earthquake in Japan. *Earthquake Engineering & Structural Dynamics* 43:1763-1784.

30. Cutter, S. L. (2013). Building disaster resilience: Steps toward sustainability. *Challenges in Sustainability* 1(2): 72-79.

31. Decò, A., Bocchini, P. and Frangopol, D. M. (2013). A probabilistic approach for the prediction of seismic resilience of bridges. *Earthquake Engineering & Structural Dynamics* 42: 1469-1487.

32. Delé, E., and Didier, M. (2014). Time-varying seismic resilience of electric supply systems. *Master Thesis* IBK, D-BAUG, ETH Zurich.

33. Der Kiureghian, A., Sackman, J. L., and Hong, K. J. (1999). Interaction in interconnected electrical substation equipment subjected to earthquake ground motions. *PEER 1999/01*.

34. Der Kiureghian, A., Sackman, J. L., and Hong, K. J. (2001). Seismic interaction in linearly connected electrical substation equipment. *Earthquake Engineering & Structural Dynamics* 30(2): 327-347.

35. Di Muro, M. A., La Rocca, C. E., Stanley, H. E., Havlin, S., and Braunstein, L. A. (2016). Recovery of interdependent networks. *Scientific Reports* 6: 22834.

36. Duenas-Osorio, L., Craig, J. I., and Goodno, B. J. (2007). Seismic response of critical interdependent networks. *Earthquake Engineering & Structural Dynamics* 36: 285-306.

37. Dueñas-Osorio, L., and Vemuru, S. M. (2009). Cascading failures in complex infrastructure systems. *Structural Safety* 31: 157-167.

38. Dunn, S., Wilkinson, S., and Ford, A. (2016). Spatial structure and evolution of infrastructure networks. *Sustainable Cities and Society* 27: 23-31.

39. Eatherton, M. R., and Hajjar, J. F. (2014). Hybrid simulation testing of a self-centering rocking steel braced frame system. *Earthquake Engineering & Structural Dynamics* 43:1725-1742.

40. Eurostat. (2015). Electricity and heat statistics. *http://ec.europa.eu/eurostat/statistics-explained/index.php/Electricity_and_heat_statistics*.

41. Fang, Y., and Sansavini, G. (2017). Optimizing power system investments and resilience against attacks. *Reliability Engineering and System Safety* 159: 161-173.

42. Farr, R. S., Harer, J. L., and Fink, T. M. A. (2014). Easily repairable networks: Reconnecting nodes after damage. *Physical review letters* 113(13): 138701.

43. Filiatrault, A., and Matt, H. (2005). Experimental seismic response of high-voltage transformer-bushing systems. *Earthquake Spectra* 21(4): 1009-1025.

44. Filiatrault, A., and Stearns, C. (2004). Seismic response of electrical substation equipment interconnected by flexible conductors. *ASCE Journal of Structural Engineering* 130(5): 769-778.

45. Franchin, P., and Cavalieri, F. (2015). Probabilistic assessment of civil infrastructure resilience to earthquakes. *Computer-Aided Civil and Infrastructure Engineering* 30: 583-600.

46. Freeman, L. C. (1977). A set of measures of centrality based upon betweenness. *Sociometry* 40(1): 35-41.

47. Fujisaki, E., Takhirov, S., Xie, Q., and Mosalam, K. (2014). Seismic vulnerability of power supply: Lessons learned from recent earthquakes and future horizons of research. *Proceedings of the 9th International Conference on Structural Dynamics (EURODYN 2014), Porto, Portugal, June 30-July 2*.

48. Gao, J., Barzel, B., and Barabási, A. L. (2016). Universal resilience patterns in complex networks. *Nature* 530 (7590): 307-312.

49. GB 50011-2010. (2010). *Code for seismic design of buildings*. Beijing: China Architecture & Building Press.

50. Ge, Y., Gu, Y. T., and Deng, W. G. (2010). Evaluating China's national post-disaster plans: The 2008 Wenchuan Earthquake's recovery and reconstruction planning. *International Journal of Disaster Risk Science* 1(2): 17-27.

51. Glaeser, E. (2011). Cities, productivity, and quality of life. *Science* 333(6042): 592-594.

52. HAZUS-MH US FEMA project web page: *https://www.fema.gov/hazus* (accessed 01.05.2015).

53. Helbing, D., Farkas, I., and Vicsek, T. (2000). Simulating dynamical features of escape panic. *Nature* 407(6803): 487-490.

54. Helbing, D. (2013). Globally networked risks and how to respond. *Nature* 497(7447): 51-59.

55. Hollnagel, E., and Fujita, Y. (2013). The Fukushima disaster-systemic failures as the lack of resilience. *Nuclear Engineering and Technology* 45(1): 13-20.

56. Hu, F., Yeung, C. H., Yang, S., Wang, W., and Zeng, A. (2016). Recovery of infrastructure networks after localised attacks. *Scientific Reports* 6: 24522.

57. Hwang, S., Park, M., Lee, H-S., Lee, S. H., and Kim, H. (2015). Postdisaster interdependent built environment recovery efforts and the effects of governmental plans: Case analysis using system dynamics. *Journal of construction engineering and management* 141(3): 04014081.

58. International Conference of Building Officials (ICBO). (1997). *Uniform Building Code 1997*.

59. International Strategy for Disaster Reduction (2005). Hyogo framework for action 2005-2015: Building the resilience of nations and communities to disasters. *World Conference on Disaster Reduction, Kobe, Japan, January 18-22*.

60. Iuchi, K., Johnson, L. A., and Olshansky, R. B. (2013). Securing Tohoku's future: Planning for rebuilding in the first year following the Tohoku-Oki Earthquake and Tsunami. *Earthquake Spectra* 29(S1): S479-S499.

61. Jeong, S. H., and Elnashai, A. S. (2007). Probabilistic fragility analysis parameterized by fundamental response quantities. *Engineering Structures* 29(8): 1238-1251.

62. Kawashima, K., Takahashi, Y., Ge, H., Wu, Z., and Zhang, J. (2009). Reconnaissance report on damage of bridges in 2008 Wenchuan, China, Earthquake. *Journal of Earthquake Engineering* 13(7): 956-998.

63. Kawashima, K. (2012). Damage of bridges due to the 2011 Great East Japan Earthquake. *Proceedings of 9th CUEE and 4th ACEE Joint Conference, Tokyo Institute of Technology, Tokyo, Japan, March 6-8*.

64. Kirschen, D. (2010). *Fundamentals of power system economics*. Wiley.

65. Klein, R. J. T., Nicholls, R. J., and Thomalla, F. (2003). Resilience to natural hazards: How useful is this concept? *Environmental Hazards* 5: 35-45.

66. Koliou, M., Filiatrault, A., and Reinhorn, A. M. (2013). Seismic response of high-voltage transformer-bushing systems incorporating flexural stiffeners I: Numerical Study. *Earthquake Spectra* 29(4): 1353-1367.

67. Koliou, M., Filiatrault, A., and Reinhorn, A. M. (2013). Seismic response of high-voltage transformer-bushing systems incorporating flexural stiffeners II: Experimental Study. *Earthquake Spectra* 29(4): 1353-1367.

68. Kramer, S. L. (1996). *Geotechnical earthquake engineering*. Prentice Hall.

69. Krishnamurthy, V., Kwasinski, A., and Duenas-Osorio, L. (2016). Comparison of power and telecommunications dependencies and interdependencies in the 2011 Tohoku and 2010 Maule Earthquakes. *Journal of Infrastructure Systems* 22(3): 04016013.

70. Kröger, W., and Zio, E. (2011*). Vulnerable systems*. London: Springer.

71. Kuwata, Y. (2012). Analysis of the impact of water-supply outages due to multiple factors caused by the 2011 Tohoku Earthquake. *Proceedings of 9th CUEE and 4th ACEE Joint Conference, Tokyo Institute of Technology, Tokyo, Japan*, *March 6-8*.

72. Kwasinski, A., Krishnamurthy, V., Song, J., and Sharma. R. (2012). Availability evaluation of

micro-grids for resistant power supply during natural disasters. *IEEE Transactions on Smart Grid* 3(4): 2007-2018.

73. Kwon, O. S., and Elnashai, A. (2006). The effect of material and ground motion uncertainty on the seismic vulnerability curves of RC structures. *Engineering Structures* 28(2): 289-303.
74. Lekkas, E., Andreadakis, E., Alexoudi, V., Kapourani, E., and Kostaki, I. (2012). The M_w=9.0 Tohoku Japan Earthquake (March 11, 2011) Tsunami impact on structures and infrastructure. *15th World Conference on Earthquake Engineering, Lisbon, Portugal, September 24-28*.
75. Linkov, I., Bridges, T., Creutzig, F., Decker, J., Fox-Lent, C., and Kröger, W. et al. (2014). Changing the resilience paradigm. *Nature Climate Change* 4: 407-409.
76. Lundberg, J., and Johansson, B. J. (2015). Systemic resilience model. *Reliability Engineering and System Safety* 141: 22-32.
77. Majdandzic, A., Podobnik, B., Buldyrev, S. V., Kenett, D. Y., Havlin, S., and Stanley, H. E. (2013). Spontaneous recovery in dynamical networks. *Nature Physics* 10(1): 34-38.
78. Manyena, S. B. (2006). The concept of resilience revisited. *Disasters* 30: 434.
79. Mensah, A. F., and Duenas-Osorio, L. (2016). Efficient resilience assessment framework for electric power systems affected by hurricane events. *ASCE Journal of structural engineering* 142(8): C4015013.
80. Michel-Kerjan, E. (2015). We must build resilience into our communities. *Nature* 524(7566): 389.
81. Midorikawa, M., Azuhata, T., Ishihara, T., and Wada, A. (2006). Shaking table tests on seismic response of steel braced frames with column uplift. *Earthquake Engineering & Structural Dynamics* 35:1767-1785.
82. Mieler, M., Stojadinovic, B., Budnitz, R., Comerio, M., and Mahin, S. (2015). A framework for linking community resilience goals to specific performance targets for the built environment. *Earthquake Spectra* 31(3): 1267-1283.
83. Mitchell, D., DeVall, R. H., Kobayashi, K., Tinawi, R., and Tso, W. K. (1996). Damage to concrete structures due to the January 17, 1995, Hyogo-ken Nanbu (Kobe) earthquake. *Canadian Journal of Civil Engineering* 23(3): 757-770.
84. Morsali, R., Mohammadi, M., Maleksaeedi, I., and Ghadimi, N. (2014). A new multiobjective procedure for solving nonconvex environmental/economic power dispatch. *Complexity* 20(2): 47-62.
85. Mosalam, K. M., Günay, S., and Takhirov, S. (2016). Response evaluation of interconnected electrical substation equipment using real-time hybrid simulation on multiple shaking tables.

Earthquake Engineering & Structural Dynamics 45: 2389-2404.

86. Naeim, F., and Kelly, J. M. (1999). *Design of seismic isolated structures: From theory to practice*. Wiley.
87. Nan, C., and Sansavini, G. (2017). A quantitative method for assessing resilience of interdependent infrastructures. *Reliability Engineering and System Safety* 157: 35-53.
88. Newman, M. E. J., Strogatz, S. H. and Watts, D. J. (2001). Random graphs with arbitrary degree distributions and their applications. *Physical Review E* 64: 02611.
89. Norris, F. H., Stevens, S. P., and Pfefferbaum, B. et al. (2008). Community resilience as a metaphor, theory, set of capacities, and strategy for disaster readiness. *American Journal of Community Psychology* 41: 127-150.
90. Omidvar, B., Malekshah, M. H., and Omidvar, H. (2014). Failure risk assessment of interdependent infrastructures against earthquake, a Petri net approach: case study-power and water distribution networks. *Natural Hazards* 71:1971-1993.
91. OpenQuake Global Earthquake Model Platform web page: *http://www.globalquakemodel.org/openquake/about/* (accessed 01.05.2015).
92. O'Rourke, T. D. (2007). Critical infrastructure, interdependencies, and resilience. *The Bridge* 37(1): 22-29.
93. O'Sullivan, D., and Haklay, M. (2000). Agent-based models and individualism: is the world agent-based? *Environment and Planning A* 32(8): 1409-1425.
94. Ouyang, M., Dueñas-Osorio, L., and Min, X. (2012). A three-stage resilience analysis framework for urban infrastructure systems. *Structural Safety* 36-37: 23-31.
95. Poljansek, K., Bono, F., and Gutiérrez, E. (2012). Seismic risk assessment of interdependent critical infrastructure systems: The case of European gas and electricity networks. *Earthquake Engineering & Structural Dynamics* 41: 61-79.
96. Porter, K. A. (2003). An overview of PEER's performance-based earthquake engineering methodology. *9th International Conference on Applications of Statistics and Probability in Civil Engineering (ICASP9), San Francisco, United States, July 6-9*.
97. Pournaras, E., and Espejo-Uribe, J. (2017). Self-repairable smart grids via online coordination of smart transformers. *IEEE Transactions on Industrial Informatics* accepted.
98. Pournaras, E., Vasirani, M., Kooij, R. E., and Aberer, K. (2014). Decentralized planning of energy demand for the management of robustness and discomfort. *IEEE Transactions on Industrial Informatics* 10(4): 2280-2289.

99. Reed, D. A., Powell, M. D., and Westerman, J. M. (2010). Energy infrastructure damage analysis for Hurricane Rita. *Natural Hazards Review* 11(3): 102-109.

100. Rinaldi, S. M., Peerenboom, J. P., and Kelly, T. K. (2001). Identifying, understanding, and analyzing critical infrastructure interdependencies. *IEEE Control Systems* 21(6): 11-25.

101. Rossetto, T., and Elnashai, A. (2003). Derivation of vulnerability functions for European-type RC structures based on observational data. *Engineering Structures* 25(10): 1241-1263.

102. San Francisco Planning and Urban Research Association (SPUR). (2009). The resilient city: Defining what San Francisco needs from its seismic mitigation polices. *spur.org.*

103. Schneider, C. M., Yazdani, N., Araujo, N. A. M., Havlin, S., and Herrmann, H. J. (2013). Towards designing robust coupled networks. *Scientific Reports* 3: 1969.

104. Senel, S. M., and Kayhan, A. H. (2009). Fragility based damage assessment in existing precast industrial buildings: A case study for Turkey. *Structural Engineering and Mechanics* 34(1): 39-60.

105. Shinozuka, M., Dong, X., Chen, T. C., and Jin, X. (2007). Seismic performance of electric transmission network under component failures. *Earthquake Engineering & Structural Dynamics* 36: 227-244.

106. Smith, K. (2013). *Environmental hazards: Assessing risk and reducing Disaster (6th Edition)*. Routledge.

107. Sun, L., Didier, M., Delé, E., and Stojadinovic, B. (2015a). Probabilistic demand and supply resilience model for electric power supply system under seismic hazard. *Proceedings of the 12th International Conference on Applications of Statistics and Probability in Civil Engineering (ICASP2015), Vancouver, Canada, July 12-15*.

108. Sun, L., Didier, M., and Stojadinovic, B. (2015b). Study of seismic recovery and resilience of Electric Power Supply System. *Proceedings of the 25European Safety and Reliability Conference (ESREL 2015), Zurich, Switzerland, September 7-10*.

109. Syner-G EU FP7 Project web page: http://www.vce.at/SYNER-G/ (accessed 01.05.2015).

110. Trovato, M., Sun, L., and Stojadinovic, B. (2015). Buckling restrained brace retrofit technique for existing electric power transmission towers. *Proceedings of the 8th International Conference on Behavior of Steel Structures in Seismic Areas (STESSA 2015), Shanghai, China, July 1-4*.

111. Wada, A., Qu, Z., Ito, H., Motoyui, S., Sakata, H., and Kasai, K. (2009). Seismic retrofit using rocking walls and steel dampers. *Proceedings of the 2009 ATC and SEI Conference on Improving the Seismic Performance of Buildings and Other Structures, San Francisco, United States,*

December 9-11.

112. Whittaker, A. S., Fenves, G. L., and Gilani, A. S. J. (2004). Earthquake performance of porcelain transformer bushings. *Earthquake Spectra* 20(1): 205-223.

113. Winkler, J., Duenas-Osorio, L., Stein, R., and Subramanian, D. (2010). Performance assessment of topologically diverse power systems subjected to hurricane events. *Reliability Engineering and System Safety* 95: 323-336.

114. Xie, Q., and Sun, L. (2012). Failure mechanism and retrofitting strategy of transmission tower structures under ice load. *Journal of Constructional Steel Research* 74: 26-36.

115. Xie, Q., and Sun, L. (2013). Experimental study on mechanical behavior and failure mechanism of latticed steel transmission tower. *ASCE Journal of Structural Engineering* 139(6): 1009-1018.

116. Xie, Q., and Zhu, R. Y. (2011). Damage to electric power grid infrastructure caused by natural disasters in China. *IEEE Power and Energy Magazine* 9(2): 28-36.

117. Yang, T. Y., Stojadinovic, B., and Moehle, J. (2012). Demonstration of a practical method for seismic performance assessment of structural systems. *Earthquake Spectra* 28(2): 811-829.

118. Ye, L. P., Qu, Z., Lu, X. Z., and Feng, P. (2008). Collapse prevention of building structures: a lesson from the Wenchuan earthquake. *Journal of Building Structures* 29(4): 42-50 (in Chinese).

119. Zhao, X., Cai, H., Chen, Z., Gong, H., and Feng, Q. (2016). Assessing urban lifeline systems immediately after seismic disaster based on emergency resilience. *Structure and Infrastructure engineering* 12(12): 1634-1649.

120. Zhao, B., and Taucer, F. (2010). Performance of infrastructure during the May 12, 2008 Wenchuan Earthquake in China. *Journal of Earthquake Engineering* 14(4): 578-600.

121. Zhao, G. F., Xie, Q., and Liang, S. G. et al. (2010). Wind tunnel test on wind-induced response of transmission tower and tower line coupling system. *Journal of Building Structures* 131(12): 69-77 (in Chinese).

122. Zheng, K. F., Chen, L. B., Zhuang, W. L., Ma, H. S., and Zhang, J. J. (2013). Bridge vulnerability analysis based on probabilistic seismic demand models. *Engineering Mechanics* 30(5): 165-171 (in Chinese).

123. Zio, E. (2016). Challenges in the vulnerability and risk analysis of critical infrastructures. *Reliability Engineering and System Safety* 152: 137-150.

124. Zio, E. and Sansavini, G. (2011). Component criticality in failure cascade processes of network systems. *Risk Analysis* 31(8): 1196-1210.